DOKUZ EYLÜL UNIVERSITY

GRADUATE SCHOOL OF NATURAL AND APPLIED SCIENCES

AN APPROACH FOR STENT SELECTION DURING ENDOVASCULAR ANEURYSM REPAIR

by

Semih UTKU

June, 2010

İZMİR

AN APPROACH FOR STENT SELECTION
DURING ENDOVASCULAR ANEURYSM REPAIR

A Thesis Submitted to the
Graduate School of Natural and Applied Sciences of Dokuz Eylül University
In Partial Fulfillment of the Requirements for the Degree of Doctor Philosophy in
Computer Engineering, Computer Engineering Program

by
Semih UTKU

June, 2010
İZMİR

PhD. THESIS EXAMINATION RESULT FORM

We have read the thesis entitled **"AN APPROACH FOR STENT SELECTION DURING ENDOVASCULAR ANEURYSM REPAIR"** completed by **SEMİH UTKU** under supervision of **PROFESSOR DR. ALP KUT** and we certify that in our opinion it is fully adequate, in scope and in quality, as a thesis for the degree of Doctor Philosphy.

....

Prof.Dr. Alp KUT

Supervisor

....

Assist.Prof.Dr. Adil ALPKOÇAK   Assist.Prof.Dr. Reyat YILMAZ

Thesis Committee Member   Thesis Committee Member

....

Prof.Dr. Hayri SEVER   Assist. Prof.Dr. Şen ÇAKIR

Examining Committee Member   Examining Committee Member

_____

Prof.Dr. Mustafa SABUNCU
Director
Graduate School of Natural and Applied Sciences

ACKNOWLEDGEMENTS

AN APPROACH FOR STENT SELECTION DURING ENDOVASCULAR ANEURYSM REPAIR

ABSTRACT

In recent years, usage of computer – aided systems has been increased tremendously in medical applications. The main purpose of these systems is to support the experts more qualified, efficient, accurate and fast way during patients' diagnosis and treatment. A 3D medical visualization application is one of the areas of computer-aided systems.

In this dissertation, a measurement tool is developed to help experts on the treatment of abdominal aortic aneurysm. Different measurements are made on aorta vein to determine which stent–graft is used. The measurements are made with user interaction in 3D environments by the developed application.

In this study, Computed Tomography images are examined and necessary steps for medical modeling; segmentation, edge detection, model construction, and surface construction phases are carried out. In order to make interactive measurements on the 3D model, required transformation is applied to the model. Contributions of this study are new surface construction method for tubular structures and measurement methods. Moreover, a new specialized measurement and evaluation tool is developed for abdominal aortic aneurysm. This specialized software will help to medical specialist in decision-making processes. To verify the accuracy and usability of the tool, the measurements are carried out on the selected patients' group by using manual methods and the tool. Obtained statistical results are evaluated and compared. It is proven statistically that the developed tool provides more reliable, more consistent, and more repeatable results.

Keywords: Computer Graphics, 3 – Dimensional Modeling, Medical Imaging, Abdominal Aortic Aneurysm, Segmentation, Stent Selection.

DAMARİÇİ GENİŞLEME TEDAVİSİ SÜRECİNDE STENT SEÇİMİ İÇİN YAKLAŞIM

ÖZ

Son yıllarda medikal uygulamalar da bilgisayar destekli sistemlerin kullanılması giderek yaygınlaşmaktadır. Bu sistemlerin temel amacı, hastaların teşhis ve tedavi sürecinde, uzmanlara daha kaliteli, etkin, doğru ve hızlı bir şekilde destek olmaktır. 3 boyutlu tıbbi görselleştirme, bilgisayar destekli uygulamalarda kullanılan yöntemlerden birisidir.

Bu çalışmada abdominal aort anevrizması durumunun tedavisinde uzmana yardımcı olacak bir ölçümleme aracı geliştirilmiştir. Anevrizma tedavisinde kullanılacak olan stentin belirlenmesi amacıyla damar üzerinde farklı ölçümlemeler yapılmaktadır. Bu araç kullanılarak, stent belirlemeye yönelik ölçümler 3 boyutlu ortamda kullanıcı ile etkileşimli olarak gerçekleştirilecektir.

Bu çalışmada uzmanların değerlendirme sürecinde kullanmış oldukları Bilgisayar Tomografi görüntüleri incelenerek tıbbi görselleştirme için gerekli aşamalar; bölütleme, kenar belirleme, model oluşturma ve yüzey oluşturma aşamaları gerçekleştirilmiştir. Model üzerinde ölçümlemelerin yapılabilmesi için gerekli dönüşümler yapılarak model kullanıcı ile etkileşimli hale getirilmiştir. Çalışma, yapılan ölçümleme yöntemleri ve yüzey oluşturmadaki çözümleriyle katkı sağlamıştır. Ayrıca Abdomianal Aort Anevrizması tedavisi için özelleştirilmiş bir uygulama geliştirilerek, uzmanların karar verme sürecinde yardımcı olacak bir yazılım sunulmuştur. Çalışma sonucunda ortaya çıkan programın kullanabilirliğini ve doğruluğunu göstermek için; belirli hasta grubuna, geliştirilen program ve manual yöntem ile ölçümlemeler yapılmış ve ölçümleme sonuçları karşılaştırılmıştır. Elde edilen sonuçlar, uygulamanın tutarlı, tekrarlanabilir ve güvenilir sonuçlar ürettiğini göstermiştir.

Anahtar Kelimler: Bilgisayar Grafikleri, 3 Boyutlu Modelleme,Tıbbi Görselleştirme, Abdominal Aort Anevrizması, Bölütleme, Stent Seçimi.

CONTENTS

CHAPTER ONE
INTRODUCTION

The use of computer systems in medical area has become increasingly widespread for last 30 years (Sakas, 2002; Russell, & et al., 1995). Several applications and specific tools help experts in medical areas. Purpose of these tools is to improve the quality and effectiveness of care and to reduce its cost while using their far reaching capabilities. Physicians expect to reach a lot of detailed information on the anatomical features of the patient as quick as possible. Three-Dimensional (3D) Medical visualization is one of these areas (Fuchs, Levoy, & Pizer, 1989). Visualization is the graphical presentation used to simplify the viewer's understanding of the information. 3D Medical visualization presents to the experts a 3D representation of the patient's anatomy which is obtained from a set of image slices. Medical Visualization applications have been developed to represents patient data in a visual form, to improve the comprehensibility and to facilitate processing of data.

1.1 Motivation

Several imaging modalities (Computed Tomography (CT), Magnetic Resonance Imaging (MRI) and ultrasonography) have been used in medical field to help physicians diagnose and treat medical conditions (Kunio, 2006). Computed Tomography uses X-Rays to generate cross-sectional, two dimensional images of the body. (Klingenbeck, & et al., 1999) Every acquired CT slice provides a matrix up to 512x512 / 1024x1024 volume elements (voxels). Intensity of the transmitted radiation is reading for each voxels by the CT detectors. Density of the tissue at each point in the CT slice is calculated by using these intensity values. According to this density value, a value is assigned for each voxel on a scale in which air has a value of −1000; water, 0; and compact bone, +1000. These scale units is named Hounsfield units (HU) (Schneider, Pedroni, & Lomax, 1996).

MRI uses a magnetic field, radio frequency pulses and a computer (Parizel, & et al., 2001). MRI collects pictures of various parts of the body without the use of x-ray.

A radio wave is used to send signals to the body and then MR scanner receive signals back. Computer generates pictures with using these returning signals. Pictures can be obtained from any particular angle of the body.

CT and MR scans produce detailed two dimensional (2D) medical images/pictures of organs, soft tissues, bone and other internal body structures. Three dimensional models can be generated by processing two-dimensional medical images / medical datasets. All these dataset are stored in the digital imaging and communication in medicine (DICOM) standard (Bidgood, & et al., 1997).

The DICOM standard was published in 1993. Its main goal was to establish norms for handling, storing, and interchanging medical images and associated digital information within open systems. DICOM is an industry standard for medical imaging format. This Standard has been developed on diagnostic medical imaging as practiced in radiology, cardiology and related disciplines; however, it is also suitable for image and non-image related information exchanged in clinical and other medical environments. DICOM standard made possible to interoperability between new medical equipments and other medical devices. Also DICOM standard provides integration within information systems in the medical and health care area (Stanberry, 2000). DICOM image files stores description of the image plane and the pixel features, values for mapping the image to color or gray scales, overlay planes, and other specific features.

CT and MRI provide three-dimensional volumetric datasets of the human body. Medical imaging is the technique and process used to create images of the human body (or parts) for clinical purposes. In medical imaging, assessment of tubular or vessel like structures is vital of interest (Krissian, 2000). Tubular structures (such as blood vessels, bronchi and colon etc.) are investigated in many clinical applications. Especially, the visualization of tubular structures such as blood vessels is an important area in the medical imaging (Kato, & et al., 1999).

Aorta is one of the well-known and important tubular structures of the body. Aorta is the largest blood vessel that carries blood to abdomen, pelvis and legs in a

human body. It supplies oxygen-rich blood to the lower part of the body. The thoracic aorta leaves the heart, ascends, arches, and descends through the chest until it reaches the diaphragm. The aorta is then called the abdominal aorta. The abdominal aorta passes the diaphragm and continues down the abdomen. The abdominal aorta ends where it splits to form the two iliac arteries that go down to the legs (Ernst, 1993).

An aneurysm is a localized dilation of a blood vessel. Abdominal aortic aneurysm occurs when a weak section on the wall of aorta expands or bulges. An abdominal aortic aneurysm becomes abnormally large or balloons outward. The blood pressure causes the aorta to bulge in the weakened part. A normal aorta has 2-3 centimeters diameter. If the weakened part over expands the healthy limits, (There is a large risk of rupture once the size has reached 5 cm.) the aorta may burst or rupture (Sternbergh, 2002). Ruptured aneurysms may cause serious internal bleeding, leading to sudden shock and death (Johnston, & et al., 2000).

This study focuses on the reliable preoperative endovascular planning of the abdominal aortic aneurysm. Reliable morphological evaluations are the most important determinant of Endovascular Aneurysm Repair (EVAR) indication. Measurement is an important step for the treatment process in the endovascular planning (Tillich, & et al., 2001). The usual measurements which are the diameter of the aneurysm neck, diameter of each iliac landing zone, length of aortic segment, between the lowermost renal artery and the aortic bifurcation, and length of each iliac segment (Aarts, & et al., 1999). These measurement values are required during the endovascular planning. Radiologists need a specialized tool for aortic aneurysm observation. As a result, faster and more reliable specialized pre-processing platform can be attained for the measurement. In this thesis, a new computer based aortic aneurysm measurement and evaluation tool was developed to fill this gap in this area.

1.2 The Problem Definition

EVAR has proven to be a less invasive alternative against to open surgery, with reduced preoperative morbidity and mortality rates, decreased intensive care unit and hospital stay (Teufelsbauer, & et al., 2002; Matsumura, & et al., 2003; Chuter, & et al., 1996; Zarins, & et al., 1999). However, it has become clear that EVAR can be associated with a substantial risk of complications that may compromise its durability (Kantonen, & et al., 1999; Stone, & et al., 2005; Waasdorp, & et al., 2005). Not all the patients with abdominal aortic aneurysms are suitable for EVAR and careful patient selection, particularly in regard to unfavorable anatomy, can be regarded as the most important determinant of EVAR outcome (Choke, & et al., 2006; Resch, & et al., 2000). Pre-procedural evaluation is needed to select inappropriate patients, to determine potential difficulties and to decide which stent graft to use (May, & et al., 1999; Slater, Harris, & Lee, 2008).

Excluding the access problems with iliac artery stenoses, the inappropriate patient group is mostly comprised of patients who have proximal aortic neck problems such as short neck, neck bulge, and angulated neck. In some aneurysms, angulations may be higher than expected and it would be impossible to implant the aortic stent-graft (Albertini, & et al., 2000; Diehm, & et al., 2008; Robbins, & et al., 2005). For instance, it is generally accepted that the angulations between proximal aortic neck and aneurysm sack should be less than 60° according to anatomical criterions for aortic aneurysm endovascular repair (Moore, & Rutherford, 1996; Balm, 1996; White, & et al., 1993; Silva, & et al., 1996; Johnston, & et al., 1991).

Reliable morphological evaluations, especially proximal neck measurements, are emerging as perhaps one of the most important determinant of EVAR indication. Post-processing studies of multidetector CT (MDCT) angiographic examinations are usually the preferred method of obtaining morphological measurements for EVAR planning (Geller, 2003; Rubin, & et al., 2000; Napel, & et al., 1992). Usually preprocedural evaluation includes the calculation of angulations over axial, sagittal or coronal images that are generated by bundled software of CT devices as a traditional method. Although well known post-processing applications provide 3-D

reconstructions of the aorta. These applications are not always specialized for abdominal aortic aneurysms, and consequently obtaining a smooth aortic model may become a very time consuming process.

Physicians may obtain different aortic measurements from different cross sectional multiplanar reformatted (MPR) images leading to inconsistent results and should choose the correct sagittal, coronal or oblique slice in this method for reliable results. As a result, a faster and more reliable specialized post-processing platform is required to avoid operator-dependency for the aortic measurements. Aortic Aneurysm Measurement and Evaluation Tool" (AMET) was developed to overcome these problems. This application platform is aimed to provide a reliable user-friendly interface to improve the measurement quality and shorten a time consuming post-processing step for EVAR.

1.3 Contributions of Thesis

This study is an interdisciplinary study that merges computer engineering and medical science (interventional radiology department). The study provides a specific application platform for automated measurement of the aorta as a part of the pre-procedural patient selection process for EVAR. With this study, a new platform – independent tool is aimed for improving the measurement quality and shortening the time needed for consuming pre-processing step of EVAR. The contributions to this study can be summarized as follows. First, this study provides platform independent specialized measurement tool for abdominal aortic aneurysm. Second contribution is about measurement methods. These methods give chance to experts' broader measurement capabilities over the 3D Model. Finally, new approach is developed to overcome surface construction problem for tubular structures in medical applications.

In this study, platform independent specialized measurement tool for abdominal aortic aneurysm was developed. Several tools and applications (Open source software, commercial software or device-dependent applications) present general-purpose platforms to help specialists in medical area. Different anatomical features

of the patient detailed three-dimensionally with these tools. In the study, customized software was provided for aortic aneurysm measurement with broader measurement capabilities. The software was developed on Java platform; therefore, it has a platform independent structure. Aorta vein and 3D model were developed with Java OpenGL (jogl). OpenGL (Open Graphics Library) is a standard specification defining a cross-language, cross-platform API for writing applications used for 2D and 3D computer graphics. In addition, the application was specialized to achieve different measurements in aortic aneurysm stent selection process.

Another contribution of the thesis is new measurement methods have been developed to measure aneurysm. In this study, shortest path, angle measurement, median centerline length, largest diameter and median luminal centerline approaches were implemented as new measurement methods. Fundamental point was based on principle of calculation midpoints of each vessel cross sections. These midpoints generated a middle path line which was passing through the middle of the vein, when three-dimensional model of veins was constructed. The middle path line was named as median luminal centerline path (MLCP) or centerline path. With this approach, different measurement problems were eliminated. Aortic neck angle measurement and actual vessel length measurement are main problems. In order to solve aortic neck angle measurement problem, experts can measure vessel aortic angle measurement with perspective sense while selecting 3 points over the MCLP. For solving actual vessel length measurement problem, experts can automatically calculate accurate vessel length by selecting two points over the MCLP. Furthermore, measurement process can be performed manually by using delta distance calculation. The other measurement method presented in this study is vessel diameter calculation. The largest diameter of the vessel can be calculated automatically from intended vessel cross-section. Experts can easily make aneurysm stent graft planning with these developed new measurement methods.

Final contribution of the thesis is a new approach for surface construction in tubular structures. For obtaining artery structures, region-growing segmentation method was used. At the end of the segmentation process, data obtained from different sections were presented at three dimensional platforms which are more

comprehensible for users. Two dimensional segmented images at different cross-sections must be united with each other to construct three-dimensional model. One of the most important problems of three-dimensional modeling is surface construction. To solve this problem, polygon and triangular structures must be gathered from related cross-sections to represent in computer graphic application. Different surface construction methods are available. The most widely known and used method is marching cube algorithm. Different object surfaces can be covered with this algorithm. A different solution method was presented to cover surface of tubular structures with this study. This solution method is only convenient for tubular structures. By using the method, surface construction can be done fast and easily.

1.4 Purpose and the Scope

In this study, an interface has been designed to model aorta aneurysm and gathered required measurements for appropriate stent in applied radiology. Stent selection process was shortened and platform specific software dependency was removed. As a result of this study, a specialized aneurysm evaluation and computation tool has been developed for aorta. During the study, the computer graphics primitive techniques, the transform of original data to computer graphic primitives, image segmentation methods, surface construction algorithms are studied.

The planning of endovascular repair of AAA puts greater requirements on preoperative imaging because it must provide accurate information on the morphological structure and quantitative dimensions of the arterial segments involved.

With this study, it is aimed that;
- ❖ To improve the understandability of the data and to facilitate processing of data (CT images) by using data visualization.
- ❖ Giving chance to experts who make preoperative endovascular planning to make measurement with a sense of perspective
- ❖ Allowing the expert mouse interaction for selection of reference points to make measurement on the 3D model

❖ Changing view of the camera / perspective with user interaction

❖ Minimizing measurement errors due to change of perspective

Currently used methods in medical services, aortic measurements are mostly manual; conventional methods of evaluation need repetition and inconsistent and time consuming. The medical application platform implemented in this study aims to focus on solutions to overcome these difficulties. The developed medical application platform targets flexible, repeatable, accurate fast and reliable measurement capabilities and might perform an important role for pre-procedural evaluation of EVAR.

1.5 Thesis Organization

The rest of the thesis is organized as follows.

Chapter 2 presents Abdominal Aortic Aneurism and related work. Initially, preliminaries knowledge and basic concepts of AAA are presented. Then, the stent graft planning process is introduced. Anatomical criteria and anatomical factors to select appropriate stent are summarized. Finally, some commercial and open source solutions are investigated and thoroughly compared.

Chapter 3 includes the basics of medical modeling steps. Data information flow for 3D applications can be grouped in three titles (Digital Image Acquisition, Data Processing, and data modeling). In this chapter, these steps are detailed.

In Chapter 4, used methods are explained. Several digital imaging methods are used to construct AMET. Some existing methods are used and some new solutions are developed during the thesis. These methods constitute the main body of the AMET. In this chapter segmentation, edge detection, middle center line path, and surface construction methods are examined.

The capabilities and usage of the tool is explained in Chapter 5. The developed tool consists of different modules. Aim of these modules and software architecture are explained in detail. Also, this chapter includes graphic rendering process of the

tool. Main objective of the developed tool made measurements over a 3D model of the aorta. Measurement principles are explained in this chapter. Finally, general menu elements and the usage of the software are discussed.

AMET provides broader measurement capabilities to the physicians. Some measurements are made to prove the AMET reliability, consistency, and accuracy by the physicians. In chapter 6 these statistical results are presented and their results are explained.

In Chapter 7, the conclusions are introduced; the chapter presents the key contributions and fundamental findings of this thesis. Finally, the possible avenue of further research is addressed based on this work.

CHAPTER TWO
ABDOMINAL AORTIC ANEURYSM and RELATED WORK

2.1 Abdominal Aortic Aneurysm

An aneurysm is an area of a localized widening (dilation) of a blood vessel. (The word *aneurysm* is borrowed from the Greek *aneurysma* meaning "a widening"). Abdominal Aortic Aneurysms (AAA) occurs if there is a weak section on the wall of main vessel (Aorta) that supplies blood from the heart to the rest of the body (Kato, & et al., 1999). Vessel pressure of the blood beats against the weakened wall then weak area expands or bulges like a balloon. There is a life-threatening danger because it can burst or rupture if the balloon exceeds safety limits. Aneurysms can occur anywhere in the aorta. Generally, AAA occurs in the portion of the vessel below the renal artery origins. The aneurysm may extend through the vessels supplying the hips and pelvis.
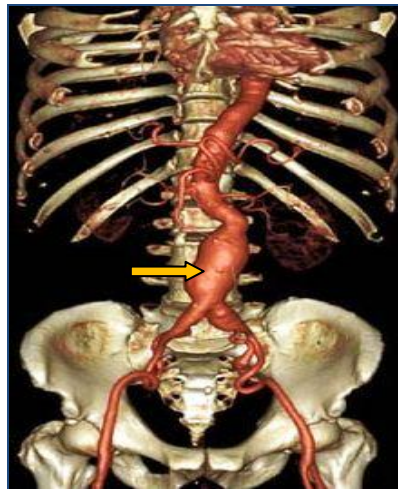

Figure 2.1 Patient who suffers from abdominal aortic aneurysm, arrow show dilation area which is so called aneurysm.

2.2 Detection of Aneurysm and Treatment

An abdominal aortic aneurysm is usually diagnosed by a physical exam, abdominal ultrasound, Computer Tomography (CT), Magnetic Resonance Imaging (MRI) or arteriography. Ultrasonography is used for the initial diagnosis of AAA. It's used to screen aneurysms and determine the size. On the other hand, MRI and angiography methods rarely use for visualization of the aneurysm. Currently, CT has been accepted as a gold standard in diagnosis of AAA process. CT scan has more sensitivity for aneurysm. CT is useful in preoperative planning and detailing the anatomy for endovascular repair. CT provides comprehensive measurement capabilities. Diameter measurements of the proximal aortic neck, aneurysm size, distance to aortic bifurcation and proximal aortic length are easily obtained with CT (Gravereaux, & et al., 2001; Bertges, & et al., 2003).

There are two well known treatment methods to cure the abdominal aortic aneurysms (Brewster, & et al., 2003). First one is the open surgery aneurysm repair. In open surgery aneurysm repair, surgeons make an incision in abdomen and replace the weakened region of the aorta with a tube-like replacement. This tube like replacement is called the aortic graft which has the size and shape of the healthy aorta. Open Surgery treatment method increase the risk of major operative complications. Also it's invasive and costly method. Patients requires at least 5-6 days of hospitalization.

Nowadays, the other method, endovascular stent graft repair / endovascular aneurysm repair (EVAR) is a fairly popular method since it is less invasive (Treiman, & Bernhard, 1998; Marin, & et al., 1998). Endovascular stent graft is used to strengthen the weakened wall of the vessel to prevent adverse events in aorta. An implant is placed inside the weakened part of the aorta to separate the aneurysm from the normal blood flow. The implant is composed of most commonly woven Dacron and supported by a rigid structure, usually metal. This structure is called a stent. Stent selection is a major difficulty of the method due to less visual feedbacks (Blum, & et al., 1997). The stent must have the same properties with the part of aorta where aneurysm occurs such as length and diameter. As a result, endovascular stent graft

repair method requires knowledge of aortic shape and accurate measurements to choose appropriate stent shape and size (Cuypers, Laheij, & Buth, 2000). EVAR has became increasingly accepted by physicians because of

- ✓ minimally invasive surgical procedure
- ✓ reduction in length of hospital stay (2 – 3 days)
- ✓ decrease the risk of major operative complications
- ✓ postoperative recovery time

EVAR has different qualification compared to open surgery method (García-Madrid, & et al., 2004). It is clear that currently reported experience shows EVAR has important potential advantages against surgical repair for AAA (Ham, & et al., 2005; Cao, & et al., 2002; Malina, & et al., 1997). Some morphological structures of the aneurysm must be measured over the images to perform EVAR operation successfully.

2.2.1 Stent Graft Planning

Selection of the appropriate stent – graft length and diameter is the most important factor to minimize complications after endovascular repair of AAA. Thus the planning of endovascular repair puts greater requirements on preoperative imaging. Physicians must be work with images to plan endovascular grafting. Exact morphological information must be determined to planning of endovascular repair (Resch, & et al., 1999; Chaikof, & et al., 2002). The planning of endovascular repair must provide accurate measurements for aneurysm. If these requirements are not provided, undesirable result may occur after endovascular grafting for AAA. Figure 2.2 illustrates all measurements during endovascular repair planning. Table 2.1 clarifies the all measurement definitions and unit for the aortic aneurysm. Commonly used anatomical criteria to select the type of the graft to use can be summarized as follows (Cheng, 2010; Stanley, & et al., 2001);

- ❖ Length of the aortic neck
- ❖ Aortic neck diameter
- ❖ supra-renal and infra-renal angle (neck angulation)

❖ between the lowermost renal artery and the aortic bifurcation length

❖ length of each iliac segment

❖ diameter of each iliac segment

Aorta anatomy is easy to understand practically, nevertheless, it is difficult to identify and measure quantitatively. Certain anatomical features should be carefully evaluated and measured before endovascular grafting. Length of the aortic neck (**L1**) is defined as the distance from the lower renal artery to the start of the aneurysm. The diameter of the aortic neck diameter (**Φ1a**) is calculated on the orthogonal cross sections of the neck. Aorta can be segmented in three parts. The first part is the aorta above the renal arteries, the second part is aortic neck and the last part is the aneurysm. These three parts create two angles. These are supra-renal angle (**α**) and infra-renal angle (**β**). Supra – renal angle is the angle between proximal AAA neck and supra-renal aortic axis. Infra – renal angle is the angle between proximal AAA neck and main axis of AAA. Aortic length is the length between the lowermost renal artery and the aortic bifurcation (**L2**). Iliac length is the length of right or left iliac segment (**L3r or L3l**). The sum of two lengths gives total stent length (**L2 + L3r or L2 + L3l**). Diameter of the iliac segment is measured to make sure that access can be obtained with the device (the implant is introduced from the femoral artery to aortic part of the aorta using a catheter delivery system).
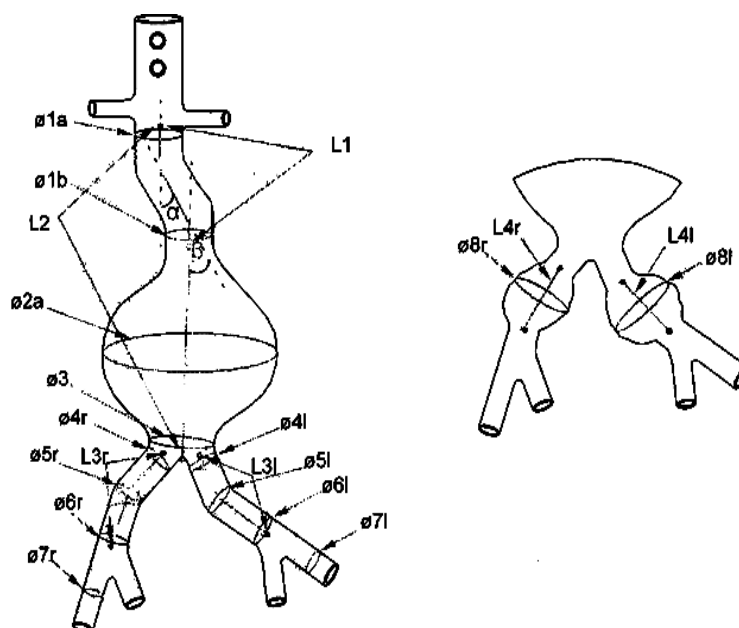
Figure 2.2 Measurements made when endovascular repair planning

Table 2.1 Measurement definitions and units

Measurement	Description	Position	Unit
α Angle	Angle between proximal AAA neck and supra-renal aortic axis (Supra – Renal Angle)		In degrees
β Angle	Angle between proximal AAA neck and main axis of AAA (Infra – Renal Angle)		In degrees
Φ1a Diameter	Proximal non-aneurysm aortic neck diameter, immediately below lowest renal		In millimeters
Φ1b Diameter	Distal non-aneurysm aortic neck diameter, immediately above aneurysm		In millimeters
Φ2a Diameter	Maximum diameter of aneurysm		In millimeters
Φ3 Diameter	Distal diameter of aorta/aneurysm above aortic bifurcation		In millimeters
Φ4r Diameter	Proximal diameter of non-aneurysm aortic neck of right iliac artery		In millimeters
Φ5r Diameter	Diameter of non-aneurysm neck of right iliac artery		In millimeters
Φ6r Diameter	Distal diameter of non-aneurysm neck of right iliac artery		In millimeters

Table 2.1 Measurement definitions and units (continued)

Measurement	Description	Position	Unit
Φ7r Diameter	Diameter of access vessels, right femoral artery		In millimeters
Φ4l Diameter	Proximal diameter of non-aneurysm aortic neck of left iliac artery		In millimeters
Φ5l Diameter	Diameter of non-aneurysm neck of left iliac artery		In millimeters
Φ6l Diameter	Distal diameter of non-aneurysm neck of left iliac artery		In millimeters
Φ7l Diameter	Diameter of access vessels, left femoral artery		In millimeters
L1 Length	Length of non-aneurismal aortic neck		In millimeters
L2 Length	Length from lowest renal artery to aortic bifurcation		In millimeters
L3r Length	Length of portion of right iliac from bifurcation to end of seal zone		In millimeters
L3l Length	Length of portion of left iliac from bifurcation to end of seal zone		In millimeters
Φ8r Diameter	Diameter of right iliac aneurysm		In millimeters
Φ8l Diameter	Diameter of left iliac aneurysm		In millimeters
L8r Length	Length of right iliac aneurysm		In millimeters
L8l Length	Length of left iliac aneurysm		In millimeters

These measurements are very important role to achieve suitable placement of the stent.

2.3 Related works: Aorta Evaluation Tools

Generally, CT and MRI data interpreted and analyzed as individual 2-D image slices. Two dimensional measurements of CT data have potentially critical measurement errors. On the other hand, the numbers of images per scan have increased while imaging technology has developed. Consequently, evaluation and decision making process have became more difficult for the specialists. Different image processing and several imaging modalities accelerate 3 − dimensional modeling in medical area. Nowadays, 3-D computer visualization and evaluation have played a major role in medical imaging and evaluation (Stytz, & Frieder, 1991).

The 3D visualization of Aorta is generated with sequence of CT cuts. Volumetric analysis of CT scans has been proposed as a more accurate method for planning endovascular repair. 3D model contains all types of body organs such as bones, lives and vessels. The needed part to analyze the aneurysm is only the abdominal aorta. Specialists use the software to clear the unwanted part from the model. But this process is very time consuming and result is sometimes not usable.

Commercial and open source solutions exist for endograft planning. In this section, Materialise Mimics (Linninger, & et al., 2005), M2S Preview, Vital Vascular Imaging, TeraRecon Endograft Planning (Lee, 2010), MITK (Zhao, & et al., 2005), OsiriX (Rosset, Spadola, & Ratib, 2004), DCMTK (Eichelberg, & et al., 2004) and Slicer (Wolf, & et al., 2005) software packages will be investigated and compared with our evaluation and measurement tool.

2.3.1 Mimics

Mimics software solution is one of the commercial products. It was developed in Belgium. It works on Microsoft windows platform. Mimics software has been in use for fifteen years. It is used for biomedical research and development from scanner data. Mimics helped the specialist to visualize and measure AAA. This software

package is not only used for AAA, but it is also used for wide variety of medical applications such as brain, surgical simulation etc. Software package provides to process and edit 2D images data. 3D model of the intended part of the body is constructed by using these 2D data. It has powerful segmentation tools and measurement capabilities over the 3D model.

Mimics has rapid reconstruction methods and user − friendly measurement tools to evaluate the AAA's morphology in details. The software allows specialists to calculate important EVAR parameters such as length, distance, angles, diameters and degree of curvature. The measurements can be calculated on 2D images or directly on the 3D model. These parameters help to specialists in examining and choosing the correct stent − graft. Stent specific planning can be materialized by using mimics centerline tool. Mimics has high graphical quality on 3D model. Because, it has REMESH module which it target to reduce the amounts of triangles. This module improves the quality of triangles while generating the 3D model.

a   **b**
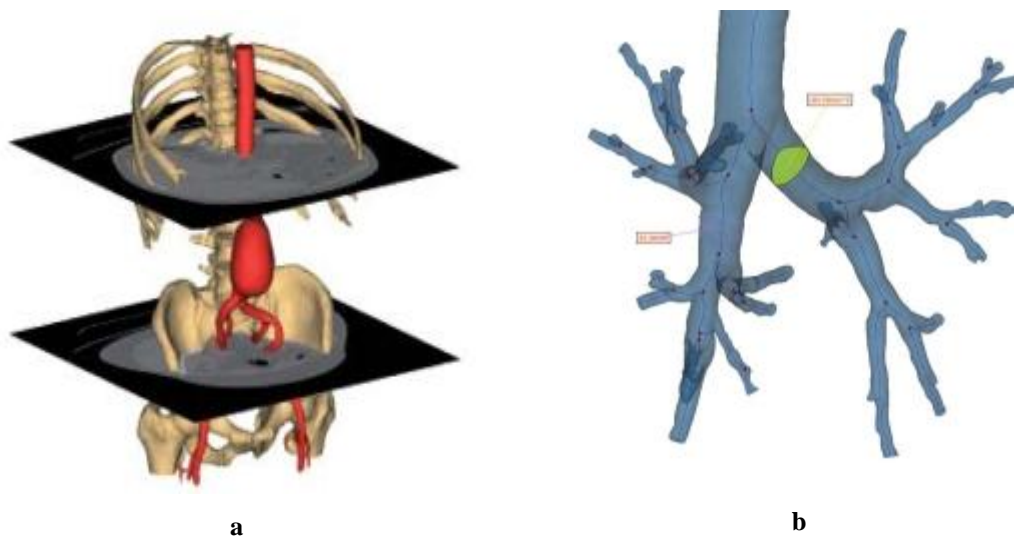
Figure 2.2 (a)Mimics Software Package(EVAR Tool) (b) A Sample view from AAA Measurement

When the Mimics software is examined according to these knowledge following results can be listed;

❖ It is platform dependent software
❖ It is commercial application

❖ It has not manipulation capabilities because it's a commercial product.

❖ High measurement capabilities

❖ Rich graphical quality

❖ It has special tool for AAA

2.3.2 M2S

Another commercial product is M2S founded in 1997. It works on windows platform. M2S specializes in data and image management services in New Hampshire. This product is used for clinical trials image management, medical registries, and advanced radiological image analysis.

M2S provides a comprehensive offering of core laboratory services for clinical trials. M2S presents medical and technical expertise with a secure and efficient electronic delivery system. This product offers broad spectrum of image management services. It works with a special project management teams for all services. Expertise areas of M2S are on mammography, angiography, spine radiology, nuclear medicine, endovascular surgery, etc…

M2S provides advanced imaging analysis including 3D modeling, tumor volumes and device migration. M2S services include 2D and 3D viewing, extensive measurement tools (including diameter, length, volumes and angles) for endovascular treatment planning. It has sophisticated measurement tools and advanced 3D computer models for aortic aneurysm. Besides, it provides virtual graft simulation with all AAA grafts available in United States.

According to these M2S knowledge, following properties can be summarized.

❖ This service is platform dependent.

❖ Commercial application (service based application)

❖ Not manipulation capabilities.

❖ It provides virtual stent graft simulation.

- ❖ Interactive measurement tools, including diameter, length, volumes and angles
- ❖ Rich graphical quality (3D modeling and reconstruction)
- ❖ Has special tool for only AAA
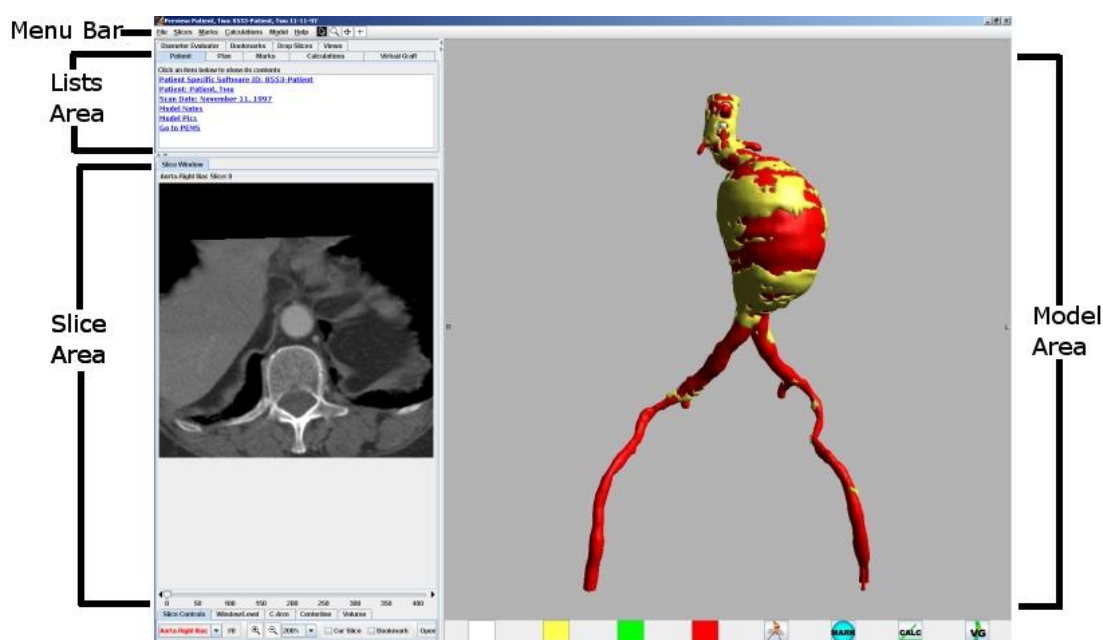
Figure 2.3 A Snapshots of M2S EVAR Solution Tool

2.3.3 Vitrea Enterprise Suite

Vitrea Enterprise Suite is another commercial product for AAA. Vitrea Enterprise Suite package provides advanced visualization tools, clinical applications, and data management systems, backed by their professional services. This solution integrated with PACS, Web and client technologies. This software has been developed for twenty years. The company's software enables the visualization and analysis of 2D and 3D images of anatomy and physiological function using CT and MR scan data. Vitrea package includes comprehensive clinical imaging solutions for; cardiac, neuro, vascular, oncologic, virtual colon and orthopedic.

Vitrea Enterprise Suite consists of two main parts. These are vital image management system (VIMS) and vital image medical imaging software (VMIS).

VIMS is a centralized server that takes huge amount of image data. This server designed for clinical applications, data management and storage management architectural principles. VIMS provide flexible access to 3D information from advanced visualization workstations, a PACS workstation, or through a Web browser.

VMIS installed on a state-of-the art, high performance Windows workstation, provides a sophisticated volume-rendering software solution. With VMIS, the following tasks can be quickly and easily accomplished: Communication with configured DICOM devices to retrieve and export patient data, Preview images by using the 2D Study Viewer feature, Adjust visualization parameters to enhance images, Measure regions of interest, Locating and observing points of interest, using 2D and 3D images, Trim with 3D and 2D segmentation to focus images on regions of interest, Fly-through or around anatomical images.

Vitrea has specialized vascular imaging tools to evaluate the AAA's morphology in details. This Vitrea comprehensive suite provides confident evaluations of CT and MR angiography studies for identification, characterization and interventional planning for vascular diseases. Specialist can effectively assess vessels and communicate results and images with clinical impact. Vital medical imaging software assesses and segments vessels remove bones, measures aneurysm and evaluate vessels. Automated Vessel Measurement feature of the vitrea solution evaluate vessels for stent placement regardless of size, tortuosity or location.

According to this Vitrea Enterprise Suite knowledge, following properties can be summarized.

- ❖ This service is platform dependent.
- ❖ Commercial application (service based application)
- ❖ Not manipulation capabilities.
- ❖ It is not provide virtual stent graft simulation.
- ❖ Interactive measurement tools, including diameter, length, volumes and angles

- ❖ Rich graphical quality (3D modeling and reconstruction)
- ❖ Special tool for Abdominal Aortic Aneurysm

2.3.4 TeraRecon

TerraRecon Company (founded in 1997) develops markets and supports systems and subsystems for professional imaging applications. TeraRecon technology solutions provide advanced 3D imaging systems for medical and industrial applications. These solutions are designed to advance the performance, quality, functionality, and integration of image processing and 3D visualization systems. (Medical, geophysical, industrial, and scientist markets) TerraRecon has been developed in a special computer framework that are used in its real-time diagnostic workstations, network – attached streaming servers, high performance reconstruction engines and real – time volume rendering hardware engines.

TerraRecon provides advanced 3D visualization techniques and image processing techniques. It has been specialized for vascular imaging tools to evaluate the AAA's morphology in details. This solution provides confident evaluations of aneurysm for planning of vascular diseases. Specialist can effectively assess vessels and measures aneurysm.

- ❖ This software solution is platform dependent.
- ❖ Commercial application (service based application)
- ❖ Not manipulation capabilities.
- ❖ It is not provide virtual stent graft simulation.
- ❖ Interactive measurement tools, including diameter, length, volumes and angles
- ❖ Rich graphical quality (3D modeling and reconstruction)
- ❖ Special tool for Abdominal Aortic Aneurysm

2.3.5 Slicer

Slicer is a free, open source software application for computer science and clinical researchers. Slicer project initiated in 1998 and supported several funding source.

This package suited for modular extension by software developers. 3D slicer is a software application written in C++. It is available on multiple platforms, including Linux, Mac and Windows. Slicer based on NA-MIC kit that includes The Visualization Toolkit (VTK), Segmentation & Registration Toolkit (ITK), Cmake, cross-platform and open-license GUI Toolkit (KWW) and TK/TCL. Slicer has a workflow engine to allow developers to introduce user – guidance into workflow. Slicer executables and source code are available under a BSD – style, free open source licensing agreement.

Slicer provides a graphical user interface to interact with the medical data. The platform provides functionality for segmentation, registration and 3D visualization for medical images data. It supports standard image file formats and the application integrates interface capabilities to biomedical research software.

The 3D Slicer package includes tools of analysis for Computed Tomography (CT) and MR. It has already been used for brain mapping, image guided surgery, virtual colonoscopy, and other biomedical research. Slicer provides advanced imaging analysis for 3D modeling and tumor volumes. It provides extensive measurement tools (including diameter, length, volumes and angles) for endovascular treatment planning. However, this software package is not specialized for abdominal aortic aneurysm.

- ❖ This software solution is platform independent.
- ❖ Open source application
- ❖ Have manipulation capabilities.
- ❖ It is not provide virtual stent graft simulation.
- ❖ Interactive measurement tools, including diameter, length, volumes and angles
- ❖ Rich graphical quality (3D modeling and reconstruction)
- ❖ Not special tool for Abdominal Aortic Aneurysm

2.3.6 Mitk

Medical Imaging Toolkit (MITK) is an open source C++ library for integrated medical image processing and analyzing software package. It is available on Windows 32bit and 64bit systems. It has been developed by Medical Image Processing Group. The image processing group started the research and development of the 3D medical image processing and analyzing system in 1996. MITK medical solutions based on the open source software VTK and ITK. Its main purpose is to provide medical image framework to combine the function of medical image segmentation, registration and visualization. MITK is free software and can be used freely in research and education purpose. MITK provides flexible and extensible framework, surface reconstruction (enhanced marching cube algorithm), various segmentation algorithms, various registration algorithms, surface rendering and volume rendering and 3D interaction. MITK is released under an open-BSD-style license. It is available for commercial or non-commercial use. MITK offer support and solutions for the different medical applications

- ❖ This software solution is platform dependent.
- ❖ Open source application
- ❖ Have manipulation capabilities.
- ❖ It is not provide virtual stent graft simulation.
- ❖ Interactive measurement tools, including diameter, length, volumes and angles
- ❖ Rich graphical quality (3D modeling and reconstruction)
- ❖ Special tool for Abdominal Aortic Aneurysm

2.3.7 Osirix

OsiriX has been designed an image processing software for navigation and visualization of multimodality and multidimensional images. OsiriX is distributed freely as open − source software under the GNU licensing. The 3D viewer offers multiplanar reconstruction, surface rendering, volume rendering and intensity projection. It has been used in medical research (radiology, nuclear imaging, and molecular imaging). It is fully compatible with the DICOM standard. It provides a

complete plug-ins architecture that allows developers to expand the capabilities of OsiriX. This software is developed on Macintosh platform under the MacOs X operating system. OsiriX is available in 32-bit and 64-bit format. It offers fast and optimized 3D graphic capabilities of the Open GL library. It has advanced user − interface design for the specific and complex tasks. It has a flexible modular structure for very specific purposes. The processing and image rendering tools are based on the open source libraries ITK and VTK. OsiriX has many features such as; read and display all DICOM files, customizable toolbars, 3D post processing, volume rendering, surface rendering, graphic board accelerated, available in 32-bit and 64- bit.

- ❖ This software solution is platform dependent. (MacOS X)
- ❖ Open source application
- ❖ Have manipulation capabilities.
- ❖ It is not provide virtual stent graft simulation.
- ❖ Interactive measurement tools, including diameter, length, volumes and angles
- ❖ Rich graphical quality (3D modeling and reconstruction)
- ❖ Not special tool for Abdominal Aortic Aneurysm

2.4 Evaluation and Comparison of the Known Tools

In this section, the commercial and open source software were examined and the general features are summarized. Table 2.1 summarizes the properties of the most popular software solutions for Abdominal Aortic Aneurysm repair. The features are classified 10 different categories and listed according to the general characteristics. These categories are platform dependency, application type(commercial / open source), type (product / service based), manipulation capabilities, measurement capabilities, graphical quality, virtual stent simulation, specialized tool, middle center line path approach, and language support. According to these general features of the programs (shortcomings and special features in the programs taking into consideration) a new software solution will be created for the abdominal aortic aneurysm.

Table 2.1 Properties of the most popular software solutions

	Mimics	M2S	Vitrea Enterprise Suite	TeraRecon	Slicer	MITK	OsiriX
Platform	Windows	Windows	Windows	Windows	Linux, MacOsX, Windows	Windows	MacOs X
Application Type	Commercial	Commercial	Commercial	Commercial	Open Source	Open Source	Open Source
Type	Product	Product	Service	Service	-	-	-
Manipulation Capabilities	Not applicable	Not applicable	Not applicable	Not applicable	Applicable	Applicable	Applicable
Measurement Capabilities	Interactive	Interactive	Interactive	Interactive	Interactive	Interactive	Interactive
Graphical Quality	rich	middle	rich	rich	rich	middle	rich
Virtual Stent Simulation	provide	provide	not provide	not provide	not provide	not provide	not provide
Specialization for AAA	Specific	Specific	Specific	Specific	Not Specific	Not Specific	Not Specific
Middle Path	Used	-	-	Used	-	-	-
Language Support	Multi lang.	Eng.	Multi lang.	Multi lang.	Eng.	Eng.	Eng.

THREE – DIMENSIONAL MEDICAL MODELING

Recent developments in computing technologies (both hardware and software) have helped the advancement of 3D modeling in medical applications (Bernardini, & Rushmeier, 2000; Bernardini, & Rushmeier, 2002). Medical modeling steps are acquisition of medical scan data, transfer and translation of data formats, processing medical data (methods of utilizing the data) and finally using the information to obtain physical 3D models, by using medical computer graphic techniques (Remondino, 2006). Figure 3.1 depicts data information flow for 3D medical applications.
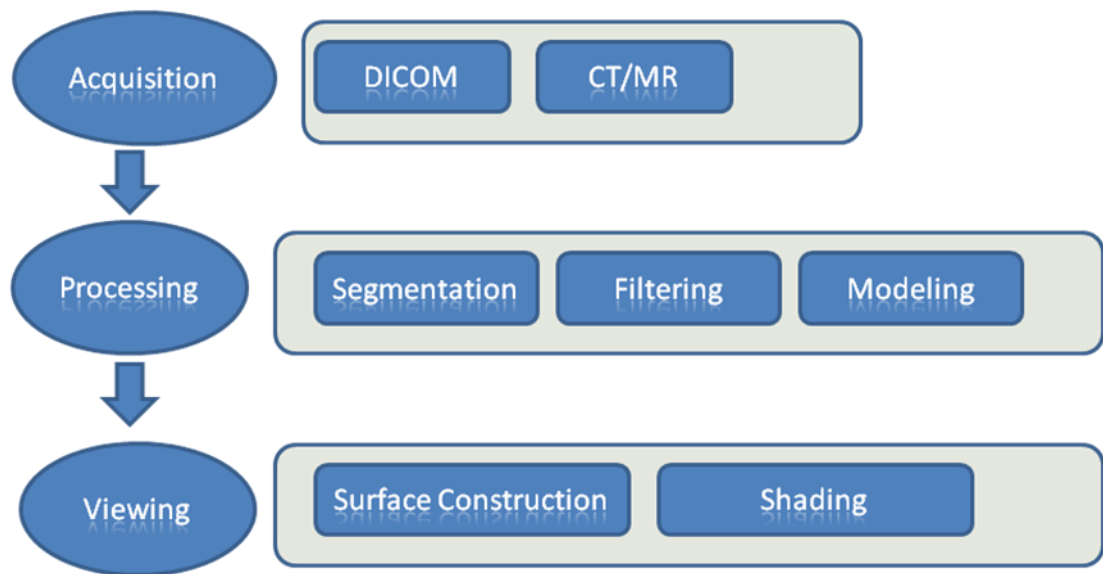
Figure 3.1 Information Flow for 3D Medical Application

3.1 Digital Image Acquisition

Data acquisition is the process of sampling physical conditions and conversion of the resulting samples into digital numeric values that can be manipulated by a computer (Aach, & et al., 1999). Patient diagnostic data are collected by hospitals that have many different digital acquisition units. These data include laboratory tests

results, digital image acquisition, etc. In each case, a specialized hardware is responsible for collecting the data and software system used for capturing, storing and managing the data.

Different image modalities are used to collect digital image data. The primary imaging modalities (CT, MRI, etc.) used in different application. Each modality has its own advantages and limitations. These modalities generate a series of 2D slice of images. Stored radiological studies are in conformance with the digital imaging and communication in medicine (DICOM) standard.

3.1.1 Dicom

DICOM is a standard in medical imaging. This standard has been developed with an emphasis on diagnostic medical imaging as practiced in radiology, cardiology and related disciplines. However, it is also applicable to a wide range of image and non-image related with information exchanged in clinical and other medical environments. DICOM file stores, handles, prints and transmits information in medical imaging. It includes a file format definition and a network communications protocol. Stored data describes the image plane and the pixels features such as, values for mapping the image to color or gray scales, overlay planes, and the other specific features (Mustra, Delac, & Grgic, 2008).

Figure 3.2 Example of a single DICOM Image of abdomen

DICOM Standard supports different types of images for different medical applications. A single dicom image is shown in figure 3.2. A single DICOM file contains: A header (which stores information about the patient's name, the type of scan, image dimensions, etc) and image data (in compressed (bitmap) or uncompressed form). Dicom header describes the image dimensions and stores other text information about the scan. Header size depends on scan configuration. Bit depth and compression applied to the image is explained in the header of the image.
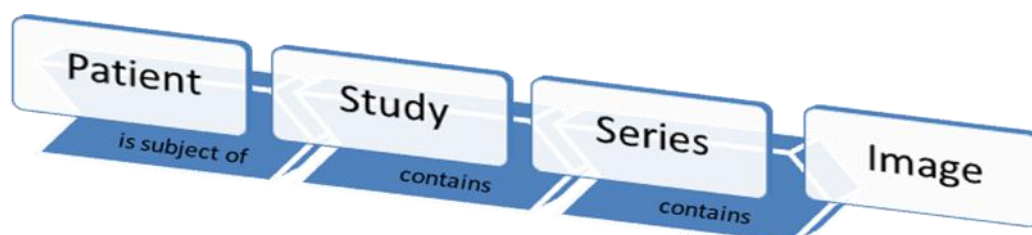
Figure 3.3 The DICOM Information Model

Figure 3.3 illustrates the dicom information model. The patient entity and Study entity contain data about the patient and examination (description, age, name, etc.). Series entity contains a set of images. Series insures the relationship of images and stores information about the imaging modality. Finally image data is stored. DICOM is a binary file, which means that an ASCII-character-based text editor like Notepad does not show it properly. A DICOM file may be encoded in Little Endian or Big Endian byte orders. A lot of special attributes are stored in a dicom file (Riddle & Pickens, 2005). These DICOM attributes are accessed via some special tag. Dicom tags give useful information in a human-readable form (the size of the image, the position of the patient, study date, modality, slice thickness, number of frames, the offset to the pixel data, and so on)

In this study, sample set of CTA images of patients was provided by Dokuz Eylül University, Faculty of Medicine, and Interventional Radiology Department. Study sample data of CTA images of patients is gathered in DICOM image format. Image data are acquired in 1-3 millimeter thick sections from a CT. A series of DICOM images consists of several axial intersections of patient body; series contents vary

from patient to patient. For instance, patient's series data contains 320 single dicom images or maybe 330. Single dicom image example is depicted in Figure 3.1. Each image contains many data such as bones, liver, aorta ...etc. Data relevant to intended part of the body must be extracted from each image of those series. The image needs to be segmented to region of interest that is easier to process. This process is called segmentation. Segmentation plays a major role in the study. The Hounsfield scale is a quantitative scale for describing radio-density. DICOM image is made up of thousands of tiny pixels. Each pixel has a computed tomography number which measured by Hounsfield unit (HU). HU is a measure of how much x-ray beam is absorbed by the tissue at each point in the body. The pixel value is indicated on a scale from -1000 to +1000 on the Hounsfield scale. Figure 3.4 shows Hounsfield scale for some objects. The Hounsfield number of a tissue varies according to the density of the tissue (Hounsfield, 1980).

air		fat	water	muscle		bone
-1000		--120	-0	-+40		+1000
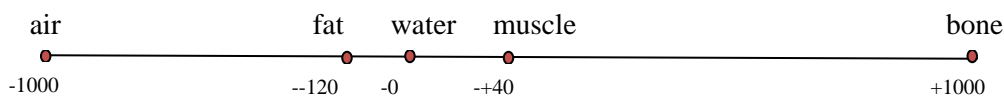
Figure 3.4 Hounsfiled Numbers of Various Tissues

HU values are stored in the DICOM file. Image segmentation can be performed by using this value.

3.2 Data Processing

Data visualization and inspection of anatomic structures are important in medical applications for diagnosis and analysis of anatomical data. Data visualization aims three important goals (Penninga, 2005; Lakare, 2000).

1) Improvement in speed, quality and dimensionality of the object
2) Improved access to the data through interactively
3) Enhance intuitive manipulation and measurement capabilities for the object.

Computer based tools allow physicians to understand and diagnose anatomical structures by virtually interacting with them. One of the important prerequisite for visualization is the availability of segmentation methods that identify and classify interesting features in the data set. Segmentation plays a critical role which is used to extract of the anatomical organ or region-of-interest. The anatomical structure or the region of interest needs to be delineated and separated out so that it can be viewed individually. This technique is known as image segmentation. This step is the processing part of the 3D information flow.

3.3 Segmantation

Medical Image Segmentation has been an important problem for image analysis (Pal 1993; Morse, 2000; Zitova, 2003). Segmentation is used to separate regions from the rest of the image. This process simplifies the image to the more meaningful object. It can be used for identifying anatomical areas of interest for diagnosis and treatment. Also, it can be used preprocessing for registration, analysis, surface extraction, visualization, simulation, etc. The main goal of medical image segmentation is to split up an image into several disjoint regions (Shi, & Malik, 2000). Given an image I the complete segmentation problem is to determine a set of K disjoint regions $R_1, R_2, \ldots, R_{K-1}$ such that

$$I = \bigcup_{i=1}^{K} R_i \qquad R_i \cap R_j = 0 \quad for\, i \neq j \qquad\qquad (1)$$

These regions correspond to whole or part of the object. In medical applications, the interested region is usually a distinct anatomical structure (liver, bone, kidney, vessel, etc.). Many segmentation techniques/algorithms have been developed by the researchers. Segmentation algorithms vary depending on the problem. Image modality and features of the anatomical structure to be segmented determine segmentation algorithm which is suitable. Selection of an appropriate algorithm may be caused a dilemma. Therefore, selection of appropriate segmentation algorithm is the most important step for the digital imaging applications. On the other hand,

segmentation algorithms can be affected by the general imaging artifacts such as motion, noise etc.

If the shape information is known, special algorithms can be applied to find certain object. Segmentation algorithms require some user interaction over the image. All segmentation algorithms keep interaction as little as possible. Graphical interface or visualization system can be very effective tool for exploring the parameters of a segmentation algorithm. In the following section, some common image segmentation techniques are reviewed.

3.3.1 Thresholding

The simplest technique to identify an object is gray – level thresholding (Weszka, Nagel, & Rosenfeld, 1974; Sahoo, Soltani, & Wong, 1988). Relevant objects in an image can be identified with intensity values. Thresholding based on intensity values. This technique uses a single threshold value; pixels above the threshold are object pixels (region of interest) and pixels below the threshold are background pixels.

Threshold value can be chosen manually or automatically. Automatic methods for threshold detection based on image histograms. Image histogram is generated by using the intensity values of each pixel. Generally,

$$g(x,y) = \begin{cases} 1 & for\ I(x,y) \in D_1 \\ 2 & for\ I(x,y) \in D_2 \\ \dots \\ n & for\ I(x,y) \in D_n \\ 0 & else \end{cases} \tag{2}$$

with a gray-level set D_i for each class, and $I(x,y) \in D_i$,

D_i refers to gray-level set,

$I(x,y)$ refers to set of regions delimited by upper and lower thresholds,

x refers to lower threshold value,

y refers to upper threshold value.

Equation 2 applies to all global thresholding algorithms. Thresholding algorithms can be classified into the six categories:

i)   Histogram shape based methods

ii) Clustering based thresholding methods

iii) Entropy based thresholding methods

iv) Thresholding based

v)   Spatial Thresholding

vi) Local adaptive methods

3.3.2 Edge Based

Edge based image segmentation methods use boundary information to split an image into regions (Pavlidis, & Liow, 1990). Very common algorithm is the Canny Edge detection (Canny, 1986). Also, another very common is the Marr-Hildreth (Smith, & et al., 1988) or Laplacian-of-Gaussian (LoG) algorithm (Sotak, & Boyer, 1989). Images resulted from edge detection cannot be used as a segmentation result. Edges have to be linked into chains which correspond better with boundaries in an image. Once the links are established, sets of linked pixels can be using as borders. The main idea of the edge based methods is to connect edges to produce object contours. There are four approaches for edge based segmentation. These are;

Thresholding with hysteresis: Firstly, the idea identifies definite edge pixels. Then, "two" values are compared for possibility pixels. If the restriction is provided, it is labeled as edge pixel.

$$t(0) \geq \begin{cases} \left|\left|\nabla f(x,y)\right|\right| \geq t(1) & \text{definitely an edge} \\ \left|\left|\nabla f(x,y)\right|\right| < t(1) & \text{maybe an edge, depends on context} \\ \left|\left|\nabla f(x,y)\right|\right| < t(0) & \text{definitely not an edge} \end{cases} \quad \textbf{(3)}$$

Edge relaxation: edge relaxation methods similar to thresholding with hysteresis. Following pseudo code shows iterative algorithms of the edge relaxation.

```
1. Evaluate initial confidence c(1)(e) for all crack edges
   (edges located between two pixels) in an image
2. Find the edge type of each edge based on the edge
   confidences c(k)(e) in its neighborhood
3. Update the confidence c(k+1)(e) according to its type
   and to its previous confidence c(k)(e)
4. Stop if all confidences have converged to either 0 or
   1. Repeat steps 2 and 3 otherwise
```

Edge linking: border tracing: This approach link adjacent edge pixels by seeing if they have similar properties.

Fitting: the Hough transform: the last approach for edge based segmentation is fitting. The Hough transform is useful for grouping isolated edge points into image structures (patterns, models). Edges to be grouped are not necessarily adjacent, connected or close.

3.3.3 Region Based

Region growing algorithm has proven to be very effective approach for image segmentation (Horowitz, & Pavlidis, 1974; Stewart, Fermin, & Opper, 2002). Region based approaches extract regions that satisfy a homogeneity criterion like gray level, color, texture, shape, spatial location and any more. One starts with one or more midpoints, and applies an iterative algorithm. Firstly all neighbors around the border are evaluated whether they satisfy the homogeneity criteria and, if they do, they are added to the region. The regions are iteratively grown by comparing all unallocated neighboring pixels to the region. Iterations continue until no changes occur.

The most important issues for region growing are suitable selection of seed points and upper – lower threshold selection. These selections are depending on the users

thus, seed points and upper - lower threshold values must be selected carefully. Region growing has several disadvantages. It is very expensive computationally. It takes both serious computing powers (processing power and memory usage). The other disadvantages are seed point selection and threshold values selection. These values are chosen by hand. These factors affect the segmentation results.
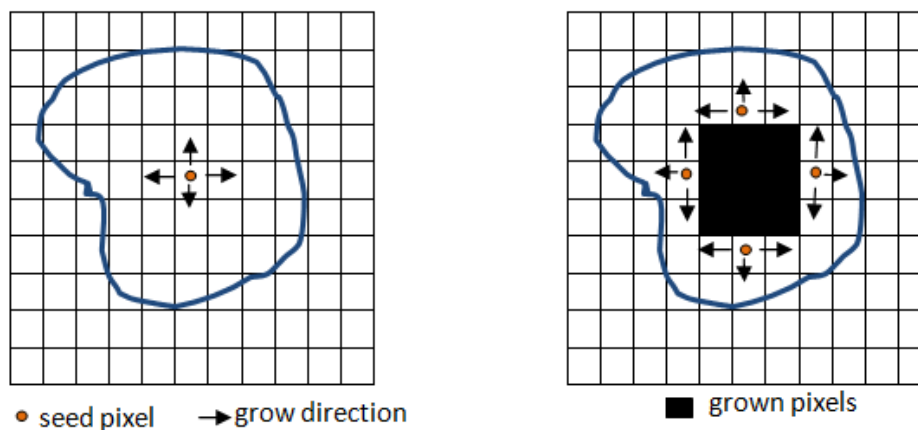
Figure 3.5 Start of growing and growing process after a few iteration

Figure 3.5 illustrates the region growing algorithm. Region growing algorithms can be summarized as follows;

1. Start by choosing an arbitrary seed pixel
2. Region is grown from the seed pixel by adding in neighboring pixels
3. Neighboring pixels are examined and added to a region class if they are same similarity constraints (compare neighboring pixels value with the given threshold values)
4. Repeat step 2 for each of the newly added pixels; stop if no more pixels can be added.

In conclusion, advantages and disadvantages of region growing are summarized as follows;

Advantages :

1. It can be correctly separated the regions that have the same defined properties.
2. It provides original images which have clear edges.
3. It only needs a small numbers of seed point to represent the property we want, then grow the region.
4. Multiple criteria can be chosen at the same time.
5. It performs well with respect to noise.

Disadvantage :

1. It takes both serious computing powers (processing power and memory usage).
2. Noise or variation of intensity may result in holes or over segmentation.
3. Seed points and threshold values are chosen by hand.

In this study, region growing algorithm is used to segment aorta. Implementation details explained in Chapter 4.

3.4 Data Modeling

The key part of the data modeling is to find suitable data structures. In this study, all segmented objects are 2D images. These images contain x, y coordinate of the segmented part. A depth (slice thickness) is added to each object for creating a 3D data model. As a result, each 2D data is transformed to 3D data format (x, y, z). 2D image pixel (x, y) become a voxel (x, y, z) which called volume pixel. Voxels are used in scientific and medical applications to generate 3D volumes. For converting these data to 3 dimensional volumetric structures, data sets for each cross – section of CT must be associated with the others. Each data must be transformed to triangular or polygonal structures for volumetric modeling.

3.5 Data Viewing

3D modeling is the process of generating a mathematical representation of any 3D surface of an object by using specialized software (Maheshwaraa, Arumaikkannu, & Gowri, 2008). The product is called the 3D model. 3D models represent a 3D object using a collection of points in 3D space. These points are connected by various geometrical structures such as triangle, lines, curves, etc. A 3D primitive (volume) has to be representing 3D objects accurately. In surface modeling, polygons and triangles are used to compose images as three-dimensional in appearance in computer graphics. Mostly triangular meshes are used to visualize objects. Advantages of the triangular primitive;

- ✓ The simplest object
- ✓ Always planar (so easy to convert a vector image into bitmap form)
- ✓ Specified with 3 vertices
- ✓ Supported in hardware

There are different ways to generate surface from point data which are called meshing algorithms, and triangulation algorithms. Delaunay triangulation and marching cube are most popular methods to generate surface data. Besides, a new custom surface construction algorithm is developed in our study. It is named fair tiling which is a simple triangulation method. Marching cube and fair tiling methods are mentioned in Chapter four in depth. In the next section Delaunay triangulation method explained.

3.5.1 Delaunay Triangulation

A triangulation is a subdivision of an area (volume) into triangles (tetrahedrons). Delaunay triangulation is the most efficient way to draw triangles between pairs of points. It is often used in the graphic representation of geometrically irregularly distributed data. Delaunay triangulation algorithm is based on the basic principle that the circumcircle (circumsphere) of every triangle (tetrahedron) does not contain any points of the triangulation. In mathematics, P is a set of points in the plane and DT is

a triangulation (Lee, & Schachter, 1980; Chew, 1989). Delaunay triangulation P is a DT such that no point in P is inside the circumcircle of any triangle in DT (P). Delaunay triangulations maximize the minimum angle of all the angles of the triangles in the triangulation; they tend to avoid skinny triangles. The circumcircle of a triangle is formed by three points. In three-dimensional spaces, circumscribed sphere is used in place of the circumcircle. For a set of points on the same line there is no Delaunay triangulation.
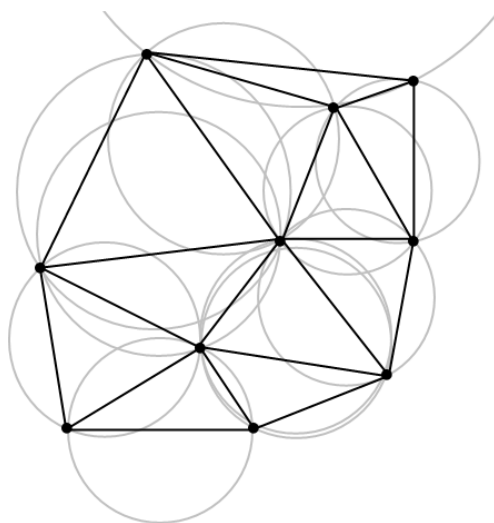
Figure 3.6 Delaunay triangulation for 10 points on a plane (2D space).

a   b
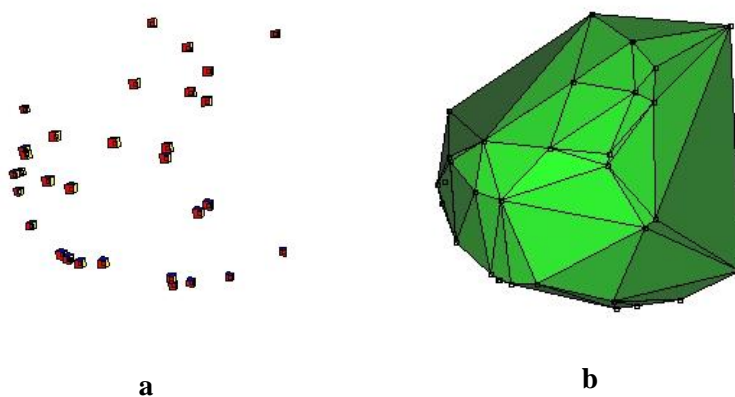
Figure 3.7 (a) Points in three dimensions, (b) Delaunay triangulation of points in three dimensions.

Widely known Delaunay algorithms are Incremental, Gift Wrap, Divide and Conquer, QuickHull.

3.5.2 Lighting and Shading

Generating realistic 3D objects is an important goal for computer graphics (Lewis., 1993; Ramamoorthi, Mahajan, & Belhumeur, 2007). As a result, interaction of light with objects is critical for a realistic view of the object. Interaction between light sources and the surface properties of objects are very complex for physically based models. Computer graphics use approximations in their models to simulate these interactions. When looking at the physical surface, eye's perception of the color depends on the distribution of photon energies that arrive and trigger cone cells (receptors inside human eye). Those photons come from a light source or combination of sources, some of which are absorbed and some of which are reflected by the surface. In addition, different surfaces may have very different properties – some are shiny, and preferentially reflect light in certain directions, while others scatter incoming light equally in all directions.

There are two basic point light types (David, 1983). These are directional light and spot light. In directional light, light source is at infinite distance, so objects receive parallel light rays. E.g. Sun. in spot light, light has a source point (defines where the light) and a target point (defines where it goes). The light can be parallel or perspective. Lighting gives special effects to surface of the objects. In reality, light is bounced off the surface or absorbed. It depends on the light angle. If the angle is steeper, light is observed by the object, thus getting darker. The light actually reflected by the surfaces to our eyes. Direct angle creates more light, steep angle create darkness. Amount of light can be calculated with two parameters. These are direction of where the light came from, and the normal of the surface. The amount of light recieved on the given spot will be the cosine of the angles between the normal and the light direction.

The objects can be shaded according to their interaction with light. Various shading models have been proposed in the literature. They describe how light is

reflected by object. Shading depends on the relative orientation of the surface, light source and viewpoint. Shading is a process used in drawing for depicting levels of darkness on an object by changing densely levels. This process can be described as more densely or with a darker shade for darker areas, and less densely or with a lighter shade for lighter areas. Shading process creates a photorealistic effect over the object. Shading is performed during the rendering process. Shading alters the colors of faces in a 3D model. Following 3D models shows the shading effects.

a   **b**
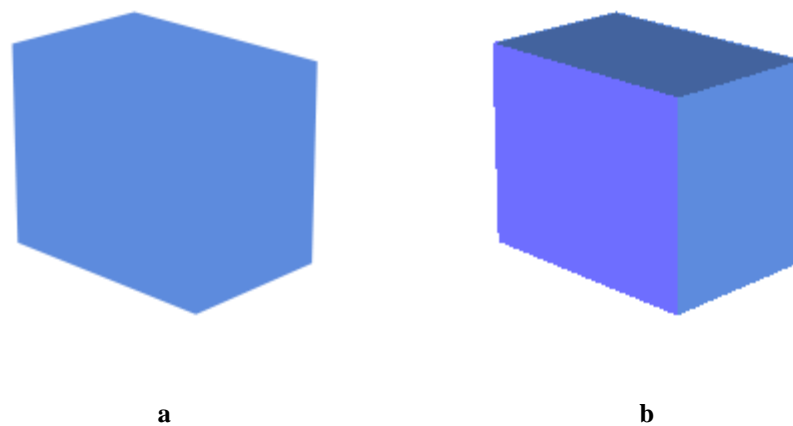
Figure 3.8 (a) Shading disable (b) Shading enable

Shading makes the image more realistic and makes face visible.or with a darker shade for darker areas, and less densely or with a lighter shade for lighter areas.

CHAPTER FOUR
METHODS AND ALGORITHMS USED IN AMET

In this study, a new specialized pre-processing platform is developed to avoid operator-dependency for the arterial anatomy measurements. This platform named as Abdominal Aortic Measurement and Evaluation Tool (AMET). AMET platform has been designed an image processing software for navigation and visualization of Aorta. It is a new tool, developed as a platform – independent tool, aimed for improving the measurement quality of EVAR preprocessing. In this section, the used methods will be explained briefly. The used methods are segmentation, edge detection, middle path calculation, and surface construction. These constitute the main body of the tool. Following figure illustrates the steps of the developed tools.
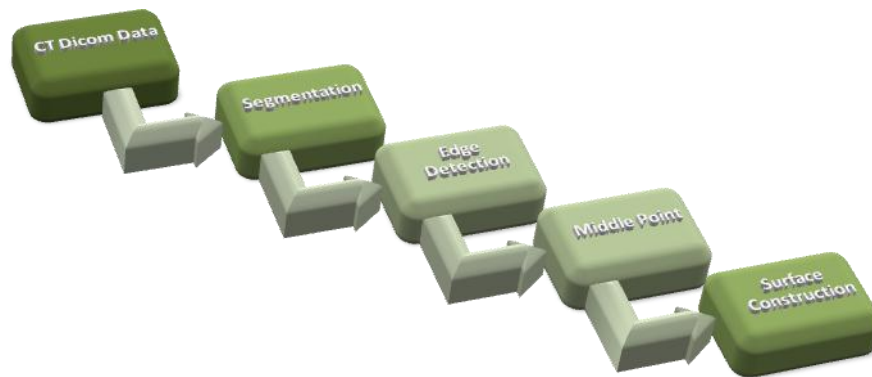
Figure 4.1 General Steps

4.1 Patient Selection

The sample set consists of CTA images and patients provided by Dokuz Eylül University, Faculty of Medicine, and Interventional Radiology Department. Data from approximately 100 consecutive patients electively treated with EVAR by the Interventional Radiology Department of our university from January 2005 to March

2010 were analyzed, retrospectively. Some patients with MR angiograms were excluded because of improper preoperative data. A target patient group was selected for the evaluation. (35 patients were selected for comparison to tool reliability.)

Multidetector CT examinations were performed by using a four–detector row scanner (Philips Medical Systems, the Netherlands). One hundred milliliters (300 mg of iodine per milliliter) of a nonionic intravenous contrast material was administered, through a 20-gauge catheter inserted into an antecubital vein, at a rate of 4 mL/sec by using a power injector. Arterial phase imaging was performed by using bolus tracking. CT parameters were set at 120 kVp and 180 mAs and a 1.00-mm detector configuration was used. Three-millimeter thick sections were reconstructed and downloaded to the picture archiving and communication system.

Institutional review board approved this retrospective study using the data of patients.

Before EVAR was considered, a high – quality CT scan with 2.5 to 3 mm cuts was obtained in most cases. A series of DICOM images consists of several axial intersections of patient body; series content varies from patient to patient. Average series data contain 340 slices. Each image contains lots of data irrelevant to aorta such as bones, liver ...etc. Data relevant to aorta must be extracted from each of images of those series. The image representation needs to be converted into something that is easier to process. That is the segmentation part of the project which plays a major role in the study.

4.2 Segmentation Process by ITK Toolkit

ITK stands for Insight Segmentation and Registration ToolKit (Ibanez, & et al., 2003). It is a toolkit for medical image segmentation and registration. ITK is sponsored by National Library of Medicine as a tool to support the Visible Human Project. The project began in 1999, and released ITK 1.0 in 2002. Now ITK is also maintained by Kitware Inc. and is distributed in Open Source form. Although ITK has got many applications in the medical imaging community. Currently the stable

version of ITK is 3.18, and it provides almost all mainstream medical image segmentation and registration algorithms. ITK has become very famous software development toolkits. It provides many conveniences to the related researchers. But they have some disadvantages which prevent them from getting more applications. Firstly, ITK doesn't provide the function of visualization. A special 3D library must be use to make a medical image processing and analyzing system. Secondly, ITK used Generic Programming. Therefore, necessary libraries must be reformed to medical image processing. Finally, ITK make use of many modern C++ language features, especially the template. All these factors restrict the application range of ITK. In this study, itk region growing segmentation method is used to segment DICOM data. (Region growing method explained detailed in section 3.2.1.3) Developed platform is implemented in Java language. So, all necessary itk libraries are converted to java code.

For Segmentation process, *ITK region growing algorithm* (Fasquel, Agnus, & Lamy, 2006) is used to segment DICOM image series via user provided reference points and upper/lower threshold values. As threshold values Hounsfield Units has been used to help with detecting aorta pattern in DICOM image.
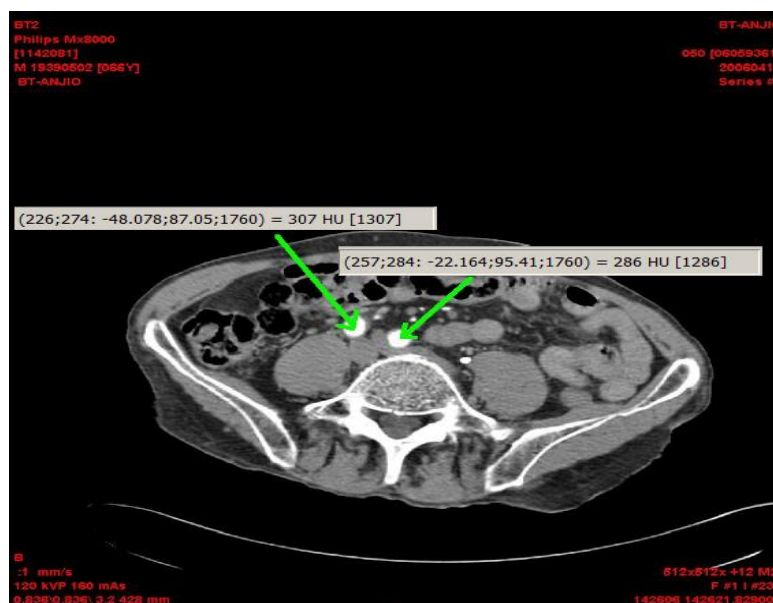
Figure 4.1 User inspects image and sets two reference points shown by green arrows in the figure ref#1 is X coordinate: 276; Y coordinate: 274 and ref#2 is X coordinate: 257; Y coordinate: 284.

In Figure 4.1, User determines two distinct regions which aorta vessel forms. To begin segmentation user needs to specify threshold values to extract the aorta pattern. At this point user observes that Hounsfield Units varies from 250 HU to 400 HU (In Figure 2.5 ref#1 is 307 HU and ref#2 is 286 HU) around the reference points. Then meaningful setting for the threshold values should be 250 as lower threshold and 400 as upper threshold respectively.

DICOM Series   After Segmentation
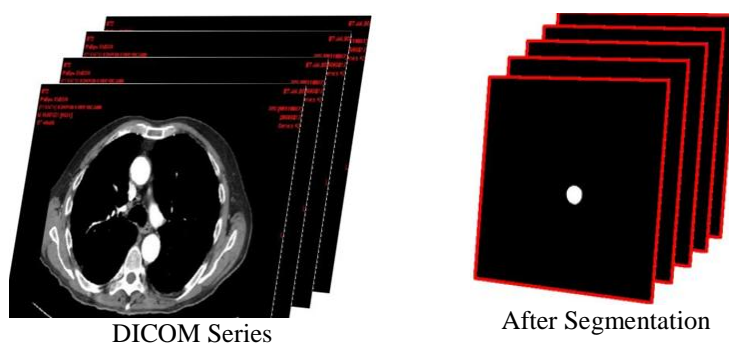
Figure 4.2 Extracting aorta vessel pattern from DICOM series.
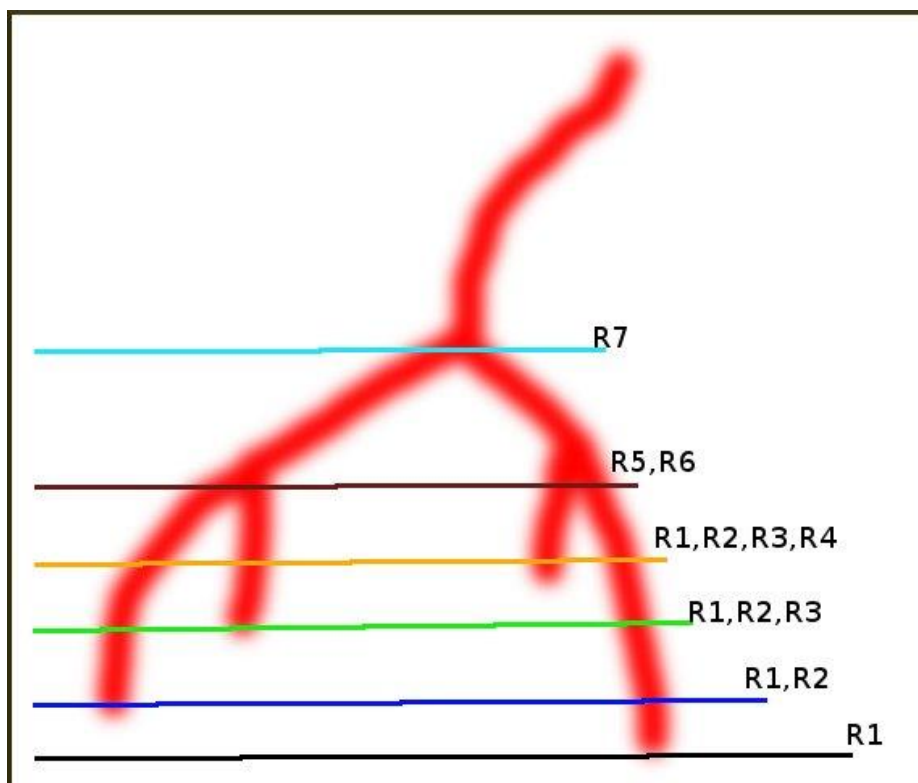
Figure 4.3 Example reference setting on multiple limbs.

Depending on the morphology of the aneurysm, complex anatomic structure of patient, and noise when CT scanning, reference setting for segmentation might be complicated. Figure 4.3 shows a guideline for setting reference points.

4.3 Edge Detection

Segmentation process generates a grayscale image set as shown in Figure 4.2. In 3D space, a volume consists of points, edges, and faces. Each image should be reprocessed to capture point and edge data (Heath, & et al., 1997). Detecting edge point is also critical since angle measurements -which are made for deciding if patient is curable- done due to middle path approach (will be mentioned in detail in section 4.4). For this reason each region's center point should be determined. Since polygon center finding algorithm (which will be covered in detail in next section) requires edge points of the polygon as input. Surface construction from edge points algorithm works only if edge points of a region in clockwise order, since rational behind the algorithm based on neighborhood relations of the points. Therefore, a new edge detection algorithm is developed to detect edge points in clockwise order.

4.3.1 Edge Detection Algorithm

Edge detection algorithm aims to detect edges of a probable non-convex shape which is defined as non-zero numbers in a two dimensional array. For instance, in the Figure 4.4 (a) in a 15x15 array black cells are non-zero numbers and white cells zero. After edge detection output should be as in Figure 4.4 (b) and sorted (numbered black cells order) through clockwise order.

Edge detection process is a little complicated since clockwise direction order of cells is vital. But approach is simple when thinking in vectors. Assume that there is an imaginary pointer pointing each cell in clockwise order. Problem is moving the pointer from one cell to another. At this point, this (probable) motion can be specified as a *motion direction*. When considering motion of the pointer around cells there are 8 possible directions -up, up-right, right, down-right, down, down-left, left, up-left-that motion direction can be one of. Motion direction of pointer should be updated after each move between two cells. Detection process starts finding upper

leftmost edge cell and setting motion direction as right direction, and process ends when first detected cell is reached.

A   B
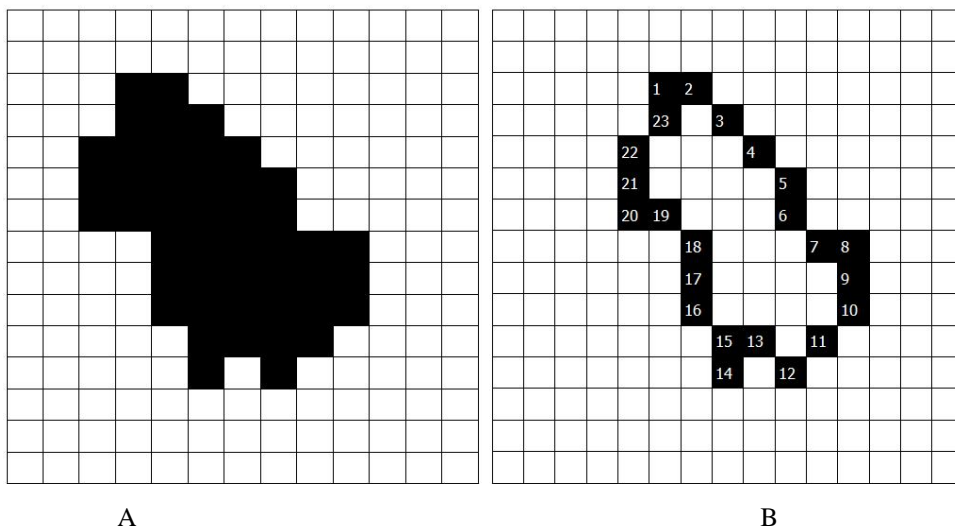
Figure 4.4 (A) A shape formed of pixels in two dimensional array (B) Shape formed of pixels after edge detection
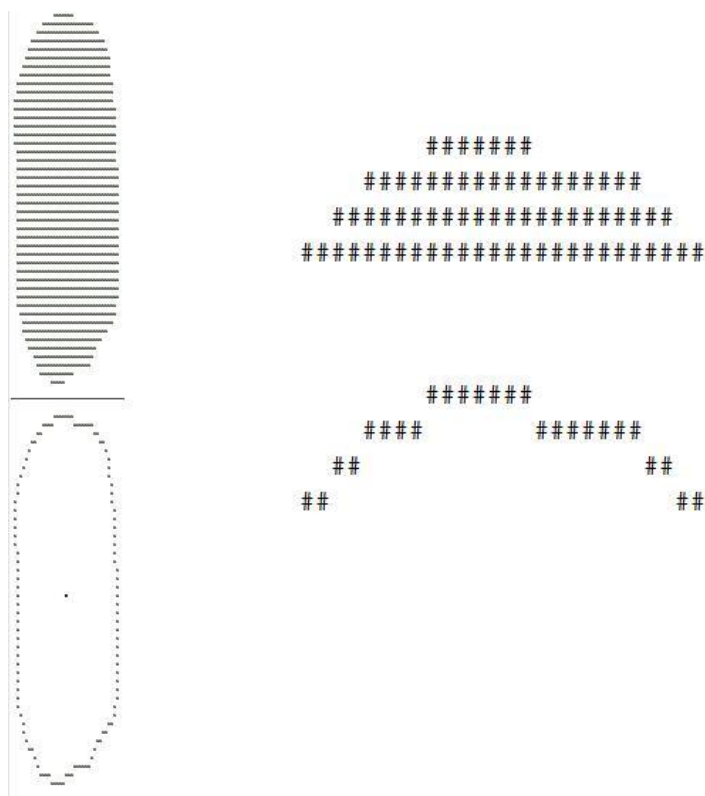
Figure 4.5 An abstract symbolizing view of pixels before and after
edge detection.

Note that algorithm takes an image and handles it as a two dimensional integer array:

```
1. Find left-upper most point and assign it as current.
2. Assign current direction as "Right".
3. Initialize direction vector starting from UP (UP, UP-
   RIGHT, RIGHT, DOWN-RIGHT, DOWN, DOWN-LEFT, LEFT, UP-LEFT)
4. Scan neighbors of the current point starting from right
   after the backwards of current direction. (ex., If
   current direction is Right, then backwards is Left, next
   direction according to clockwise is UP-LEFT)
5. If found a legal point while scanning, assign it as
   current point and assign direction at which point found
   as current direction.
6. Continue from step 4, until left-upper most point is
   found.
```

4.4 Finding Middle Point (Centroid) of the Shape

The problem of determining the area of a polygon seems at best messy but the final formula is particularly simple. Consider a polygon made up of line segments between N vertices (x_i, y_i), i = 0 to N-1. The last vertex (x_N, y_N) is assumed to be the same as the first and the polygon is closed.
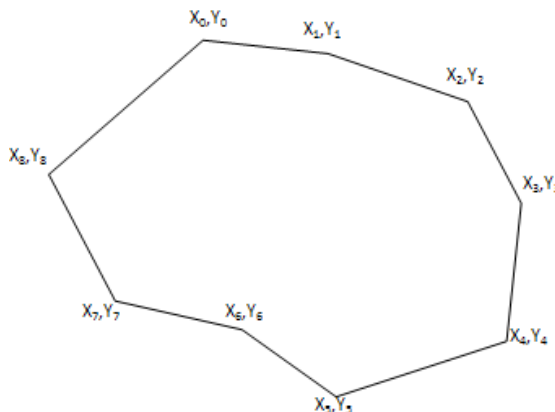
Figure 4.6 A polygon with n=9 point data

The area is given by;

$$A = \frac{1}{2} \sum_{i=0}^{N-1} (x_i y_{i+1} - x_{i+1} y_i)$$

(**4**)

The holes are usually defined by ordering the vertices of the enclosing polygon in the opposite direction to those of the holes. This algorithm still works except that the absolute value should be taken after adding the polygon area to the area of all the holes. That is, the holes will be of opposite sign to the bounding polygon area.

The sign total areas of the expression above (without the absolute value) can be used to determine the ordering of the vertices of the polygon. If the sign is positive then the polygon vertices are ordered counter clockwise about the normal, otherwise clockwise. To derive this solution, draw lines from each vertex to some horizontal line below the lowest part of the polygon. The enclosed region from each line segment is made up of a triangle and rectangle. Sum these areas together noting that the areas outside the polygon eventually cancel as the polygon loops around to the beginning.
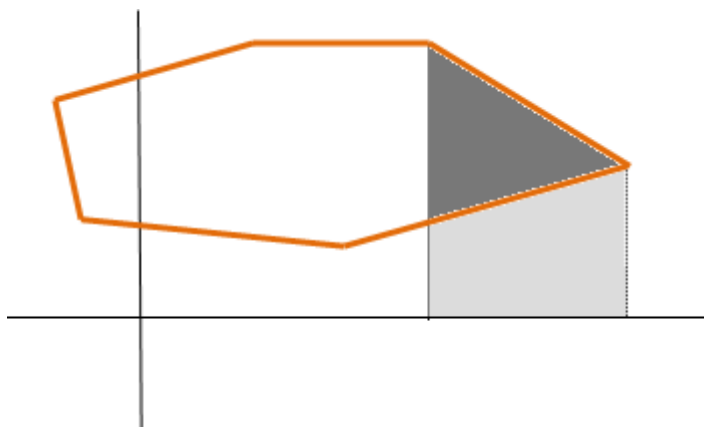
Figure 4.7 Polygon Area

The only restriction that will be placed on the polygon for this technique to work is that the polygon must not be self intersecting.

The centroid is also known as the "centre of gravity" or the "center of mass". The position of the centroid assuming the polygon to be made of a material of uniform density is given below. As in the calculation of the area above, x_N is assumed to be x_0, in other words the polygon is closed (Bourke, Fuhrman, & Dephi, 1988).

$$c_x = \frac{1}{6A} \sum_{i=0}^{N-1} (x_i + x_{i+1}) \, (x_i \, y_{i+1} - x_{i+1} \, y_i) \qquad \textbf{(5)}$$

$$c_y = \frac{1}{6A} \sum_{i=0}^{N-1} (y_i + y_{i+1}) \, (x_i \, y_{i+1} - x_{i+1} \, y_i) \qquad \textbf{(6)}$$

4.5 Modeling Vessel as a Tree

Since the aorta vessel is multi limbed and forked around distal arteries, its nature is modeled as general tree data structure. Since the data is captured as axial intersections, the model is formed of a bunch of slices. Each slice may include 1 to N regions –sections of aorta limbs. Each region consists of edge points and of course a centroid coordinate data of which calculation is explained in detail in section 4.4. Following figure show the data model of the aorta vessel. Aorta vessel structures like a tree therefore, its data structure constructed with tree structures. Modeling as a general tree, each region (R0 to RN) is a list of point data, each slice is a list of regions and model consists of list of slices.
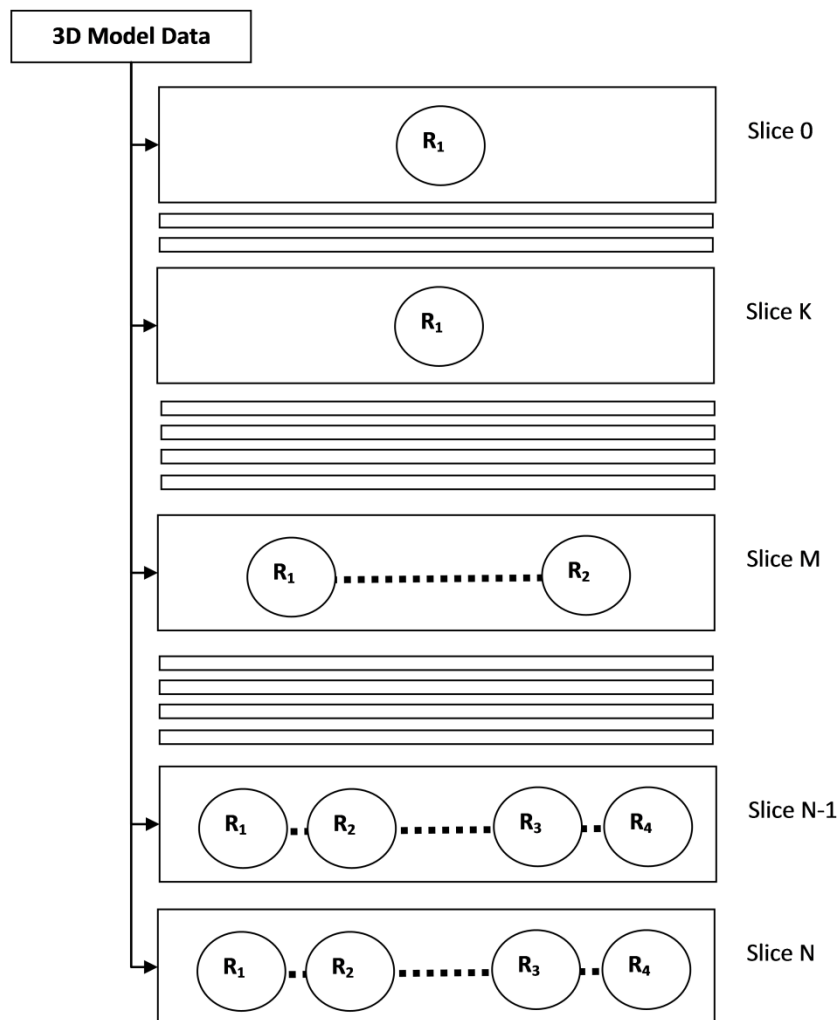
Figure 4.8 Modeling Vessel as a Tree

4.6 Surface Construction

Medical visualization was examined at two different techniques as surface generation and volumetric imagining. Surface generation is a 3D visualization technique which displays the tissue density isosurface whereby points, straights, vectors, triangles and polygons and not interested in interior of object (Choi, & et al., 1988). Volumetric imagining is a 3D visualization technique which displays the interior of object with parts and layers at different tissue density. This technique monitorizes surface of object and also interior region of object with different density and opacity values.

In the medical field, 3D visualization has an effective role at diagnosis and treatment process. Segmentation process provides two – dimensional dataset. This data are obtained from different cross – sections of the BT. It is more comprehensible for 3D volumetric modeling. Structures at two – dimensional sequential sections must be generated as 3D. For converting these data to 3 dimensional volumetrical structures, each section must be associated with the others and, tirangular or polygonal surfaces must be indicated for volumetric imaging (modeling).

So far here, medical images are read and segmented, edge points detected on segmented images and modeled the data, but all we got is point data (X, Y, Z) coordinates in 3D space. To model an object –actually a volume- in 3D space we also need relations (or simply connections) between points. We know that points which have same Z coordinate belongs to the same slice. However this is a partial relation. How about relations (connections) between points on different slices? (Regions' points on two consecutive slices for example) To create a volume in 3D space; this question should be answered: which points construct a surface? There are ways to generate surface data from point data called meshing algorithms, triangulation algorithms…etc. Most of these algorithms cover sophisticated numeric analysis methods, heuristics…etc. Delaunay triangulation is explained in Chapter 3. In this thesis, Marching Cube and new simple triangulation method are used to surface construction process. In this section these methods will be explained.

4.6.1 Marching Cubes

Marching Cubes (Lorensen, & Cline, 1987) is an algorithm for generating iso-surfaces from volumetric data. The marching cubes algorithm is a 3D iso-surface representation technique. In a 3D space, 256 different situations are enumerated for the marching cubes representation. All these cases can be reduced in 15 cases by rotations and symmetries. 15 unique cube configurations are illustrated in Figure 4.9. In order to be able to determine each case, a notation has been adopted. It aims at referring each case by an index created from a binary interpretation of the corner weights. Marching Cubes Algorithm is based essentially on two lookup tables. These are Edge table and Triangle table. A part of these tables are given below.

```
Int edgeTable[256] =
{ 0x000, 0x109, 0x203, 0x30a, 0x406, 0x50f,
0x605, 0x70c, 0x80c, 0x905, 0xa0f, 0xb06,
0xc0a, 0xd03, 0xe09, 0xf00, 0x190, 0x99,
0x393, 0x29a, 0x596, 0x49f, 0x795, 0x69c
.....}


Int triTable[256][16] =
{{-1,-1,-1,-1,-1,-1,-1,-1,-1,-1,-1,-1,-1,-1,-1,-1},
 {0, 8, 3,-1,-1,-1,-1,-1,-1,-1,-1,-1,-1,-1,-1,-1},
 {0, 1, 9,-1,-1,-1,-1,-1,-1, -1,-1,-1,-1,-1,-1,-1},
 {1, 8, 3, 9, 8, 1,-1,-1,-1, -1,-1,-1,-1,-1,-1,-1},
 {1, 2, 10,-1,-1,-1,-1,-1,-1, -1,-1,-1,-1,-1,-1,-1},
.....}}
```

It classifies vertices as positive or negative, according to their comparison with a given isovalue. Then, it uses a lookup table to tile the surface inside the cube. Marching Cubes Algorithm steps can be explained as follows;

Each of the eight vertices of a cell is assigned a value, comparing which against the minimum determines if that cell is intersected by the surface. Any vertex with a value less than or equal to the minimum is defined to be inside the surface. For each inside vertex a bit is inserted into a designated index at a position representing that vertex. The index is used with edge Table return the edges of the cube that intersect the surface, again as bits of an integer. If none of the edges are intersected the process goes back to the beginning and tests another cell. Otherwise that number is checked bit by bit and a point of intersection is determined for each intersected edge. That point is saved into an array at the index corresponding to its edge. Finally triangles are created by connecting points on intersected edges of the cell in the order returned by triangle Table at index formed earlier. Triangle Table is 256x16 arrays of integer values, which are used as indices for the array of 12 points of intersection. It defines the right order to connect the intersected edges to form triangles. The process for one cell stops when index of -1 is returned from the table.
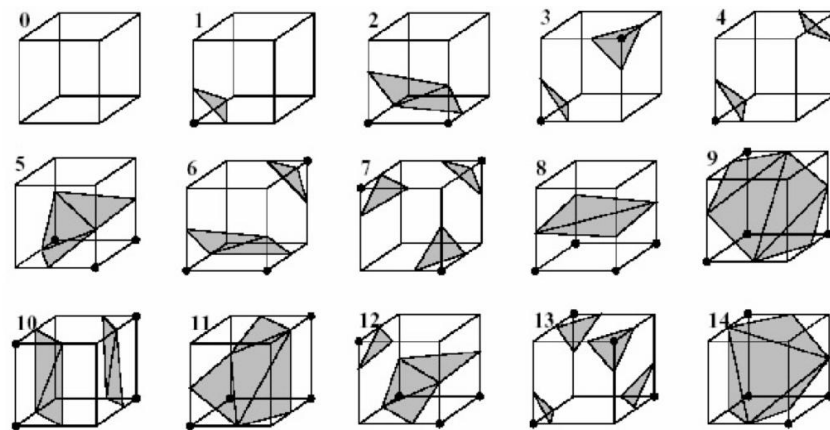
Figure 4.9 15 unique cube configurations

The marching-cubes algorithm is conventionally used in the field of computer graphics. Input image dataset can range from medical images to geological scans.

Basic Steps:

Locate the surface corresponding to a user-specified value.

Create triangles.(using edge table and triangle table)

To locate the surface, it uses a logical cube created from eight pixels.
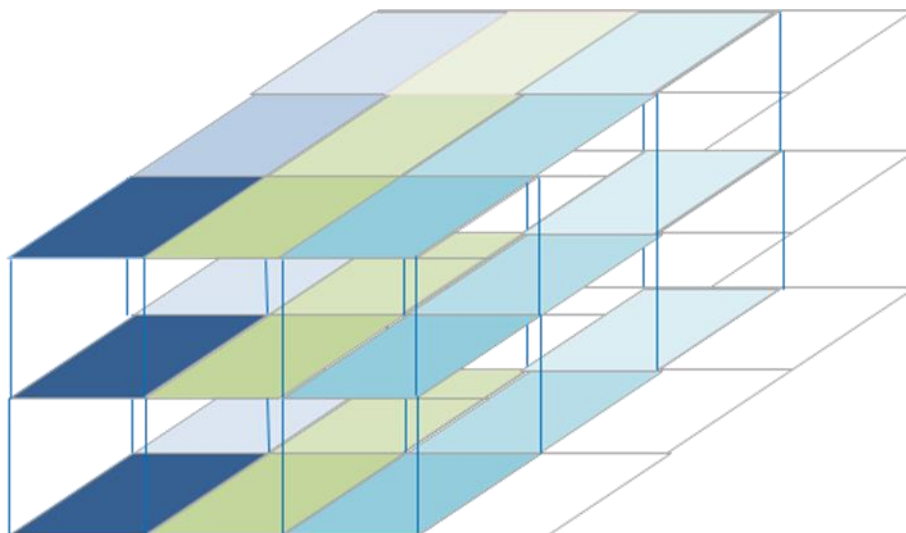
Figure 4.10 Logical Cube

There are many data for each slice. The program needs high memory capacity to hold these data if all of them are transferred to main memory. Therefore, marching cube algorithm works on the following principles: The consequent slice data are transferred to memory and marching cube algorithms then starts to work. Created triangles are stored in a special data structures and first slice data are removed from the memory. Next slice data are transferred to memory and algorithm is applied again for the all slice. Figure 4.10 illustrates this step for the three consequent slices.

4.6.2 Custom Triangulation for This Study: Fair Tiling

Smooth geometrical objects can be expressed with certain mathematical functions. Such as; ellipse, sphere shapes etc. If the surface has irregular geometry, it can't be expressed with certain functions. Irregular surfaces can be identified by using small surface component. (12) The limitation points of the objects must be found to describe real surface structure ideally. Main purpose of this process is combination of object surface points by using polygonal principles (like triangle) for modeling of the object. Simulated polygonal surface model can be displayed as colored and lighted by utilizing computer graphic techniques.

In this section, surface generation method, which had been developed for 3D visualization of vascular structure among the CT based imagining, will be detailed. By using surface data obtained from developed method, related region is readily created with polygon and triangular based visualization in computer once again and it can be monitored in other application. This new method is developed for this thesis. It is a simple triangulation method and named Fair Tiling.

Triangulation methods/algorithms mentioned in previous section requires some computations over and over again such as computation of circumcircle center and radius, query if a point is in the circle or any other point is in the circle. Several times repetition of these operations in those algorithms requires fast access to point data, using a partition of data and portioning the data. For all those of reasons a relatively simpler algorithm is developed to solve the triangulation problem. This solution is much customized to 3D modeling of aorta.

Fair Tiling Method is based on forming the least triangular structure from coordinates corresponding to the mutual cross-sectional by distributing point values in consecutive sections regularly. In this approach, consecutive sections are scanned by using midpoint of structure (like tube or convexhull structure). Scanning process is done with lines between midpoints of a section and edge points of the other section. Obtained triangular structure includes intersecting points on scanning area. Before the application of Fair Tiling Method, edge and midpoint determination processes are implemented from segmented images. These processes are explained in section 4.3 and section 4.4.

Algorithm simply handles two successive regions in two successive slices and discovers which point of the region will connect to which point of the other region. In other words, algorithms takes one point from a region connects it to single or N points on the other region.
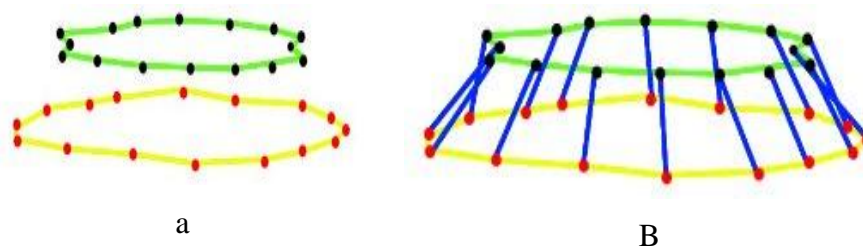
Figure 4.11 (a) two successive regions' points. (b) One-to-one connection

From the view of the rational that taking one point from the region and connect it to the point from the other region is easy when number of points in regions is the same and/or fairly separated. For such scenario it would be quite easy to make one-to-one connection as shown in Figure 4.11 (b), in that case for N points there would be N quads and if we subdivide the quads by 2, we would form 32 triangles as shown in Figure 4.12.
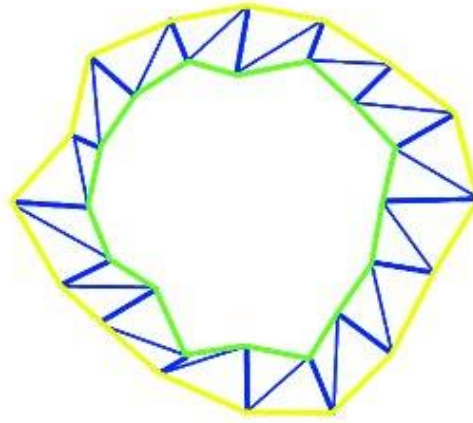
Figure 4.12 Final top view of the two regions
after triangulation.

In the scenario of different number of the points that regions formed of, the solution method should fairly assign each required point a fair number of connections. At this point problem turns out to be a fair assignment of some specific resources to some specific consumers. Figure 4.13 is an example of fair assignment of connections to the points.
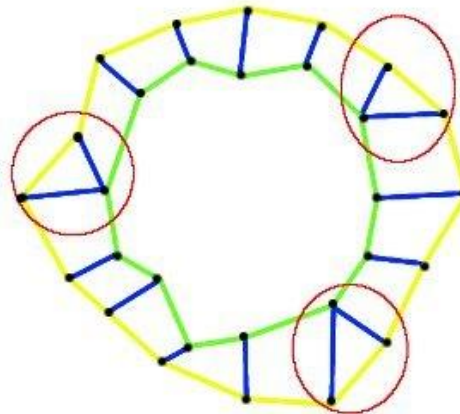
Figure 4.13 One-to-N matching, occurs when number of points is not equal or inadequately separated

For adequately connection of points we have developed neighborhood by center approach to solve this problem. If we consider two consecutive regions as shown in

Figure 4.14, an adjustment needs to be take place initially; this adjustment is overlapping the centers of the regions as shown in the Figure 4.15.
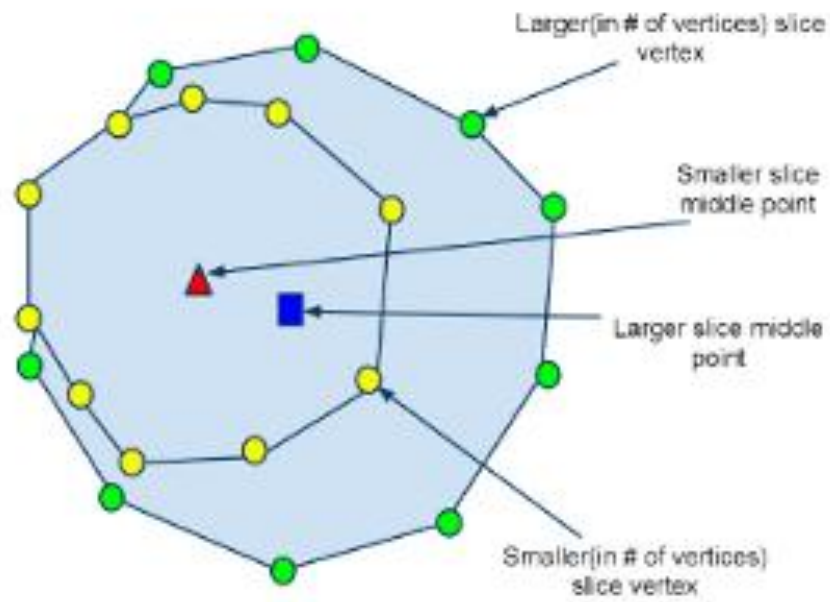
Figure 4.14 Top view of the region points
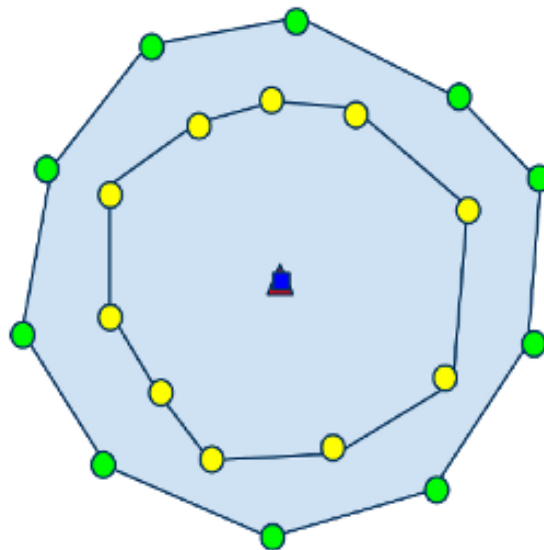
Figure 4.15 Overlapped centroids of the regions

After overlapping, draw an imaginary circle large enough to enclose both regions. For each point in smaller (size is determined in terms of number of points that region is formed of) region, calculate delta distances to its neighbors (there is always two, before and after the point) and mark the halfway of this distance (this marker point is called D point). Now an imaginary line is drawn that crosses both center point and D point. Then the intersection point that both the line and the circle cross must be found and noted. All these process must be done for the other neighbor to find second intersection point. After finding these two intersections an imaginary triangle is drawn and for each point of the bigger (size is determined in terms of number of points that region is formed of) region is tested if the point is fall into this triangle area. This operation for single point in smaller region is depicted in Figure 4.16.
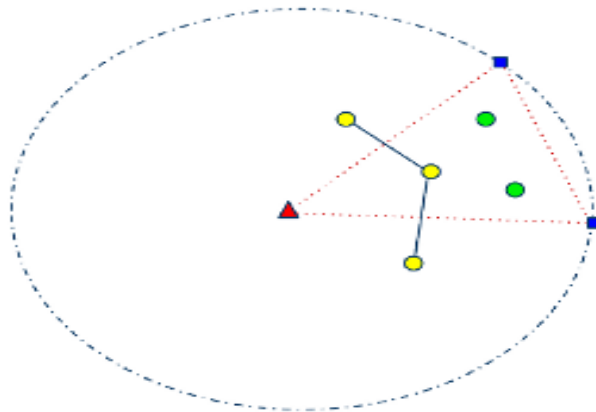
Figure 4.16 Figure Point in triangle test

At this another problem arises, how a point is tested if it is in triangle or not? This problem is actually a ray tracing problem to calculate shading over pixels. And solved by the following;
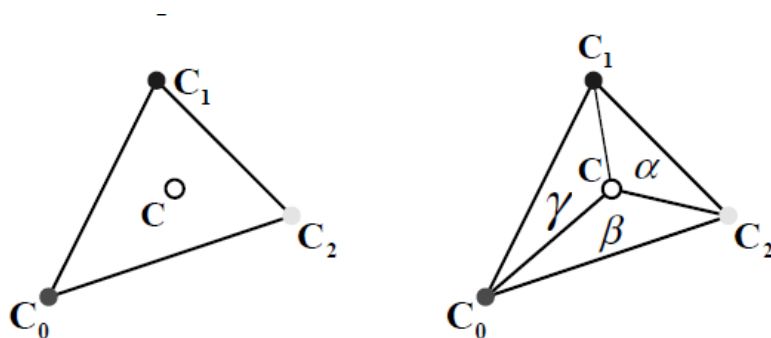
Define 3 Barycentric (Warren, Schaefer, Hirani, & Desbrun, 2006) coordinates; α, β, γ

$$C = C_0\alpha + C_1\beta + C_2\gamma \quad \text{where} \quad \alpha + \beta + \gamma = 1$$

C is inside $C_0C_1C_2 \Leftrightarrow \alpha, \beta, \gamma \in [0,1]$

$$\alpha = \frac{Area(C\ C_1C_2)}{Area(C_0C_1C_2)} \tag{7}$$

$$\beta = \frac{Area(C_0C\ C_2)}{Area(C_0C_1C_2)} \tag{8}$$

$$\gamma = \frac{Area(C_0C_1C\ )}{Area(C_0C_1C_2)} \tag{9}$$

And calculating a triangle area of which all three coordinates are known is as follows;

$$X_1Y_2 = C_{0_X} * C_{1_Y}$$

$$X_2Y_3 = C_{1_X} * C_{2_Y}$$

$$X_3Y_1 = C_{2_X} * C_{0_Y}$$

$$X_2Y_1 = C_{1_X} * C_{0_Y}$$

$$X_3Y_2 = C_{2_X} * C_{1_Y}$$

$$X_1Y_{3'} = C_{0_X} * C_{2_Y}$$

$$A = \tfrac{1}{2}\left(X_1Y_2 + X_2Y_3 + X_3Y_1 - X_2Y_1 - X_3Y_2 - X_1Y_3\right) \tag{10}$$

Point $\mathbf{r}$ lies inside the triangle if and only if $\alpha, \beta, \gamma > 0$. Otherwise, $\mathbf{r}$ lies outside the triangle.

General algorithms for fair tiling can be summarized as follows;

```
1. Take 2 consecutive slices from different z-coordinates
2. Make a reference slice which has smallest number of
   points. (Inner slice) Take 2 consecutive points in
   reference slice
   2.1 Find center (delta point) of these points.
   2.2 Find a line which is passing from inner slice center
   to delta point
   2.3 Intersection points for the inner slice are stored
   in a special data structure. Found line (in 2.2) is used
   to find intersection points.
3. For each points at the inner slice
   3.1  Two stored points and inner slice center creates a
      triangle
   3.2  Each point is tested in the outer slice, point is
      inside the triangle or not? If point is inside the
      triangle a triangle mesh created with this point.
```

For obtaining artery structures, region growing segmentation method was used. While artery structure was segmented, the vascular structures corresponded to each section was gained from DICOM imaginations. 3D models generated by various visualization methods. During 3D model generation, several problems arise. One of the major problems of generating 3D models from consecutive 2D slices is surface construction. This study presents a surface construction method, fair tiling, which is used to generate surfaces of from arbitrary points. These points are gathered from CT images to construct vessel-like structures. Fair tiling presents an easier structure compared to other methods in the area.

4.7 Marching Cube vs. Fair Tiling

Fair tiling is used to construct surface with triangular structures. It uses coordinate points of the object which can be expressed with 3 dimensional x, y, z coordinates. Marching Cube is the most popular method for the surface construction and its details are explained in section 4.6.1. There are some disadvantages and advantages of the fair tiling when comparing with marching cube.

In marching cube, all object points have to be stored in a special 3 dimensional data structures. Because, It uses index base search methods (this index structure are stored in a lookup table) with using unit cube points during triangular creation process. All points have to be converted to standard structures in accordance with lookup table. Fair tiling works on the real values of object. Marching Cube algorithm produces a triangle mesh by computing iso-surfaces from discrete data. It can be used to generate surface for all volumetric data. There is no limitation. But, fair tiling only works on tubular structures. Fair tiling works on convex like structures. If one of the two consecutive slices is not convex, algorithms can't be generating correct surface.

Working principle of the Fair Tiling based on middle point calculation approach of the object. Therefore, edge points of the object must be determined to calculate middle of the object. This process is not necessary for the Marching Cube approach.

Parallel processing can be applied for the each algorithm. Marching Cube algorithm works on "computation in space", Fair Tiling works on "computation in time" principles. These relationships are given in Table 4.1. Both algorithms are applied for the AAA patients. (10 patients' data are used) Their 3D aorta model was created with these methods. Total number of triangles and execution times are compared. Results are given in Table 4.1.

Table 4.1 MC (Marching Cube) FT(Fair Tiling)

Execution Times (milisecond)		Total Triangle Number	
MC	FT	MC	FT
174203	458	308146	128666
81645	181	152210	56496
97695	154	221060	49539
75064	118	127578	41143
99511	193	171692	60790
76926	101	123538	31696
90627	243	189842	65358
91844	251	217172	69838
80735	217	157774	57820
97229	258	224170	72730

The 3D models of the aorta are given in figure 4.17. The model given in figure 4.17 (a) was created with marching cube algorithm where the other model was created with fair tiling.

a   **b**
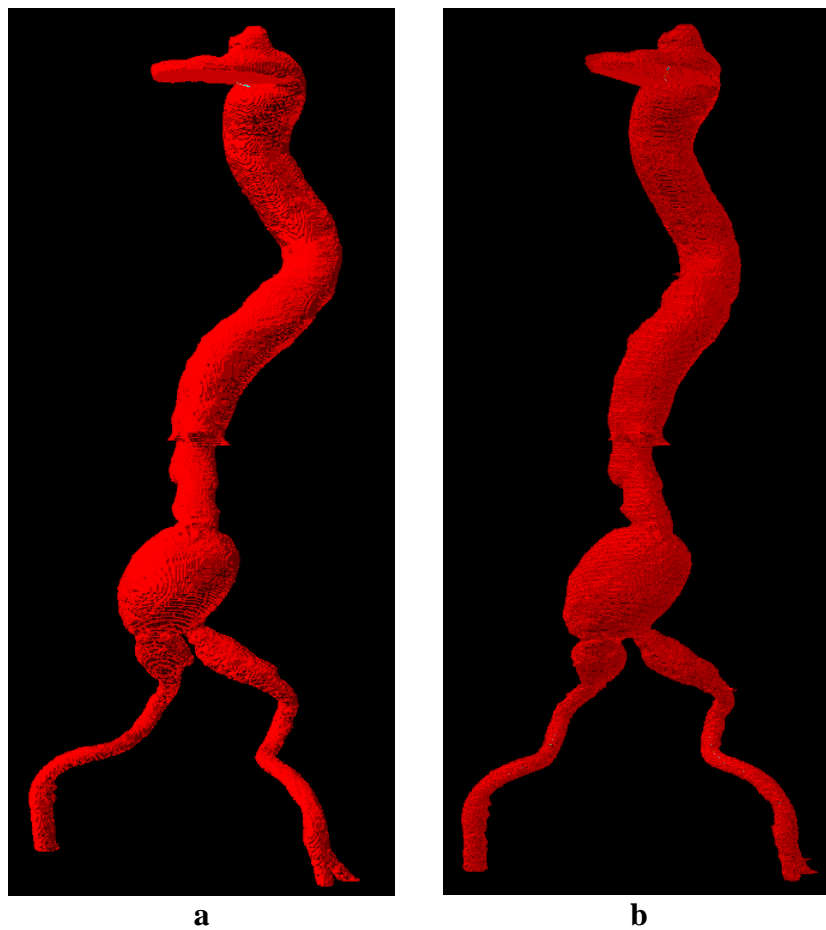
Figure 4.17 a) Output of Marching Cube for AAA b) Output of Fair Tiling Method for AAA

CHAPTER FIVE
SOFTWARE CONCEPTS

The AMET is used for making measurement and evaluation related with aortic dimensions and characteristics of aneurysm. With the help of this tool, navigation and visualization of the aorta in 3D perspective was made possible. AMET was developed on Java platform; therefore it has a platform independent infrastructure. Aorta 3D model was developed with Java Open Graphics Library *(jogl)*. Used methods to construct the AMET were explained in Chapter 4. In this chapter, the capabilities and usage of AMET will be explained..

5.1 Program Capabilities

Developed software tool consists of four main modules. These are,

- ❖ Dicom Viewer,
- ❖ Segmentation,
- ❖ Data Manager,
- ❖ Graphics Render Engine.

PixelMed DICOM Toolkit is used as a preprocessor to read, display and manage CT images. PixelMed is a stand-alone DICOM toolkit which is used for reading and creating DICOM data, supports the display of directories, images, and DICOM object validation. The toolkit is open source and freely available for both non-commercial and commercial use, under BSD License and freely available. PixelMed provides java libraries to manage DICOM data. DICOM viewer part was developed by using PixelMed toolkit. The DICOM viewer part of AMET provides many opportunities for managing DICOM images. These are;

- ❖ Opens any DICOM image
- ❖ Visualization of DICOMDIR files in typical structure patient/study/series/study

❖ Standard navigation (pan, zoom, magnification)

❖ Advanced tools to measure area and distance

❖ Brightness and contrast change with a simple mouse movement

❖ Simultaneous visualization of two or more DICOM files.

❖ Export single frame in JPEG, BMP format

Segmentation is an important part of the AMET. Segmentation is the pre–processing part of the tool. This part provides aorta boundaries for the each slice. 3D model of the aorta is generated by using these boundaries. AMET used region growing segmentation algorithms of ITK library which have been proven to be a very effective approach for image segmentation. Details of region growing approach were explained in section 3.2.1.3. Firstly, a set of seed pixels are selected from the target images for the basic region growing algorithm. After this step, algorithm adds neighboring pixels to the set according to similarity criteria repetitively. Finally, an interested part from the target image is found. Aorta boundaries are represented as x-y coordinates. This coordinates are called aorta edge points in the AMET. Aorta edge points are generated for each slice and these points are stored in a common database for the patients by the tool.

Data Manager part of the tool operates and manages the parameters taken from 3D Manager, Visual Manager, Shortcut Manager and database. All data obtained from the segmentation is stored in a database. Therefore, the segmentation is not repeated for each patient. Edge points of a segmented vessel are gathered with edge detection algorithm. Edge detection algorithm details were explained in section 4.3.2. These data are stored in database as x, y, z coordinates. All these model data are transferred to the 3D view panel by using Data Manager. Transformation process is organized by data manager. All measurement values which are measured in 3D view panel are transferred to the Data Manager and these data are stored by the Data Manager. AMET provides some shortcut features to the users. These shortcuts work on menus and 3D model. In 3D model, it provides that translate, rotate, zoom, etc. features. Data manager manages these shortcuts. In data manager, database access information was created dynamically.

Visual Manager arranges the position of the user menus used in AMET. In addition, model color, size and some other visual properties can be arranged in Visual Manager. Last selected menus are stored in data manager by visual manager.

After segmentation step, the edge points of the slice are stored in database. To create 3D model, a volumetric view have to be obtained from these point data. Graphics Render Engine part of the AMET is used in this step. OPENGL is used for 3D modeling of the aorta. OPENGL panel of the AMET shows the 3D model of the aorta. Different processes can be made over this model (translate, zoom, pan, etc.). User interaction could be provided with these features. The most fundamental aim of the AMET is to perform measurement on the 3D model. So that, user can be select anywhere from the model and signed points.

OpenGL does not allow the points (which are entities does not fills a volume) to be selected (or interact with). Therefore any point which is required to be interacted with should be wrapped by a volume. At this point a tetrahedron volume is chosen to be right for this purpose. A tetrahedron is a polyhedron composed of four triangular faces, three of which meet at each vertex.
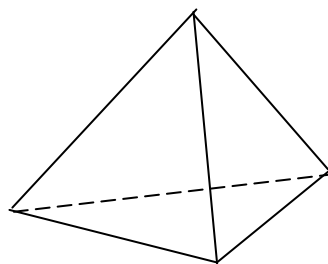
Figure 5.1 a tetrahedron

The user can measure by using these selected points from the menus. The measurements are the diameters, the angle, the distance, and the delta distance of the aorta. Graphics Render Engine parts of the AMET interactively works with 3D Control Panel. Each measurement results are transferred to 3D Control Panel and displayed. Measurement history is created in 3D Control Panel. Physicians can use these measurement data in stent selection process.

OPENGL supports interactive applications. Objects drawn on the screen are exposed different operations such as multiple rotations, translations and perspective transformations. In 3D scene, determination of selected object is difficult. At this point, OPENGL provides a special selection mechanism. This mechanism assures position of the objects drawn inside a specified region of the window. This feature of OPENGL can be used together with a special routine to determine the position of the object with the cursor. Figure 5.2 illustrates the overall 3D modeling software architecture. The class diagrams of the AMET are presented in Appendix A.
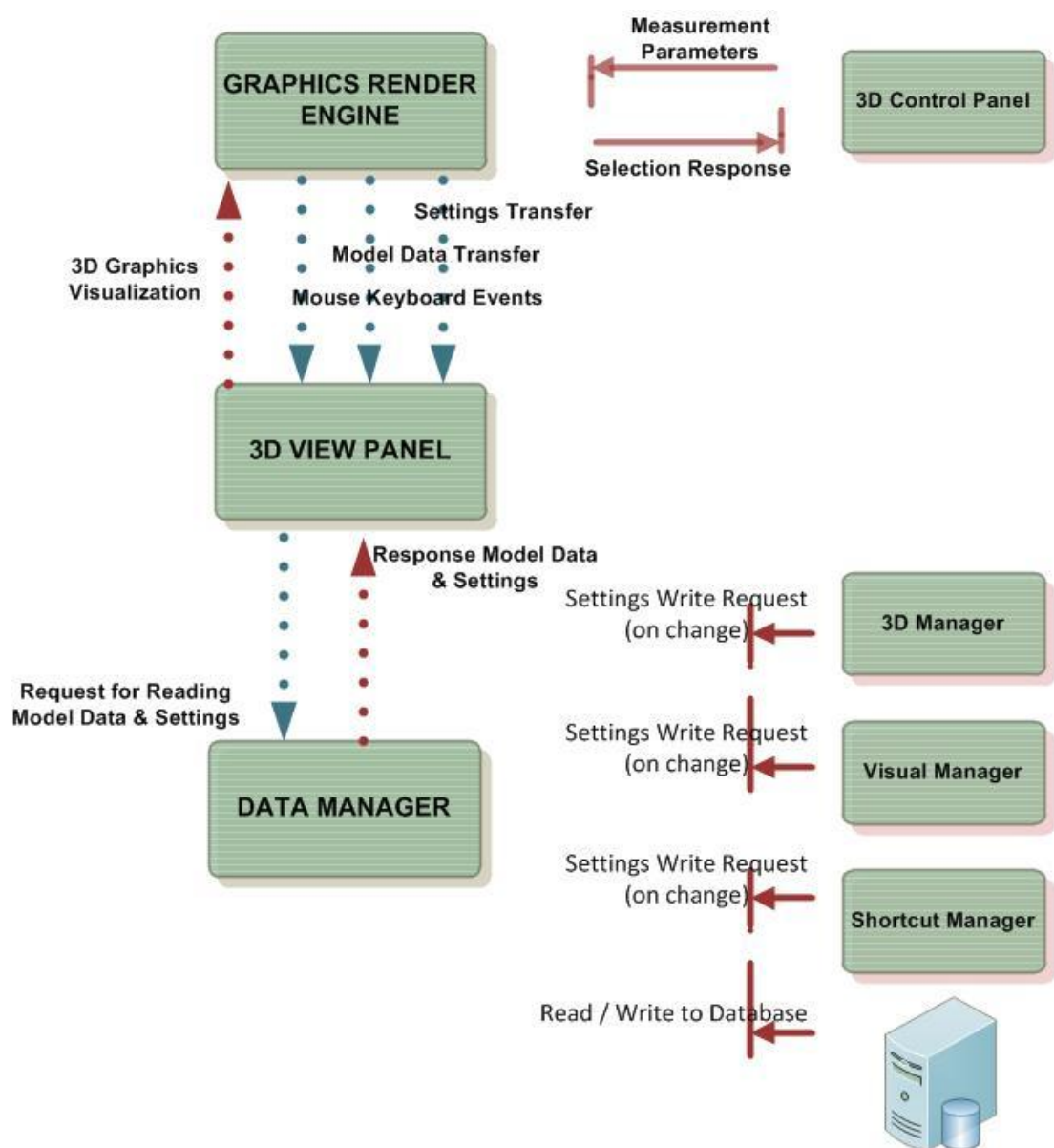
Figure 5.2 Software Architecture

5.2 Graphic Rendering

Open Graphic Library is used for graphical rendering to take advantage of a widely used cross-platform availability. By the nature of the OpenGL, there are four functions needed to be implemented to conform the interface of graphic rendering; init(), display(), reshape(), displayChanged(). Init() function is called when rendering initially started, this function is where lighting, shading, performance factors, projection configuration, display lists, frame per second (FPS) settings are set. display() function is always called in loop to render each frame, interactive drawings are made by using this function. reshape() function is called when the window is reshaped, this function is where reconfiguration of the projection is made. displayChanged() function is for multi display systems and not required to be implemented for single display systems. In this study, java wrapping of the OpenGL framework: JOGL is used. JOGL pack for the OpenGL comes together with such useful objects; one of them is Animator class. Animator is a thread class that calls display() function, conforming the frame per second setting which is set in the init() function. In the study graphic rendering operations and functions implemented together as a render engine modulo. In this modulo graphic rendering layout is set as follows;

- ❖ Initialization function of rendering
    - ✓ Projection configuration
    - ✓ FPS(Frame per second) configuration
    - ✓ Clearing graphic rendering area
    - ✓ Positions and types of lights
    - ✓ Initial model drawing by using display lists
    - ✓ Shading configuration
- ❖ Display function of rendering
    - ✓ Clearing graphic rendering area
    - ✓ Scene drawing methods (Selection Mode or Render Mode)
- ❖ Reshape function of rendering
    - ✓ Projection configuration (Every time when window is resized projection needs to be reconfigured)

Projection transformation defines a viewing volume. The viewing volume is used to project an object on the screen and it defines which objects or portions of objects are clipped out of the final image. Viewpoint could be thought of existing end of the viewing volume. In this study, perspective projection is chosen to take action in the graphic rendering as projection method.

In this study, GLU (Graphic Utility Library) is used which is a complement library for OpenGL to ease the coding of projection. The gluPerspective is a utility function which configures the perspective in accordance with these parameters; fovy, aspect, near, far. This function creates a matrix for a symmetric perspective-view frustum and multiplies the current matrix by it. The fovy argument is the angle of the field of view in the x-z plane; its value must be in the range [0.0, 180.0]. The aspect ratio is the width of the frustum divided by its height. The near and far values are the distances among the viewpoint and the clipping planes, along the negative z-axis. They should always be positive (Angel, 2001). For the study, standard perspective values are chosen as; 30 degrees for fovy, one unit for near and 1000 units for far value, width and height values parametrically changed as window of the graphic rendering frame resized by the user.
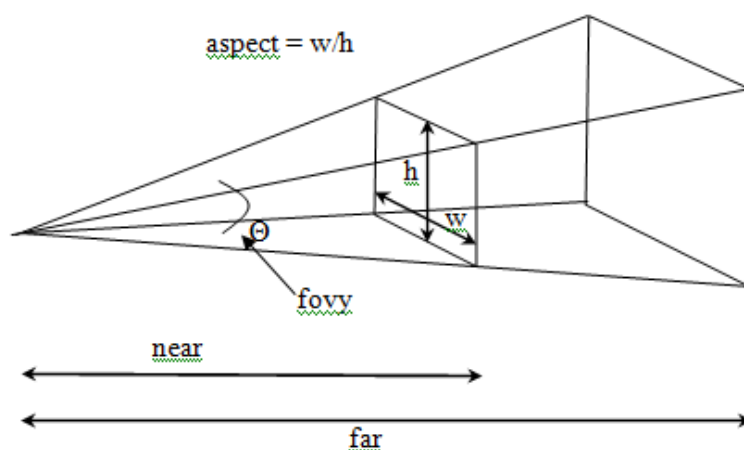
Figure 5.3 Perspective Projection

5.3 User Interaction

User interaction with the model is either by keyboard or mouse. Keyboard controls include changing camera view such as zooming, panning, rotating the model and of course resetting the model back to its initial position. Desired point is selected with mouse at anywhere on the model by left mouse clicking.

5.3.1 Rotation, Zoom and Pan

Rotation, zoom, and pan functionality are connected to mouse drag events. These properties are very important for user interaction with the object. The position and orientation of the viewpoint can be changed by using viewing transformation. The camera is positioned by the viewing transformation. Transformation achieved in two ways, either you can move the camera or you can move all the objects in the opposite direction.

Projection method is chosen as a perspective projection. Perspective projection moves the object scene along the z-axis. It will give a feel of coming near to object or going far from the object to the user. As a zooming functionality we used this trick, if graphic render engine detects parameters from the user as input, all transformation is applied to object -move it along the negative/positive direction of the z-axis. To transform the object in $x - y$ axis, similar transformation method is used. Rotation is provided by glRotate function in OPENGL. When user wants to rotate the object is rotated by 10 degrees (by default) in the user specified direction.

5.3.2 Point Selection by mouse

Selection is important for interaction on the model. Users have to select any part on the model to measures of the interested part. All measurement is calculated by using these selected points. Therefore, all points which generate the model are transformed to selection mode in OPENGL. But, OpenGL does not allow the points to be selected (or interact with). For this reason points are transformed to tetrahedron volume. This transformation provides an interaction between points and user. Another problem in selection process is to determine which object was selected in a

three dimensional scene. At this point, OpenGL provides a selection mechanism that automatically tells to user which objects are drawn inside a specified region of the window. This mechanism can be used together with a special utility routine to determine which object is within the region and which object is specified, or picked, with the cursor by the user.

Selection is actually a mode of operation for OPENGL; feedback is another such mode. The usual rendering calculations are performed by using graphics hardware and OpenGL in feedback mode. OpenGL returns (or feeds back) the drawing information to user. In both selection and feedback modes, drawing information is returned to the application rather than being sent to the frame buffer, as it is in rendering mode. Thus, the screen remains frozen –no drawing occurs- while OpenGL is in selection or feedback mode.

5.4 Measurements and Calculations

The main objective of the developed tool is to make measurements over a 3D model of the aorta. This process helps experts in the stent selection for the patient. After the model is generated, different measurements can be made on 3D aorta model with interactively. These measurements are used in the process of stent selection. Different mathematical formulas are used in three dimensional spaces in the process of measurements. Quantitative data have been obtained with these formulas by using point value of the 3D model. On the basis of measurement, selecting of points on the model has critical importance. Because, each calculation performed by using these values. Developed tool provides length, angle, and diameter measurements over the model. These measurements are important during the stent selection process. All the measurements and measurement 3D position are transferred to the Control Panel. Appropriate measurement values are transferred to Report panel by the physicians. These values determine the final measurement value.

Anatomical criteria used to select the type of the graft were explained in section 2.2.1. The length of the aortic neck, aortic neck diameter, supra-renal and infra-renal angle (neck angulations'), between the lowermost renal artery and the aortic

bifurcation length, length of each iliac segment and diameter of each iliac segment are the most important measurement values. These measurements are very important to planning of endovascular repair. According to these criteria, tool must provide length, diameter and angle measurement properties to the physicians.

Length measurements are calculated in two ways: Delta length or cumulative length. Delta length calculation is based on Euclid distance. It can be measure between two selected points or it can be measure across any pair of points on the model. Cumulative length can be measure only via center points. Cumulative length is calculated between slices from first selected point to second selected point cumulatively. Figure 5.4 clearly points the difference between delta and the cumulative measurement.

a   b
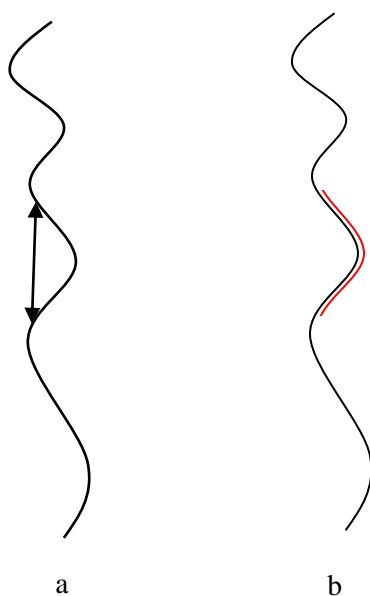
Figure 5.4 (a)Delta distance
(b) Cumulative distance

To facilitate the angle measurement of the aorta, the Middle Center Line Path (MCLP) is created. Center point for each cross section is composing the MCLP. Middle point is calculated using the formulation described in section 4.4. The MCLP provides a line in the aorta. This line is used for realistic model of the angulation calculation process. Aortic neck angulation is generated from selected reference

points on the middle path. To obtain an angle measurement, at least 3 reference points are necessary. However, points located on each slice must be selected carefully to get more accurate results. AMET calculates the aortic neck angulations from selected reference points on the 3-D model using formulations below.

$$\overrightarrow{BA} \cdot \overrightarrow{BC} = \left|\overrightarrow{BA}\right| \cdot \left|\overrightarrow{BC}\right| \cdot Cos(\alpha) \tag{11}$$

$$\overrightarrow{BA} \cdot \overrightarrow{BC} = (x_1 - x_2)(x_3 - x_2) + (y_1 - y_2)(y_3 - y_2) + (z_1 - z_2)(z_3 - z_2) \tag{12}$$

$$\left|\overrightarrow{BA}\right| = \sqrt{\left((x_1 - x_2)^2 + (y_1 - y_2)^2 + (z_1 - z_2)^2\right)} \tag{13}$$

$$\left|\overrightarrow{BC}\right| = \sqrt{\left((x_3 - x_2)^2 + (y_3 - y_2)^2 + (z_3 - z_2)^2\right)} \tag{14}$$
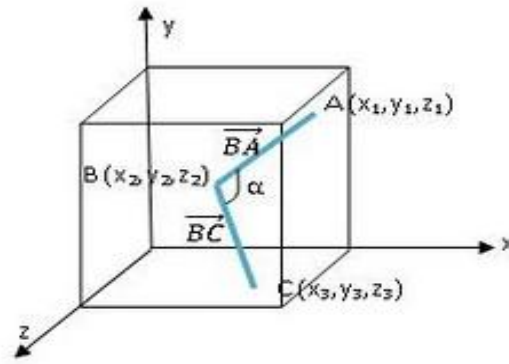
Figure 5.5 Angle calculation

If equation 11 is rewritten as,

$$\alpha = Arc\cos\left(\frac{\overrightarrow{BA} \cdot \overrightarrow{BC}}{\left|\overrightarrow{BA}\right| \cdot \left|\overrightarrow{BC}\right|}\right) \tag{15}$$

Where A, B, C are the reference points and alpha is the angle. AMET has a flexible user interface where users can easily rotate or transform model to decide reference points located on middle-path.

Diameter measurements are made in two ways: Manual and/or automatic. In the manual method; two points are selected in relevant cross − section to determine the diameter by the physicians. Diameter calculation is based on Euclid method. Physicians can measure diameter across any pair of points over the 3D model. In automatic method, physicians selects relevant cross − section from the model. After that, the maximum diameter is calculated automatically. To obtain automatic diameter calculation, physicians should push the diameter button on the 3D Control Panel. This calculation brings the program as a novelty. To perform automatic diameter, the distance is calculated according to the Euclidean distance formula for each two points over the selected slice and the maximum diameter value is calculated.

5.5 Basic User's Guide

The AMET software has the capability to process DICOM images, to segment the aorta via the parameters determined through the DICOM images, to create the model of the aorta from the point data obtained as a result of this segmentation and to make measurements using this model. The AMET software has specialized menus for various functions. These menus allow the specialist to use the software. This part is presented in Appendix B. In this section the software usage steps are explained

5.5.1 Workflow.

The steps below serve as a general guide for the sequence to the physicians for create a new 3D aorta modeling and measurement process.

At the first stage, the specialist loads the CT data for the relevant patient in the software. During this period, the data of the patient are loaded to the DICOM image editor panel. It is possible to navigate the CT cross sections of the patient by using DICOM tree panel. The patient's personal information is loaded to the Patient Info panel. Figure 5.9 illustrates the cross section image from the DICOM image editor for a patient whose CT images have been loaded.
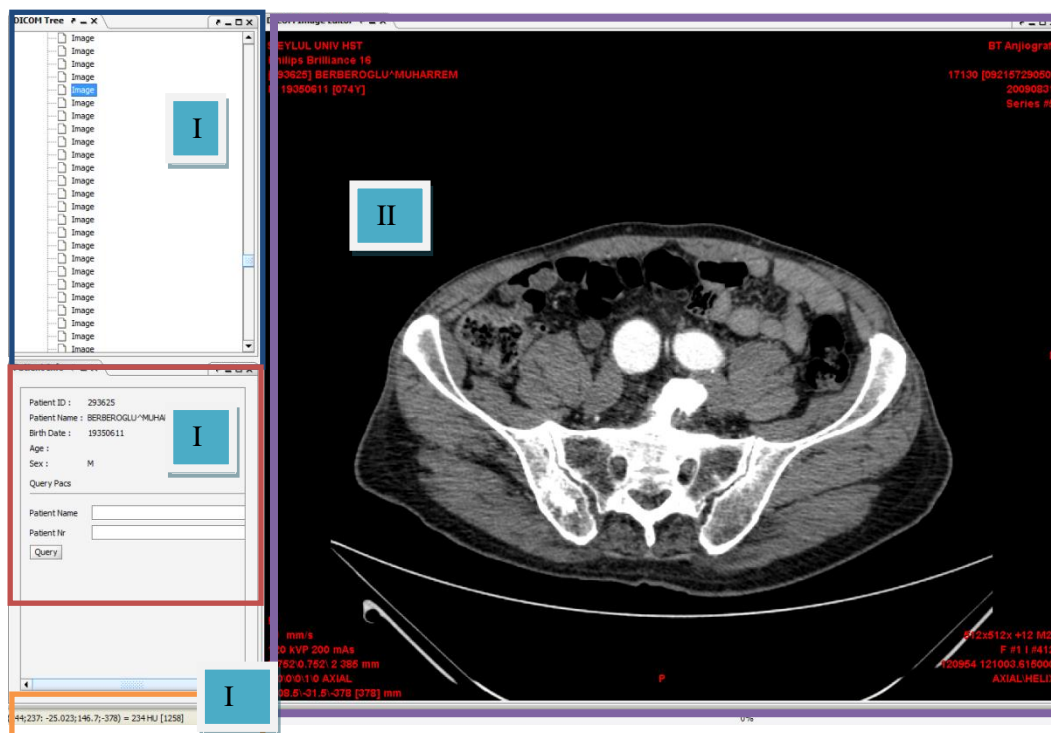
Figure 5.9 (I) DICOM Tree Panel, (II) Patient Information Panel, (III) DICOM Image Editor
Panel. (IV) HU values according to mouse position over the image

For the specialist to create the 3D model of the aorta, having assessed the patient's
CT cross sections, he / she needs to select the aorta by marking the reference points
on the relevant cross sections. The specialist needs to go to the relevant place on the
image, right click, and choose the option "set reference point" for the selection
operation from the popup menu. The selected reference points are automatically
transferred to the Segment panel. Once all reference points are selected, the specialist
needs to start the segmentation period by inputting the relevant threshold values. The
Hounsfield Unit (HU) values of the tissue are presented as a mouse dependant
interaction on the lower part of the DICOM panel to identify the threshold values.
The specialist should select the threshold values in accordance with these values.
Figure 5.10 illustrates the necessary function and segmentation the specialist needs to
carry out for the segmentation period.
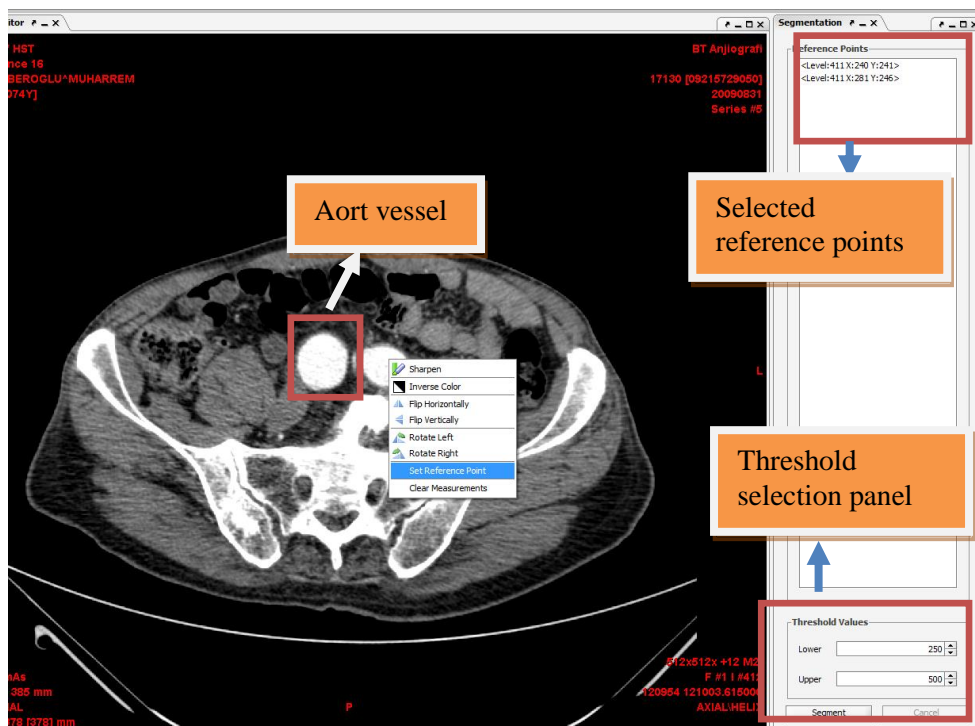
Figure 5.10 Segmentation Process

After the segmentation period, AMET will automatically navigate through all of the relevant cross sections and find the aorta in every single cross section. The cross sectional values obtained will be transformed into point data by passing through edge and midpoint determining algorithms. Here, a 3D value is appointed for the 2D point data. This value is determined in accordance with inter – slice interval between each cross section. Thus, the two dimensional cross sectional structure becomes a three dimensional point structure. By using the "Generate 3D" button on the toolbar, a 3D model of the aorta is established. By using the OPENGL model, it is established in the "3D View" panel. Selecting "3D" from the View menu enables the specialist to see the model formed.

The environment where the aorta is established and the user can interact with the model is the 3D view panel. Either by using a mouse or the short cut keys the specialist can carry out activities such as transformation, pan, and zoom on the model. The established model is a point display. Also established within the model, is the Middle Center Line Path (MCLP) obtained from the midpoints found. Every point forming the MCLP has the necessary features allowing the specialist to select.

The specialist can choose any points on the line in order to carry out measurements. Figure 5.11 illustrates the established aorta after the segmentation period. On the left is a point aorta display and on the right is a surface view. Illustrated in the picture on the left is the MCLP.
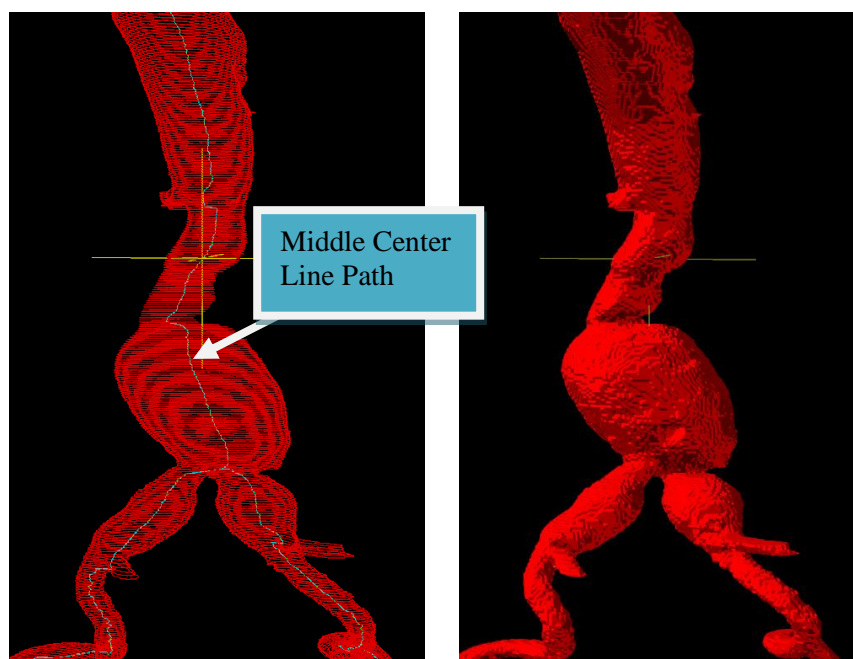
Figure 5.11 3D Model of Aorta (left side model generated by using point data, in right side surface constructed)

Once the specialist moves onto the 3D display 5 panels appear. These panels are the slice view panel, the DICOM Image editor, the 3D view, the 3D Control panel, and the Measurement report.

At the Slice view panel, the point display of the selected cross section is presented to the specialist. The specialist can either carry out measurements on the model or by using the point data given in the slice view. This measurement provides the diameter of the aorta cross section.

The DICOM Image editor panel has been designed to give the specialist information on the selected cross section. At this panel, the CT cross section is

displayed as a whole (not segmented). This panel enables the specialist to choose during the measurement stage.

The 3D view panel is where the model is established. It is where user interaction takes place and where the model is displayed. The model is established on this panel using OpenGL. The specialist can carry out observations of the model from all perspectives. By using rotate, zoom, and pan it is possible for the specialist to focus on the desired region of the aorta and carry out measurements.

The entire measurement period is managed through the 3D Control panel. The 3D Control panel is the panel that marks the measurement chosen on the model by the specialist. The specialist is able to measure diameter, length, and angles using the options on the panel. The measurement values taken are transferred to the measurement history section as position and value automatically. Later on, the specialist can carry chosen values from this panel to the Measurement Report panel. The specialist can change the values in the report panel anytime they want if they have made a mistake. The values transferred to the measurement report section are finally presented to the specialist as a report. Figure 5.12 illustrates all the panels that appear before the specialist in 3D mode.
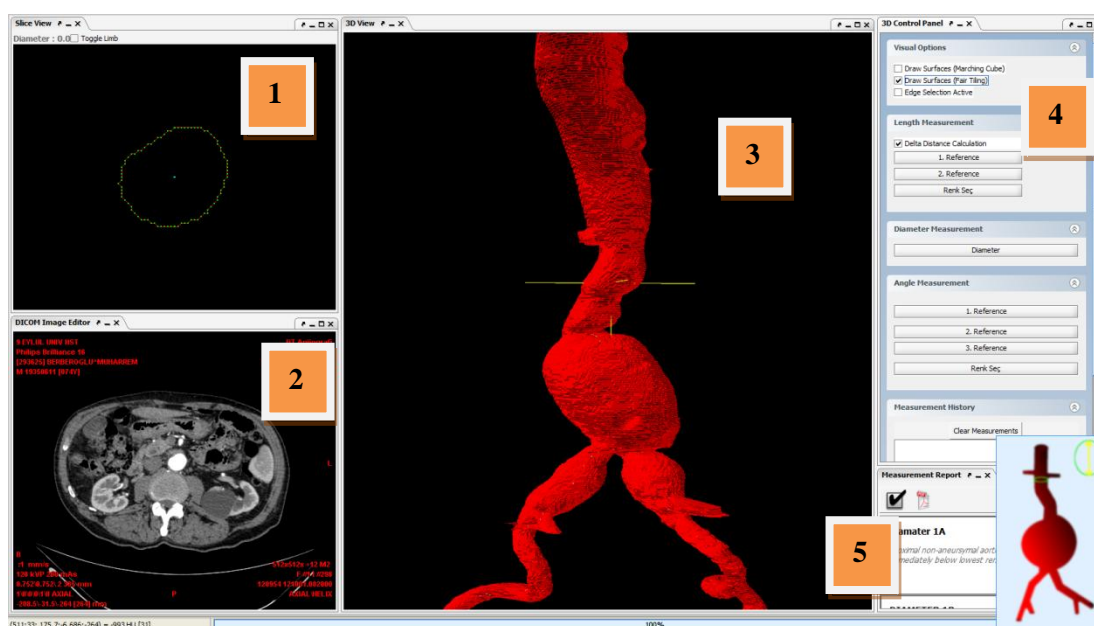
Figure 5.12 AMET in 3D View Mode (1) Slice Viewer (2) DICOM Image Editor (3) 3d View Panel (4) 3D Control Panel (5) Measurement Report.

The objective of preparing AMET is to enable the specialist to carry out measurements during the stent selection period via the aorta. The diameter, length, and angle calculations made using AMET are in accordance with the options chosen from the 3D Control panel. Visual Options, Diameter Measurement, Angle Measurement, Length Measurement, and Measurement History are the fields that constitute the 3D Control panel. The specialist determines the measurement values required using the available options. Figure 5.13 illustrates the Control Panel.

Options in forming the surface are available in the Visual Options section. The specialist can move from point data to volumetric display in two ways, either by using the marching cube method or by using the Fair Tiling method. In sections 4.6.1 and 4.6.2 are detailed explanations of both methods. The other important part of the Visual Options section is the "edge selection active" option. This option makes all points forming the model selectable. This option is set to 'closed' as default. Performance decreases graphically once in this mode. The aim of this mode is to allow the specialist to measure from any edge point requested. Whether it is diameter or length calculations the specialist can carry out these calculations from any edge point it wants when in this mode.

Figure 5.13 3D Control Panel

It is possible to carry out two different measurements on the aorta. The reference points in the Length Measurement section need to be determined in order to enable the specialist to carry out these measurements. Figure 5.14 illustrates the measurement values carried out by delta length and cumulative length on the model.
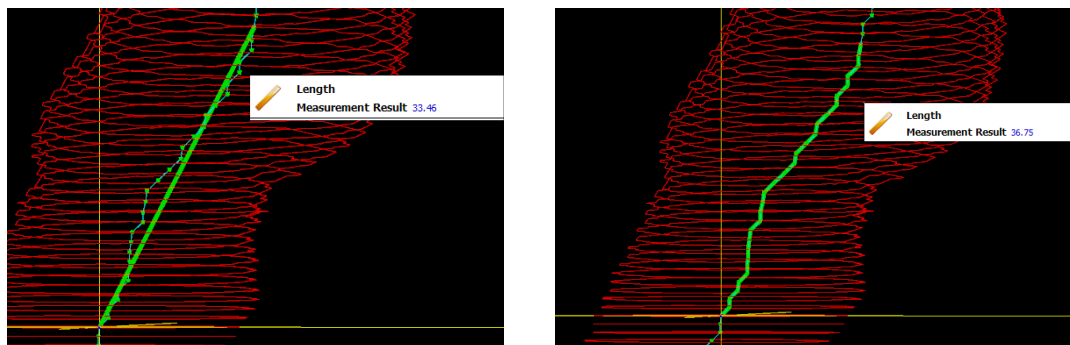
Figure 5.14 Length calculations over the 3D model (Delta length and cumulative length.)

Measuring the diameter is the other measurement carried out on the model. Information in regards to the longest diameter of the cross section is given to the specialist automatically. The specialist either may use this information or may carry out measurements using the points selected specifically. The specialist must choose the Diameter option on the 3D Control panel for measuring the diameter. This option provides the specialist with information on the longest diameter within the cross section. Another option is choosing two points and calculating the length using the Slice View panel. Figure 5.15 illustrates forms of measuring diameter.
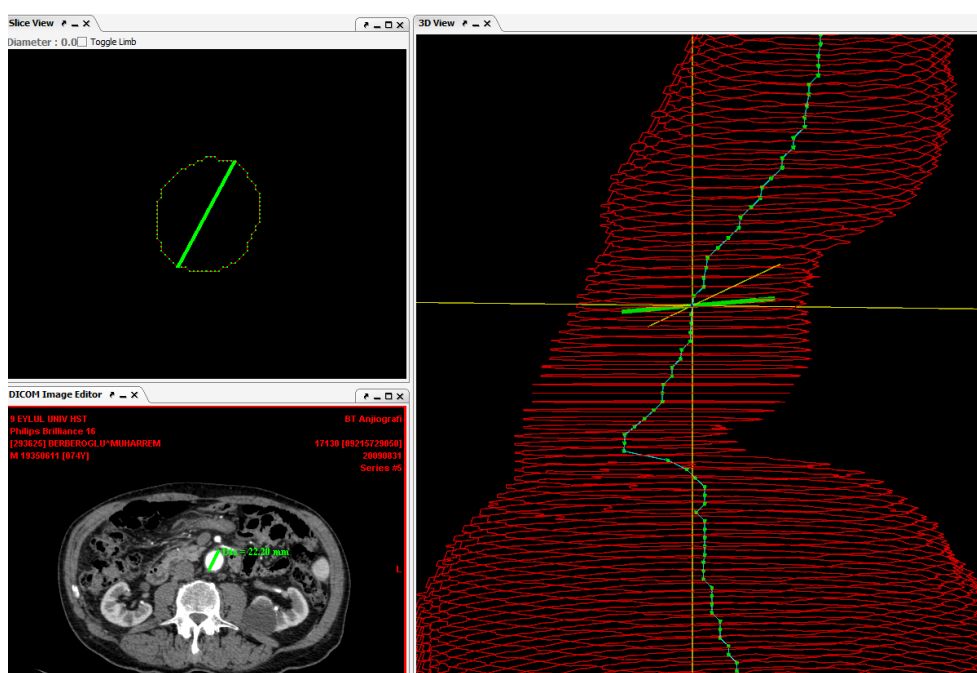
Figure 5.15 Diameter

The diameter value appears on the slice view panel, the DICOM Image editor, and the 3D View Panel for the specialist to see. Calculating the angle is another measurement stage. An angular value appears for the specialist from a three dimensional perspective in calculating angles. The specialist needs to choose the Angle Measurement option on the 3D Control panel when calculating angles. In this section, the specialist needs to select three points from the midpoint. After selecting three points, an angular value appears for the specialist. Figure 5.16 illustrates the angle measurement display.
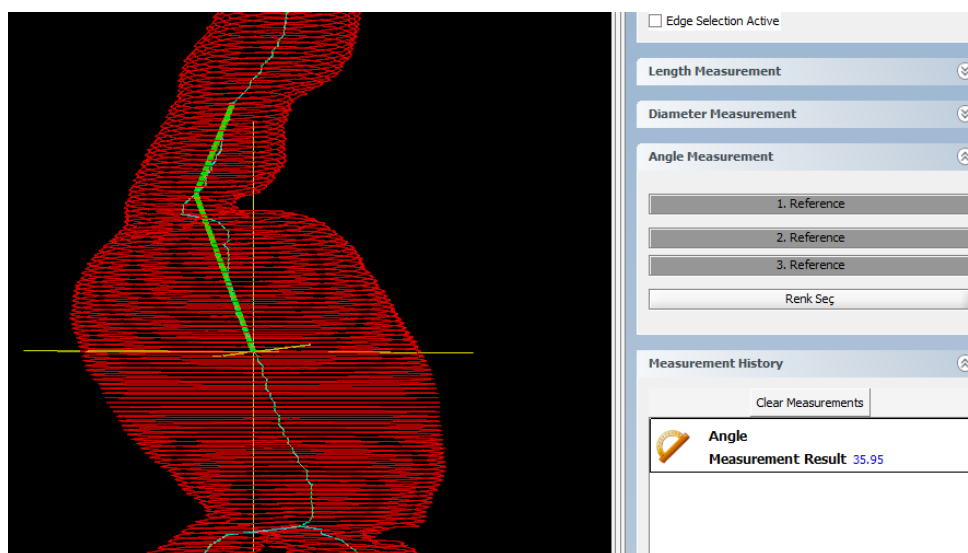
Figure 5.16 Angle Measurement

This whole process displays how the AMET software works. This software enables the specialist to carry out measurements rapidly, from a 3D perspective, and with a user-friendly interface. AMET enables different measurement capabilities to the specialist during stent determination period. The developed software is a specific tool to the modeling of the aorta and to enabling measurements on the aorta.

CHAPTER SIX
EVALUATION OF AMET ON THE TEST DATASET

An accurate measurement of the arterial anatomy (reliable morphological evaluations) is one of the most important determinants of the endovascular abdominal aneurysm indication. Aorta iliac anatomy is easy to understand conceptually, however, it is difficult to define and measure quantitatively. Therefore, AMET is developed for arterial anatomy measurements. AMET provides broader measurement capabilities to the physicians. Measurements were made to prove the AMET reliability, consistency, and accuracy by the physicians. These measurements were made in both methods to compare each method (Manual method and AMET). In this chapter statistical results are presented and their results are explained.

6.1 Properties of the Test Dataset

Data obtained from 100 consecutive patients electively treated with EVAR by the Interventional Radiology Department, university of Dokuz Eylul from January 2005 to March 2010, were analyzed retrospectively. Among the patient group, 33 patients were randomly selected which are suitable for the evaluation of the automated measurement platform. Preoperative investigation of 33 patients consisted of MDCT scans.

Multidetector CT examinations were performed by using a four–detector row scanner (Philips Medical Systems, the Netherlands). One hundred milliliters (300 mg of iodine per milliliter) of a nonionic intravenous contrast material was administered, through a 20-gauge catheter inserted into an antecubital vein, at a rate of 4 mL/sec by using a power injector. Arterial phase imaging was performed by using bolus tracking. CT parameters were set at 120 kVp and 180 mAs and a 1.00-mm detector configuration was used. Three-millimeter-thick sections were reconstructed and downloaded to the picture archiving and communication system.

6.2 Anatomical Factors

Suitable patient selection is the most important determinant of EVAR outcome. Clinical studies show that especially aortic neck diameter, proximal aortic neck angulations and proximal aortic neck length are critical parameters to perform aneurysm repair successfully. Therefore, these measurements must be made correctly to achieve suitable placement of the stent.

Several studies have reported that adverse proximal aortic necks were correlated with adverse outcomes. Many researchers have showed the associations between anatomic features and stent graft repair success. (Hovsepian, & et al, 2001) used the AneuRx device and found that short proximal neck was significantly associated with an increase complications and death. Stanley et al. found that risk of proximal endoleak increased with every millimeter of decrease in neck length less than 20 mm. (Dillavou, & et al., 2003) showed the neck anatomy is the major determinant for suitability of the patients for endovascular repair. Parody has reported that the length and the diameter of the proximal aortic neck and distal iliac arteries have to be precisely known for perfect stent fixation. (Aarts, & et al., 1999) reported their experiences that neck length and iliac arteries diameter are essential for successive exclusion of the aneurysm. On the other hand increasing degrees of aortic neck angulations have been associated with adverse outcomes following endografting for AAA. (Sternbergh, 2002) described their experience with the AneuRx endograft and showed aortic neck angulation appears to be an important determinant of outcome after EVAR. (Robbins, & et al., 2005) examined the association of such anatomic factor, proximal aortic neck angulation, with the incidence of adverse events following EVAR. Also (Albertini, & et al., 2000) showed a direct association between aortic neck angulation and adverse outcomes. (Rockman, & et al., 2002) reported their experience that shows the association between endoleaks and aortic neck angulations.

All these study showed that determination of aneurysm morphology is very important step for patient evaluation and selection before the endovascular planning.

6.3 Measurement Methods

Aortic anatomy was acquired from preoperative CT scans and angiograms. CT is required preoperatively to define the arterial anatomy, to make the necessary diameter and length measurements, and to permit patient selection and determination of the required implant size. Three-dimensional reconstructions of MDCT images were prepared using multiplanar maximum intensity projections (View Forum 4.1 – PMS 1.1 MIMIT, Philips Medical Systems) and MPR reformatted images which provides the measurement in 2-D over sagittal, coronal or axial images which are generated by post-processing software as the manual method. In manual method, aortic diameter was assessed directly from digital CT scans displayed on a workstation. The diameter measurements were performed on the minor axis with digital calipers. Neck length, the presence of a neck bulge, or reverse taper neck was assessed from CT scans with confirmation as needed from the angiography. Preoperative arteriograms were obtained selectively for questionable access or neck anatomy. Pre – deployment angiography with a marked catheter was taken in anterior – posterior with approximately 15 degrees of cranial – caudal angulations before endovascular graft selection. Manual measurement method screen shots are given in Appendix – C.

Two radiologists (Prof. Dr. Ahmet Yiğit Göktay and Asst. Prof. Dr. Aytaç Gülcü with 10 years and 7 years of CT angiography experience, respectively) in consensus evaluated and verified the arterial phase data to perform post-processing studies and calculate the proximal aortic neck, proximal aortic diameter and aneurysm length with manual method and a few weeks later with AMET. Same radiologists evaluated a subgroup of previously selected patients (13 patients) two months later with same manner.

Measurement results are summarized in table 6.1 for 33 patients. The results of all groups were compared statistically. The Paired Samples T-Test analysis was used to evaluate the relationship between these two data groups. Paired Sample T – Test assesses whether the means of two groups are statistically different from each other.

This analysis is suitable to compare the means of two groups. All statistical analysis was performed using SPSS 17.0 (SPSS Inc. Chicago, IL).

In order to verify the accuracy of the tool, measurements are carried out on the patients' CT images at different times by using both manual methods and the AMET. Thirty-three (33) patient groups were used to carry out these measurements. Table 6.1 illustrates the results of measurements carried out by specialists using the manual method and the AMET. Two months after the completion of measurements using the manual method, measurements were carried out using the AMET. During measuring, the patients were chosen at random and in no particular order.

The measurement took place in accordance with the anatomical criteria used by the specialists. Therefore, the chosen measurements were the aneurysm length, the proximal neck diameter, the proximal neck length.

Table 6.2 illustrates the general statistical distribution of the 33 patients. The mean values and the interclass correlation values of the measurements are given in this table. It has been previously reported that, if correlation value is $> 0.90 =$ excellent, $> 0.80\text{-}0.89 =$ high, and $>0.70\text{-}0.80 =$ acceptable (Vincent, 1999). There is an acceptable level of compliance between the manual method and AMET in accordance with values of the proximal neck diameter, and the proximal neck length (acceptable level: 0.70). There is not an acceptable level of compliance among the measurements carried out for the aneurysm length.

Tablo 6.1 AMET - Manual Method Measurement Results (for 33 patients)

	Manual Method			AMET		
	Aneurysm Length	Proximal Neck Length	Proximal Neck Diameter	Aneurysm Length	Proximal Neck Length	Proximal Neck Diameter
1	132,9	31,5	23,4	118,24	20,9	30,38
2	123,9	51,6	22,5	144,98	61,74	23,88
3	121,6	44,5	22,5	124,05	46,44	22,31
4	99,4	32,8	18,7	127,48	18,71	18,8
5	125	28,8	25,1	141,61	33,39	26,77
6	148	46,7	28,6	157,93	48,58	27,3
7	97,5	46,1	22,3	129,11	29,67	20,97
8	129,4	64,7	21,8	127,53	25,05	22,39
9	125	54,7	21,1	143,49	35,66	20,88
10	145,1	50	16,5	169,99	40,91	17,8
11	100,4	26,7	21,2	109,7	31,95	22,83
12	109,4	45,3	20,4	113,67	49,85	18,93
13	123	50	23	142,69	23,49	22,58
14	130,9	28,9	18,3	121,1	33,59	18,4
15	154	18	17	159,48	26,26	20,4
16	141,2	44,4	25,8	144,29	31,52	21,98
17	154,9	16,9	22,9	152,38	24,74	32,67
18	140	46,3	22,1	170,94	31,14	22,92
19	185,8	7	22,8	123,83	18,74	23,95
20	108,1	28,5	18	119,68	30,34	19,66
21	97,9	14,7	20,1	129,25	15,83	20
22	120	40	16,8	106,97	18,19	18,86
23	113	39,7	18	120,32	43,12	18,46
24	142	36	21,8	166,28	38,6	21,81
25	160,6	52	20,4	147,6	54,76	19,91
26	145,1	41,5	21,5	161,27	20,25	21,18
27	115,7	41,9	23	126,44	34,93	30,43
28	175,7	64,7	21	131,44	43,56	25,14
29	144,4	61,2	22,6	149,43	70,09	27,18
30	103,4	43,2	21,8	132,36	48,99	20,65
31	124,5	36,5	16,8	137,97	38,07	17,59
32	93	7	20,3	115,57	9,36	22,5
33	177,7	42,5	28,2	134,15	27,2	29,24

Table 6.2 Patient Statistics for 33 patients (A.L. * Aneurysm Length, P.N.L. * Proximal Neck Length, P.D. *Proximal Diameter)

	Patient Statistics		Intraclass Correlation Coefficient		
				95% Confidence Interval	
	Mean	Std. Deviation	Intraclass Correlation (average measures)	Lower Bound	Upper Bound
Manual Method(A.L.)	130,5606	24,15836	0,604	0,214	0,803
AMET (A.L.)	136,4006	17,66399			
Manual Method (P.N.L)	38,918	14,8781	0,732	0,451	0,869
AMET (P.N.L.)	34,11	13,7588			
Manual Method (P.D.)	21,403	2,96337	0,79	0,534	0,901
AMET (P.D.)	22,6894	3,96259			

For the aneurysm length, the interclass correlation coefficient between the manual method and the AMET was founded 0,604, and the 95% confidence interval was founded 0.214 – 0.803. These values verified that the compliance was below the acceptance level (acceptance level: 0.70).

After evaluating the statistical result belonging to the Proximal neck length, the interclass correlation coefficient between the manual method and the AMET was 0,732, and the 95% confidence interval was 0.451 – 0.869. These values verified that the compliance was at an acceptable level (acceptance level: 0.70).

For the Proximal diameter, the interclass correlation coefficient between the manual method and the AMET was 0,790, and the 95% confidence interval was 0.534 – 0.901. These values verified that the compliance was at an acceptable level (acceptance level: 0.70).

In addition to all these general measureable values, the differences between the measurement values were compared by applying a T-Test to the measurements. Table 6.3 illustrates these values.

Table 6.3 T – Test Results for 33 patients (A.L. * Aneurysm Length, P.N.L. * Proximal Neck Length, P.D. *Proximal Diameter)

	Paired Samples Correlations	Mean	Std. Deviation	Std. Error Mean	Sig. (2 - tailed)
Manual Method(A.L.) **AMET (A.L.)**	0,464	-5,84	22,35	3,89065	0,143
Manual Method (P.N.L.) **AMET (P.N.L.)**	0,605	4,8085	12,7607	2,2213	0,038
Manual Method (P.D.) **AMET (P.D.)**	0,721	-1,28636	2,748	0,47847	0,011

The paired samples correlation coefficient in the table verifies relations between group distributions. The values of the paired sample test, illustrated in the table 6.3, determine whether or not there are different significances between the samples. The mean of the samples represents the values of the paired samples. Thus, if there is a significant difference between their two-tailed test values this shows that these two clusters belong to different samplings. The value taken into account for the two-tail test is whether it is below or over 0.05. When the measurement values for the proximal neck length and the proximal neck diameter is evaluated, it is clearly seen that they are below 0.05. This verifies that there is a significant difference between these samplings. This value appeared on the border for proximal neck length. There is no significant difference for the aneurysm length measurements.

As seen from the values, different statistical results are obtained between the manual method and the AMET. According to the T-test results, there are no significant differences between the means of the aneurysm length. The difference for the proximal neck length is close to the border (the two-tail test result for the proximal neck length was 0.038), But, there was significance difference in the proximal diameter (the two-tail test result for the aneurysm length was 0.011).

According to the overall statistical results obtained for the measurement values, there is a similarity between measurements by the manual method and the AMET. In order to test which method is more reliable, consistent, and repeatable a sub-group of

the 33 patients was chosen at random. The number of patients seen adequate for the sub-group was thirteen. Testing of the systems was carried out by redoing the measurements on the sub-group, both with the manual method and the program. Table 6.4 illustrated the manual measurement values obtained by the specialists for the thirteen patients. Table 6.5 illustrates the AMET measurement information. AMET measurements achieved three weeks after the completion of measurements using the manual method on the sub-group patients. During measuring, patients were chosen at random and in no particular order.

Table 6.4 Manual Measurement Results (for 13 patients)

	Manual Method I			Manual Method II		
	Aneurysm Length	Proximal Neck Length	Proximal Neck Diameter	Aneurysm Length	Proximal Neck Length	Proximal Neck Diameter
1	160,6	52	20,4	160	51	18,5
2	97,9	14,7	20,1	123,2	21,3	18,6
3	154	18	17	149,9	20,7	19,4
4	175,7	64,7	21	175,3	77,1	18,2
5	124,5	36,5	16,8	130,4	51,5	16,8
6	141,2	44,4	25,8	125,8	50,2	22,9
7	177,7	42,5	28,2	173,2	56,4	22,3
8	113	39,7	18	116	45,6	14,9
9	100,4	26,7	21,2	111,3	31,9	21,6
10	144,4	61,2	22,6	187	102	17,9
11	115,7	41,9	23	113,9	43,9	21,1
12	125	54,7	21,1	114,9	65,5	20,9
13	121,6	44,5	22,5	133,4	57,7	21

Table 6.5 AMET Measurement Results (for 13 patients)

	AMET I			AMET II		
	Aneurysm Length	**Proximal Neck Length**	**Proximal Neck Diameter**	**Aneurysm Length**	**Proximal Neck Length**	**Proximal Neck Diameter**
1	147,6	54,76	19,91	141,43	59,17	19,87
2	129,25	15,83	20	132,66	15,26	18,44
3	159,48	26,26	20,4	155,11	21,89	22,08
4	131,44	43,56	25,14	131,44	51,2	22,2
5	137,97	38,07	17,59	131,97	38,07	18,46
6	144,29	31,52	21,98	144,55	35,36	24,62
7	134,15	27,2	29,24	139,62	30,61	27,88
8	120,32	43,12	18,46	116,29	42,86	18,46
9	109,7	31,95	22,83	108,7	26,02	23,24
10	149,43	70,09	27,18	147,05	69,49	25,99
11	126,44	34,93	30,43	123,98	25,55	28,76
12	143,49	35,66	20,88	141,73	42,15	24,37
13	124,05	46,44	22,31	124,35	50,11	22,31

Table 6.6 Patient Statistics via the manual method repeated for 13 patients (A.L. * Aneurysm Length, P.N.L. * Proximal Neck Length, P.D. *Proximal Diameter)

	Item Statistics		Intraclass Correlation Coefficient		
				95% Confidence Interval	
	Mean	**Std. Deviation**	**Intraclass Correlation (average measures)**	**Lower Bound**	**Upper Bound**
Manual Method 1(A.L.)	134,746	26,523	0,906	0,705	0,971
Manual Method 2(A.L.)	139,562	26,431			
Manual Method 1 (P.N.L)	41,654	15,129	0,854	0,136	0,963
Manual Method 2 (P.N.L)	51,908	21,987			
Manual Method 1 (P.D.)	21,362	3,238	0,742	0,018	0,927
Manual Method 2 (P.D.)	19,546	2,328			

Table 6.6 illustrates the general statistical distribution of patients used in the repeated manual method. The mean values and the interclass correlation values of the measurements are given in table 6.6. In accordance, there is an acceptable level of compliance between measurement values in the first manual method and measurement values from the repeated manual method (acceptance level: 0.70). While this level was "excellent" between the aneurysm lengths, it was "high" for the proximal neck length, and "appropriate" for the proximal neck diameter.

A T-Test was applied to the measurement values obtained via the manual method repeated for the thirteen patients in order to compare the differences between the measurements. Table 6.7 illustrates these values. The paired samples correlation coefficient in the table 6.7 verifies relations for the group distribution. However, according to 2-Tail test results, the values for the proximal neck length and the proximal diameter are lower than 0.05. There is a significant difference between these measurement groups. There is no significant difference between the means of the aneurysm length.

Table 6.7 T – Test Results via the manual method repeated for 13 patients (A.L. * Aneurysm Length, P.N.L. * Proximal Neck Length, P.D. *Proximal Diameter)

		Paired Differences			
	Paired Samples Correlations	Mean	Std. Deviation	Std. Error Mean	Sig. (2-tailed)
Manual Method 1(A.L.)	0,831	-4,815	15,371	4,263	0,281
Manual Method 2(A.L.)					
Manual Method 1 (P.N.L.)	0,906	-10,253	10,456	2,900	0,004
Manual Method 2 (P.N.L.)					
Manual Method 1 (P.D.)	0,737	0,607	2,190	0,670	0,011
Manual Method 2 (P.D.)					

According to obtained values from the manual methods, the reason can be explained behind why the proximal neck length and the proximal diameter values illustrated in table 6.3 are low or near the border. When measurements for the proximal neck length and the proximal diameter are repeated (by using the manual method) their values show no consistency. Results illustrated by Table 6.3, which compare the manual method to AMET, reflect this consistency.

Table 6.8 illustrates the general statistical distribution of patients used in the repeated AMET method. The mean values and the interclass correlation values of the measurements are given in table 6.8. In accordance, there is an acceptable level of compliance between measurement values obtained from the first AMET method and measurement values from the repeated manual method (acceptance level: 0.70). The all values were at a level of "excellent" for the entire measurement criteria

Table 6.8 Patient Statistics via the program method repeated for 13 patients (A.L. * Aneurysm Length, P.N.L. * Proximal Neck Length, P.D. *Proximal Diameter)

| | Item Statistics | | Intraclass Correlation Coefficient | | |
| | | | | 95% Confidence Interval | |
	Mean	Std. Deviation	Intraclass Correlation (average measures)	Lower Bound	Upper Bound
AMET 1(A.L.)	135,200	13,626	0,982	0,940	0,994
AMET 2(A.L.)	133,760	13,015			
AMET 1 (P.N.L)	38,414	13,772	0,972	0,910	0,992
AMET 2 (P.N.L)	39,056	15,609			
AMET 1 (P.D.)	22,796	4,050	0,942	0,808	0,982
AMET 2 (P.D.)	22,821	3,462			

In order to compare the differences between the measurements, the T-Test was applied to the measurement values obtained via the AMET method, repeated for the thirteen patients, Table 6.9 illustrates these values. The paired samples correlation coefficient in the table 6.9 verifies the group distribution relations. When the 2-Tail test results are examined, it can be seen that the values for the entire measurement criteria are above 0.05. There is no significant difference between these measurement groups. In other words, there is no meaningful difference for these measurement groups.

Table 6.9 T – Test Results via the program method repeated for 13 patients (A.L. * Aneurysm Length, P.N.L. * Proximal Neck Length, P.D. *Proximal Diameter)

	Paired Samples Correlations	Paired Differences			Sig. (2-tailed)
		Mean	Std. Deviation	Std. Error Mean	
AMET 1(A.L.)	0,968	1,440	3,414	0,947	0,154
AMET 2(A.L.)					
AMET 1 (P.N.L)	0,950	-0,642	4,978	1,380	0,650
AMET 2 (P.N.L)					
AMET 1 (P.D.)	0,893	-0,025	1,826	0,506	0,961
AMET 2 (P.D.)					

If the repeated AMET measurement values examined as a whole, it can be concluded that measurements repeated using AMET are more consistent and repeatable.

Cronbach's Alpha Model enables comparison of the reliability of the measurement values. Table 6.10 illustrates Cronbach's Alpha results for the repeated tests. As seen from the table 6.10, values obtained for repeated measurements by both the manual method and AMET are high.

Table 6.10 Reliability Test Results

	RELIABILITY
	Cronbach's Alpha
AMET 1 vs AMET 2 (Aneursym Length)	0,983
Manual Method 1 vs Manual Method 2 (Aneursym Length)	0,908
AMET 1 vs AMET 2(Proximal Neck Length)	0,971
Manual Method 1 vs Manual Method 2 (Proximal Neck Length)	0,917
AMET 1 vs AMET 2(Proximal Diameter)	0,938
Manual Method 1 vs Manual Method 2 (Proximal Diameter)	0,822

According to depending on these obtained results, the reliability values obtained from measurements made by AMET are better than values obtained from measurements made by the manual method. AMET produced more reliable statistical values for its repeated measurements. There is measurable evaluation studies carried out on the patients in literature for Endovascular Aneurysm Repair (EVAR). Upon assessing these studies, manual method measurements, carried out by specialists, differ within each other. When the obtained results are evaluated, specialists produce different measurement results statistically.

As a result of the statistical study carried out, it is evident and proved statistically that the AMET provides more reliable, more consistent, and more repeatable results.

CHAPTER SEVEN
CONCLUSIONS

There are many software solutions offered in medical imaging. The developed software solution Aortic Measurement and Evaluation Tool (AMET) overcomes to aneurysm measurement and evaluation problems during the stent selection process for Abdominal Aortic Aneurysm. Hardware needs and operating system independency properties are important features of the AMET. The application offers privatization opportunities and the study presents an aortic measurement and visualization application platform, which is specialized for physicians. The application provides a user-friendly interface and improved measurement capabilities.

The aim of this study is to model of the aortic vein and to provide measurement capabilities on this model. These measurements help to the physicians in the stent selection process. Therefore, the physicians can easily determine stent – graft type. AMET is a platform – independent package, and customized for the modeling and measurement of an aortic vessel.

During the application development process, necessary 3D medical visualization steps were successfully carried out and 3D models of the aorta were obtained. In 3D modeling, different edge detection and surface construction algorithms are available for the medical applications. At the same time, brand new edge detection and surface construction algorithms were constructed and applied. The problems encountered during implementation of these algorithms had been overcome by current medical imaging solutions and the developed new solution methods.

In order to determine the measurable characteristics of the aorta aneurysm new approaches and methods were applied for angle calculation, median centerline determination, the largest diameter and median luminal centerline length calculation. The physicians can easily take measurements with 3D perspective over the 3D model

by using these methods. The middle center line path approach used in this study brings a new perspective to the aortic angle measurement.

In stent–graft, the importance of appropriate stent choice the placement of the selected stent into the suitable location, and identification of possible complications after stent placement cannot be considered separately. Stent selection process which is the first step of the stent–graft is sometimes the most time consuming step. Moreover, monitoring of intravascular stent location before the operation affects the treatment results. In order to overcome these problems the AMET was developed. Depending on the obtained results, it was seen that by using AMET, the time required stent selection process was strictly reduced.

In order to verify the accuracy, reliability, consistency, and repeatability of the AMET, randomly selected patients data obtained from D.E.U Medical Department is used as test data set.

The measurements were made in accordance with the anatomical criteria used by the physicians. The aneurysm length, the proximal neck diameter, and the proximal neck length were selected depending on these criteria. After the statistical studies carried out on the results, obtained from AMET and from the manual method, it was seen that AMET was more reliable, consistent, and repeatable.

Although some commercial and open source software exists for Abdominal Aortic Aneurysm, open source software provides more general purpose solutions and commercial software provides specialized solutions with high cost. To combine advantages of platform independency and specialization in one area, AMET was developed for aorta vein with Java programming language and OPENGL. The AMET is specialized for endovascular planning and also not for profit with its open source property. By using the AMET, the physicians can make measurements easily, reliably, and fast with a user friendly interface.

In the future, the AMET can be enhanced by adding some features to it. One of these features is adding web capability. By using web environment, the 3D model can be transferred to physician's browsers regardless of their physical locations. With these facility physicians can reach the patients' data and can share information with other colleagues. Besides, the data security should also be considered and applied. At the same time, depending on the data obtained from AMET virtual stent applications can be carried out by the physicians and the stent position on the aorta can be monitored before the operation. In this way, the complications can be foreseen by the physicians before the stent – graft.

REFERENCES

Aach, T., Schiebel, U., Spekowius, G., & Gmbh, P. (1999). Digital image acquisition and processing in medical x-ray imaging. *Journal of Electronic Imaging*,7 - 22.

Aarts, N.J.M., & et al. (1999). Abdominal aortic aneurysm measurements for endovascular repair: intra-and interobserver variability of CT measurements, *European Journal of Vascular and Endovascular Surgery,* 18, 475 – 480.

Albertini, J.N., & et al. (2000). Anatomical Risk Factors for Proximal Perigraft Endoleak and Graft Migration Following Endovascular Repair of Abdominal Aortic Aneurysms. *European Journal of Vascular & Endovascular Surgery,* 19, 308–312.

Angel, E. 2001 *Open GL Primer*. 1st. Addison-Wesley Longman Publishing Co., Inc.

Balm, R. (1996). *Transfemoral Endovascular Aneurysm Management*. PhD thesis. Univ. Utrecht, Netherlands.

Bernardini, F., & Rushmeier, H. (2002). The 3D Model Acquisition Pipeline, *Computer Graphics. 21*(2), 149-172.

Bernardini, F., & Rushmeier, H. E., (2000). 3D Model Acquisition, Eurographics 2000, *State of the Art Reports Proceedings, Eurographics Association*. 41- 62.

Bertges, D. J., & et al. (2003). Abdominal aortic aneurysm size regression after endovascular repair is endograft dependent. *Journal of vascular surgery*, *37*(4), 716-23.

Bidgood, W.D., Horil, S.C., Prior, F.W., Syckle, D.E. (1997). Understanding and using DICOM, the data interchange standard for biomedical imaging. *Journal of the American Medical Informatics Association,* 4, 199 – 212.

Blum, U., & et al. (1997). Endoluminal Stent–Grafts for Infrarenal Abdominal Aortic Aneurysms. *The New England Journal of Medicine*, 336(1), 13-20.

Bourke, P., Fuhrman, C., & Dephi, P. (1988). Calculating The Area And Centroid Of A Polygon. Area, (C), 3-5.

Brewster, D.C., & et al. (2003). Guidelines for the treatment of abdominal aortic aneurysms. Report of a subcommittee of the Joint Council of the American Association for Vascular Surgery and Society for Vascular Surgery. *Journal of vascular surgery. 37*(5), 1106-17.

Canny, J. (1986). A computational approach to edge detection. *IEEE Transactions on Pattern Analysis and Machine Intelligence,* 8(6), 679-698.

Cao, P. & et al. (2002). Predictive factors and clinical consequences of proximal aortic neck dilatation in 230 patients undergoing abdominal aorta aneurysm repair with self-expandable stent-grafts. *Journal of Vascular Surgery,* 37, 1200-1205.

Chaikof, E. L., & et al. (2002). Reporting standards for endovascular aortic aneurysm repair. *Journal of Vascular Surgery*, *35*(5), 1048-1060.

Cheng, S.W. (2010). Endovascular Stent Graft for Aortic Diseases. *Graft*, 91-92.

Chew, L.P.(1989). Constrained delaunay triangulations, *Algorithmica*, 4, 97-108.

Choi, B.K., & et al.(1988).Compound surface modelling and machining, *Computer-Aided Design*,20(3),127-136.

Choke E., & et al. (2006). Outcomes of endovascular abdominal aortic aneurysm repair in patients with hostile neck anatomy. *CardioVascular and Interventional Radiology,* 29, 975-980.

Chuter T.A.M., & et al. (1996). Clinical experience with a bifurcated endovascular graft for abdominal aortic aneurysm repair. *Journal of Vascular Surgery,* 24, 655–666.

Cuypers, P. W., Laheij, R. J., & Buth, J. (2000). Which factors increase the risk of conversion to open surgery following endovascular abdominal aortic aneurysm repair? The EUROSTAR collaborators. *European journal of vascular and endovascular surgery*, *20*(2), 183-189.

David, R.W. (1983). Lighting controls for synthetic images, *International Conference on Computer Graphics and Interactive Techniques*,13-21.

Diehm, N., & et al. (2008). Sixty-four–detector CT Angiography of Infrarenal Aortic Neck Length and Angulation: Prospective Analysis of Interobserver Variability, *Journal of Vascular and Interventional Radiology,* 19, 1283-1288.

Dillavou, E. D., & et al.(2003). Does hostile neck anatomy preclude successful endovascular aortic aneurysm repair. *Journal of Vascular Surgery*, *38*(4), 657-663.

Eichelberg, M., & et al. (2004). Ten years of medical imaging standardization and prototypical implementation: the DICOM standard and the OFFIS DICOM toolkit (DCMTK). *Medical Imaging*, 57-68.

Ernst, C.B. (1993). Abdominal Aortic Aneurysm, *The New England Journal of Medicine* 328(16),1167-1172.

Fasquel, J., Agnus, V., & Lamy, J. (2006). An efficient and generic extension to ITK to process arbitrary shaped regions of interest. *Computer methods and programs in biomedicine*, 81(1), 1-7.

Fuchs, H., Levoy, M., Pizer, S.M., (1989). Interactive Visualization of 3D Medical Data,*Computer*, 22(8), 46-51.

García-Madrid, C., & et al. (2004). Endovascular versus open surgical repair of abdominal aortic aneurysm: a comparison of early and intermediate results in patients suitable for both techniques. *European journal of vascular and endovascular surgery*, *28*(4), 365-72.

Geller, S.C. (2003). Imaging guidelines for abdominal aortic aneurysm repair with endovascular stent grafts. *Journal of Vascular and Interventional Radiology,* 14, 263-264.

Gravereaux, E. C., & et al. (2001). Risk of spinal cord ischemia after endograft repair of thoracic aortic aneurysms. *Journal of vascular surgery*, *34*(6), 997-1003.

Ham, A.C., & et al. (2005). Two-Year Outcomes after Conventional or Endovascular Repair of Abdominal Aortic Aneurysms. *Society*, *20*(2), 183-189.

Heath, M.D. , Sarkar, S., Sanocki, T., & Bowyer, K.W.(1997). A Robust Visual Method for Assessing the Relative Performance of Edge-Detection Algorithms IEEE Trans. *Pattern Analysis and Machine Intelligence*, 19(12), 1338-1359.

Horowitz, S., & Pavlidis, T. (1974). Picture segmentation by a directed split and merge procedure. *In Procdings of the 2nd International Joint Conference on Pattern Recognition*, 424 – 433.

Hounsfield, G.N. (1980). Computed medical imaging. *Journal of Computer Assisted Tomography*,4, 665–674.

Hovsepian, D.M. & et al.(2001). Endovascular abdominal aortic aneurysm repair in 144 patients: correlation of aneurysm size, proximal aortic neck length, and procedure-related complications, *Journal of Vascular Interventional Radiology,* 12, 1373–1382.

Ibanez, L. & et al., (2003). The ITK Software Guide. Insight Software Consortium, August 2003. URL http://www.itk.org/ItkSoftwareGuide.pdf.

Johnston, K.W., & et al. (1991). Suggested standards for reporting on arterial aneurysms. Subcommittee on Reporting Standards for Arterial Aneurysms, Ad Hoc Committee on Reporting Standards. *Journal of Vascular Surgery,* 13, 452-458.

Johnston, S.C., & et al. (2000). Endovascular and surgical treatment of unruptured cerebral aneurysms: comparison of risks. *Annals of Neurology*, 48,11-19.

Kantonen, I., & et al. (1999). Mortality in ruptured abdominal aneurysms. *European Journal of Vascular and Endovascular Surgery,* 17, 208–212.

Kato, Y., & et al. (1999). Application of Three-Dimensional CT Angiography (3D-CTA) to Cerebral Aneurysms. *Surgical Neurology*, 52, 113-122.

Kato, Y., Sano H., Katada, K., Ogura, Y., Hayakawa, M., Kanaoka, N., & Kanno, T. (1999). Application of three-dimensional CT angiography (3D-CTA) to cerebral aneurysms, *Surgical Neurology*,52(2),113-122.

Klingenbeck, R.K., Schaller, S., Flohr, T., Ohnesorge, B., Kopp, a.F. & Baum, U. (1999) Subsecond multi-slice computed tomography: basics and applications. *European journal of radiology*, 31, 110-24.

Krissian, K. (2000). Model-Based Detection of Tubular Structures in 3D Images. *Computer Vision and Image Understanding*, *80*(2), 130-171.

Kunio, D., (2006). Diagnostic imaging over the last 50 years: research and development in medical imaging science and technology. *Physics in medicine and biology,* 51(13), 5-27.

Lakare, S. (2000). 3D Segmentation Techniques for Medical Volumes. *Neural Networks*.

Lee, D.T. & Schachter, B.J. (1980). Two algorithms for constructing a Delaunay triangulation,*International Journal of Parallel Programming*,9 (3), 219-242.

Lee, W.A. (2010). Endovascular abdominal aortic aneurysm sizing and case planning using the TeraRecon Aquarius workstation. *Vascular and endovascular surgery*, *41*(1), 61-7.

Lewis., R.R. (1993). Making shaders more physically plausible. *In Fourth Eurographics Workshop on Rendering*, 47-62.

Linninger, A.A., & et al. (2005). Mimics Image Reconstruction for Computer - Assisted Brain Analysis. *Imaging*, 1-12.

Lorensen, W. E., &Cline, H. E. (1987). Marching cubes: A high resolution 3D surface construction algorithm. *In Proceedings of the 14th Annual Conference on Computer Graphics and interactive Techniques SIGGRAPH '87*. ACM, 163-169.

Maheshwaraa, N. U., Arumaikkannu, G., & Gowri, S. (2008). Three-dimensional reconstruction and rapid prototyping of femur bone using multiple digital X-rays. *Journal of medical engineering & technology*, *32*(1), 30-9.

Malina, M., & et al. (1997). Changing Aneurysmal Morphology After Endovascular Grafting: Relation to Leakage or Persistent Perfusion, *Journal of Endovascular Surgery*, 4, 23-30.

Marin, M. L., & et al. (1998). Impact of transrenal aortic endograft placement on endovascular graft repair of abdominal aortic aneurysms. *Journal of Vascular Surgery*, 638-646.

Matsumura, J.S., Brewster, D.C., Makaroun, M.S., Naftel, D.C. (2003). A multicenter controlled clinical trial of open versus endovascular treatment of abdominal aortic aneurysm. *Journal of Vascular Surgery,* 37, 262-271.

May, J., & et al. (1999). Adverse events after endoluminal repair of abdominal aortic aneurysms: A comparison during two successive periods of time. *Journal of Vascular Surgery,* 29, 32-39.

Moore, W.S., & Rutherford, R.B. (1996). Transfemoral endovascular repair of abdominal aortic aneurysm: results of the North American EVT phase I trial. *Journal of Vascular Surgery*, 23, 543-545.

Morse, B. S. (2000). Lecture 18 : Segmentation (Region Based). *Reading*, 1998-2000.

Mustra, M., Delac, K., & Grgic, M. (2008). Overview of the DICOM Standard. *Veterinary Medicine*,10-12.

Napel, S., & et al. (1992). CT angiography with spiral CT and maximum intensity projection. *Radiology,* 185, 607-610.

Pal, N.R., & Pal, S. K. (1993). review on image segmentation techniques. *Pattern Recognition*, *26*, 1277-1294.

Parizel, P.M, Makkat, S., Miert, E., Goethem, J.W., Hauwe, L., Schepper, A.M. (2001) Intracranial hemorrhage: principles of CT and MRI interpretation. *Euro Radiology*, 11, 1770 – 1783.

Pavlidis, T., & Liow, Y. (1990). Integrating region growing and edge detection. *IEEE Transactions on Pattern Analysis and Machine Intelligence*, *12*(3), 225-233.

Penninga, F. (2005). 3D Topographic Data Modelling : Why Rigidity. *Network*, 409-425.

Ramamoorthi, R., Mahajan, D., & Belhumeur, P. (2007). A first-order analysis of lighting, shading, and shadows. *ACM Transactions on Graphics*, *26*(1), 2-es.

Remondino, F. (2006). Image-based 3D modelling : a review. *Photogrammetric Record,* 269-291.

Resch, T. & et al. (2000). Midterm changes in aortic aneurysm morphology after endovascular repair. *Journal of Endovascular Therapy,* 7, 279-285.

Resch, T., & et al. (1999). Abdominal aortic aneurysm morphology in candidates for endovascular repair evaluated with spiral computed tomography and digital subtraction angiography. *Journal of Endovascular Surgery*, 6, 227-32.

Riddle W.R. & Pickens, D.R. (2005).Extracting data from a DICOM file.Medical Physics ,32(6), 1537-1541.

Robbins, M., & et al. (2005). Comerota, Suprarenal Endograft Fixation Avoids Adverse Outcomes Associated with Aortic Neck Angulation, *Annals of Vascular Surgery,*19, 172-177.

Rockman, C.B., & et al. (2002).Aneurysm morphology as a predictor of endoleak following endovascular aortic aneurysm repair: do smaller aneurysm have better outcomes?. *Annals of Vascular Surgery*; 16, 644-651.

Rosset, A., Spadola, L., & Ratib, O. (2004). OsiriX: an open-source software for navigating in multidimensional DICOM images. *Journal of digital imaging*, *17*(3), 205-16.

Rubin, G.D., & et al. (2000). Aorta and Iliac Arteries: Single versus Multiple Detector-Row Helical CT Angiography. *Vascular and Interventional Radiology,* 215, 670-676.

Russell, H., Stephane, L., Grigore, C.,Ralph, M. (1995). Computer integrated surgery: technology and clinical applications. *Cambridge, MA: MIT Press*.

Sahoo, P.K., Soltani S., &Wong, A.K.C. (1988). A survey of thresholding techniques. *Computer Vision, Graphics, and Image Processing,*41(2), 233-260.

Sakas, G. (2002). Trends in medical imaging: from 2D to 3D. *Computers & Graphics*, 26, 577-587.

Schneider, U., Pedroni, E. & Lomax, A. (1996) The calibration of CT Hounsfield units for radiotherapy treatment planning. *Physics in medicine and biology*, 41, 111-24.

Shi, J., & Malik, J. (2000). Normalized Cuts and Image Segmentation. *Analysis*, *22*(8), 888-905.

Silva, M.B., & et al. (1996). A program of operative angioplasty: Endovascular intervention and the vascular surgeon. *Journal of Vascular Surgery,* 24, 963-973.

Slater, B.J., Harris, E.J., & Lee, J.T. (2008). Anatomic Suitability of Ruptured Abdominal Aortic Aneurysms for Endovascular Repair. *Annals of Vascular Surgery,* 22, 716-722.

Smith, T.G., & et al. (1988). Edge detection in images using Marr-Hildreth filtering techniques. *Journal of Neuroscience Method* 26:75-82.

Sotak, G.E., & Boyer, K.L. (1989). The Laplacian-of-Gaussian kernel: a formal analysis and design procedure for fast, accurate convolution and full frame output. *Comp. Vis. Graph. Im. Proc.* 48, 147–189.

Stanberry, B. (2000). Telemedicine: barriers and opportunities in the 21st century. *Journal of internal medicine*, *247*(6), 615-28.

Stanley, B.M., & et al. (2001). Evaluation of Patient Selection Guidelines for Endoluminal AAA Repair With the Zenith Stent-Graft : The Australasian Experience. *Journal of Endovascular Therapy*, 457-464.

Sternbergh, W.C., Carter, G., York, J.W., Yoselevitz, M., & Money, S.R. (2002). Aortic neck angulation predicts adverse outcome with endovascular abdominal aortic aneurysm repair. *Journal of Vascular Surgery,* 35, 482-486.

Stewart, R. D., Fermin, I., & Opper, M. (2002). Region growing with pulse-coupled neural networks: an alternative to seeded region growing. *IEEE transactions on neural networks*, *13*(6), 1557-62.

Stone, P.A., & et al. (2005). Ruptured abdominal aortic aneurysms: 15 years of continued experience in a southern West Virginia community. *Annals of vascular surgery,* 19, 851-857.

Stytz, M.R., Frieder, G., & Frieder, O. (1991) Three-dimensional medical imaging: algorithms and computer systems. *ACM Computing Surveys (CSUR),*23(4), 421-499.

Teufelsbauer, H., & et al. (2002). Endovascular stent grafting versus open surgical operation in patients with infrarenal aortic aneurysms. *Circulation,* 106, 782–787.

Tillich, M, & et al. (2001). Prediction of aortoiliac stent-graft length: comparison of measurement methods. *Radiology,* 220:475–48.

Treiman, G. S., & Bernhard, V. M. (1998). Endovascular treatment of abdominal aortic aneurysms. *Annual review of medicine*, *49*, 363-73.

Waasdorp, E.J., & et al. (2005). Aneurysm Diameter and Proximal Aortic Neck Diameter Influence Clinical Outcome of Endovascular Abdominal Aortic Repair: A 4-Year EUROSTAR Experience. *Annals of Vascular Surgery*, 19, 755-761.

Warren, J., Schaefer, S., Hirani, A. N., & Desbrun, M. (2006). Barycentric coordinates for convex sets. *Advances in Computational Mathematics*, 27(3), 319-338.

Weszka, J.S., Nagel, R.N., & Rosenfeld, A. (1974). A threshold selection technique. *IEEE Transaction Computing,* 23, 1322 -1326.

White, R.A., & et al. (1993). Endovascular surgery credentialing and training for vascular surgeons. *Journal of Vascular Surgery,* 17, 1095-1102.

Wolf, I., & et al. (2005). The medical imaging interaction toolkit. *Medical image analysis*, *9*(6), 594-604.

Zarins, C.K. , & et al. (1999). AneuRx stent graft versus open surgical repair of abdominal aortic aneurysms: Multicenter prospective clinical trial. *Journal of Vascular Surgery,* 29,292-308.

Zhao, M.C., & et al. (2005) Design and Implementation of MITK for 3D Medical Image Processing and Analyzing. *Journal of Software, 16*(4), 485-495.

Zitova, B. (2003). Image registration methods: a survey. *Image and Vision computing*, *21*(11), 977-1000.
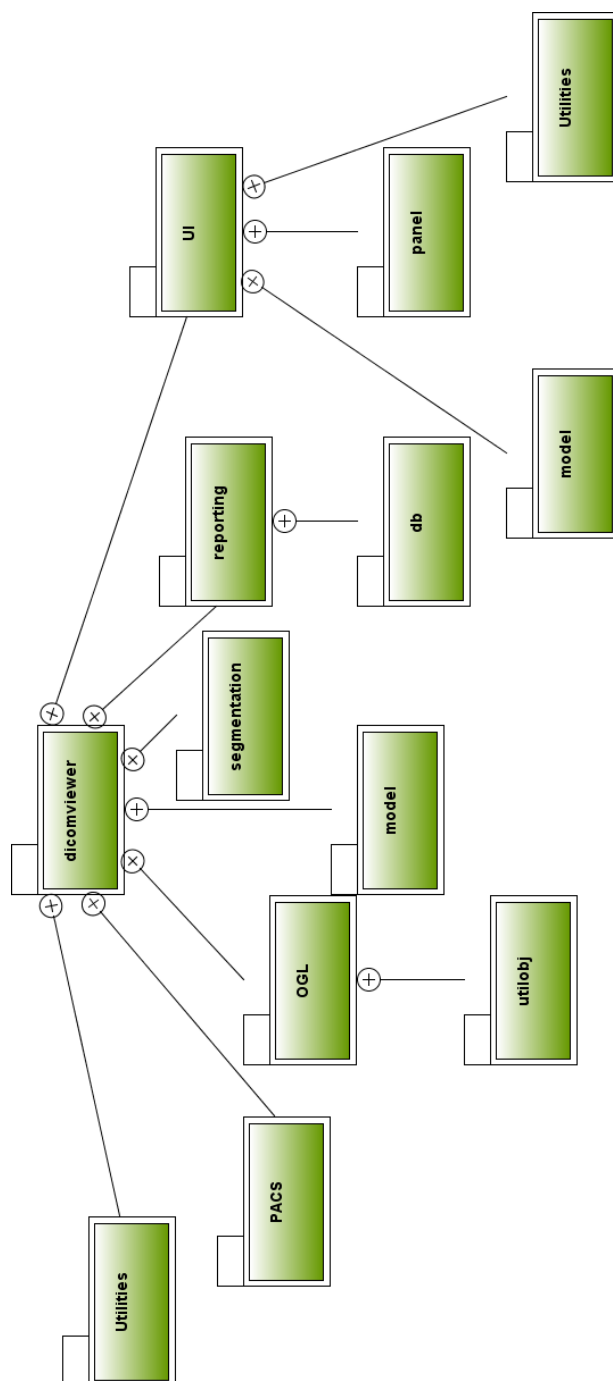
APPENDICES

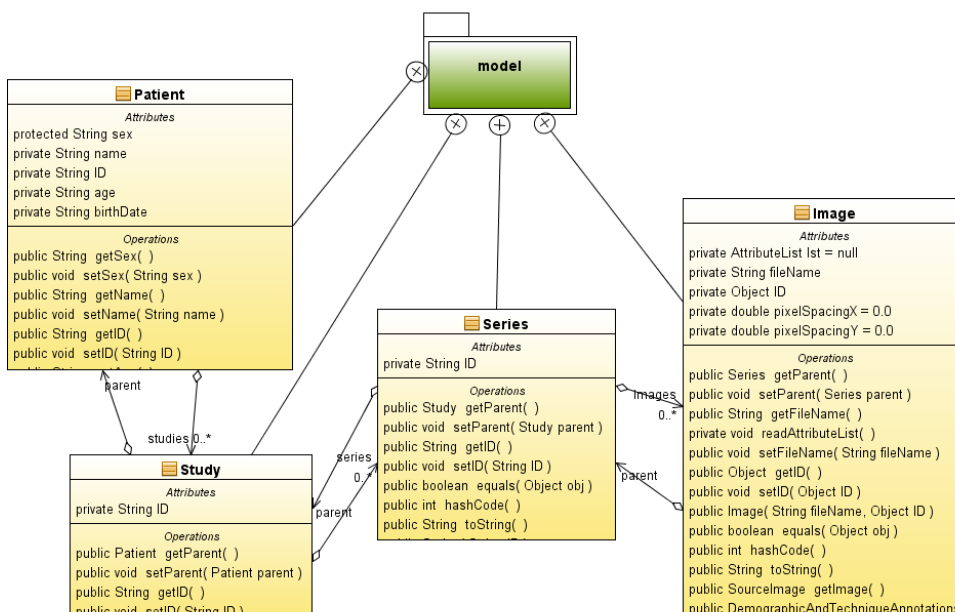### A. Class Diagrams Of The Amet

Figure A.1 Package Hierarchy of AMET

Patient

Attributes
protected String sex
private String name
private String ID
private String age
private String birthDate

Operations
public String getSex( )
public void setSex(String sex)
public String getName( )
public void setName(String name)
public String getID( )
public void setID(String ID)

model

Series

Attributes
private String ID

Operations
public Study getParent( )
public void setParent(Study parent)
public String getID( )
public void setID(String ID)
public boolean equals(Object obj)
public int hashCode( )
public String toString( )

Image

Attributes
private AttributeList lst = null
private String fileName
private Object ID
private double pixelSpacingX = 0.0
private double pixelSpacingY = 0.0

Operations
public Series getParent( )
public void setParent(Series parent)
public String getFileName( )
private void readAttributeList( )
public void setFileName(String fileName)
public Object getID( )
public void setID(Object ID)
public Image(String fileName, Object ID)
public boolean equals(Object obj)
public int hashCode( )
public String toString( )
public SourceImage getImage( )
public DemographicAndTechniqueAnnotations

Study

Attributes
private String ID

Operations
public Patient getParent( )
public void setParent(Patient parent)
public String getID( )
public void setID(String ID)

parent

studies 0..*

Images
0..*

series
0..

parent

parent

Figure A.2 Class Hierarchy of Model Package (Patient Class, Study Class, Image Class, and Series Class)

RenderEngine

Attributes
private int BUFSIZE = 512
private int NO_ID = -65568
private int modelGLId
private int surfacesGLId
private int surfacesGLId2
private int compassGLId
private boolean isMouseClicked =
private boolean isModelInitialized

OGL

DrawingParametersObject

Attributes
public float tetrahedronSize
public float pointerSize

SliceRenderEngine

Attributes
private int BUFSIZE = 12
private int NO_ID = -65568
private boolean isMouseClicked = false
private boolean isModelInitialized = false
private GLU glu
private Point pickpoint

SegmentationData

Attributes
private String files[0..*]
private String dataSourcePath
private String reflmageName
private int reflmageNumber
private double pixelSpacingX

Measurement

Attributes
public int NoVertex = 0x0
public int Vertex1 = 0x1
public int Vertex2 = 0x2

ShortcutsObject

Attributes
public int scRotationXPositive
public int scRotationXNegative
public int scRotationYPositive
public int scRotationYNegative

SegmentReferenceData

Attributes
private int level
private int X

SelectedVertex

Attributes
public int slice_id
public int region_id

Operations

SceneParametersObject

Attributes
public float rotationAxisX = 0.0f
public float rotationAxisY = 0.0f
public float rotationAxisZ = 0.0f

utilobj

Polygon

Attributes

Operations
public Polygon(top)
public boolean isMultiple(

CameraControlParametersObject

Attributes
public float xDelta
public float yDelta

Triangle

Attributes

Operations
public Triangle(v1, v2,
public Triangle(v1, v2,
public [0..*] getVertices
public getNormal( )
public String toString( )

glRenderer

sliceRenderer

measurementList 0..*

measurement

selectedVertexExt

v1 v2 v3

spo scene scene

dpo

dpo

shortcuts

shortcuts
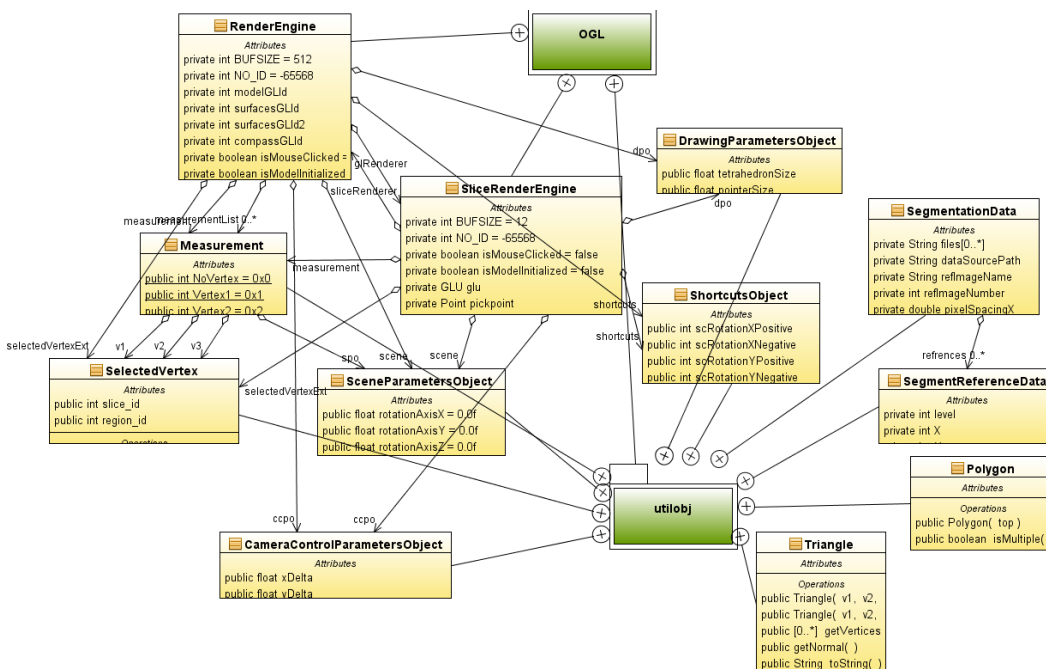
selectedVertexExt

refrences 0..*

ccpo ccpo

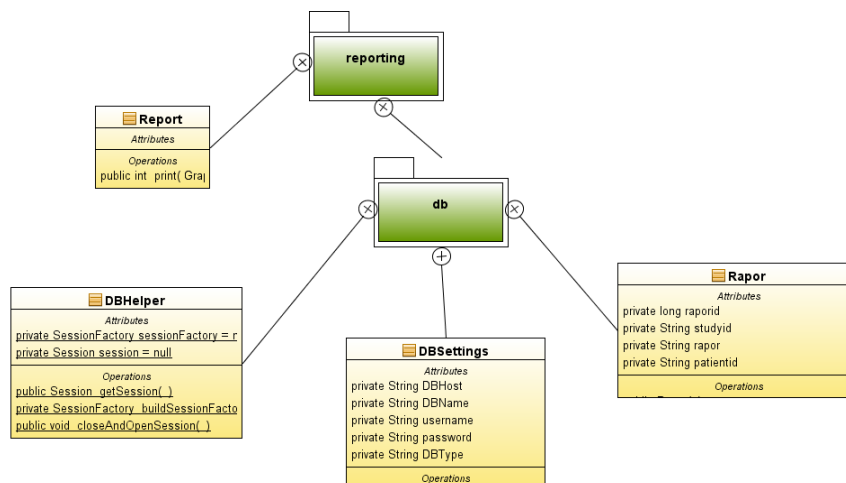Figure A.3 Class Hierarchy of OPENGL and Utility Package

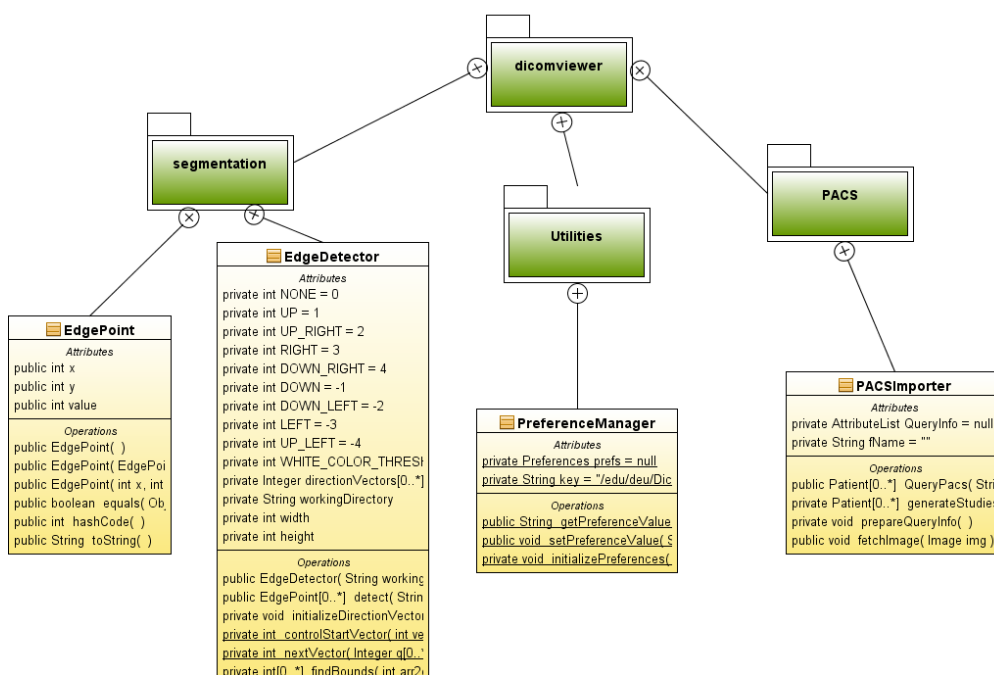Figure A.4 Class Hierarchy of Reporting and Database Package

Figure A.5 Class Hierarchy of Segmentation, Utilities, and PACS Package
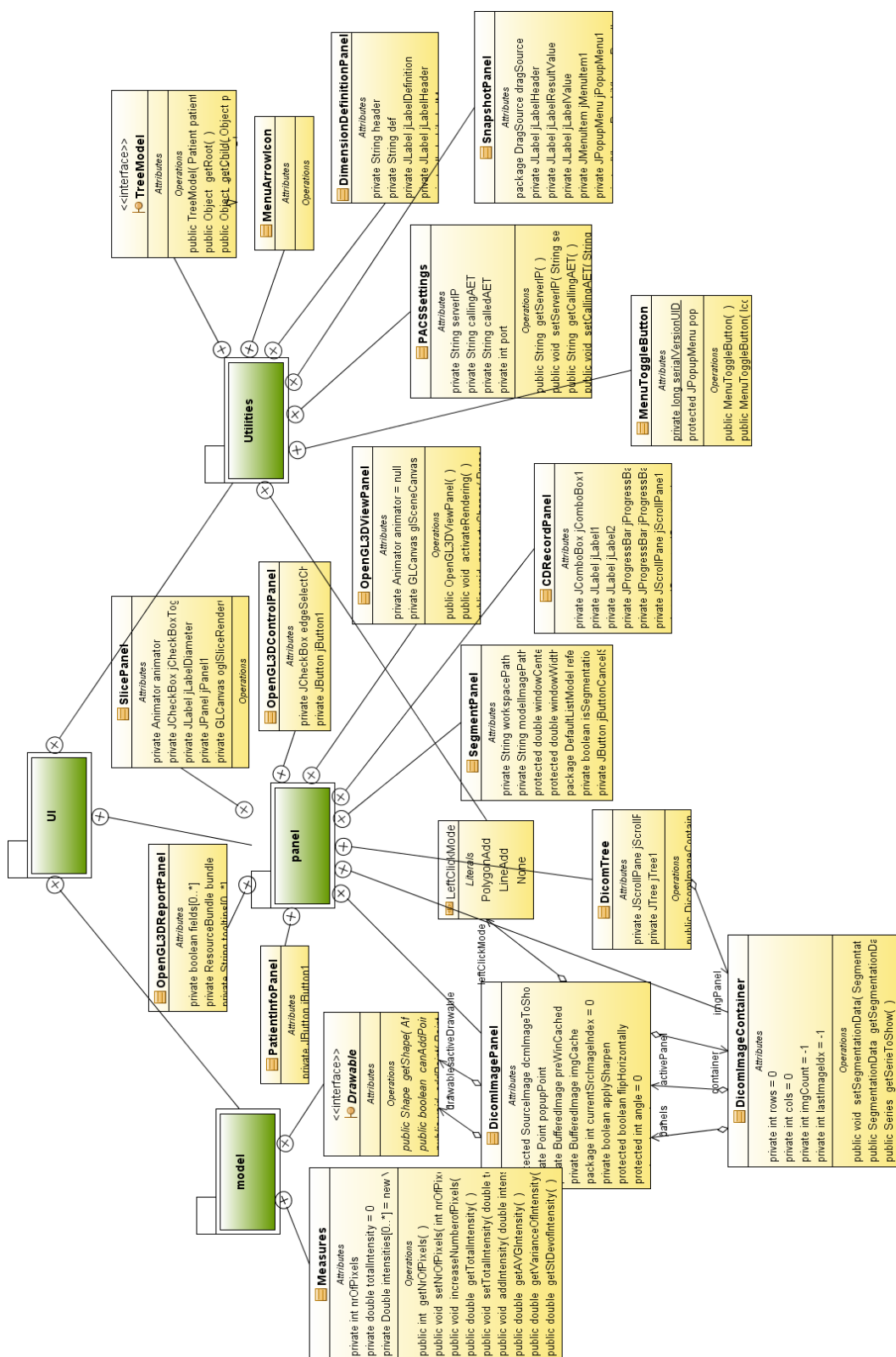
Figure A.6 Class Hierarchy of User Interface, Model, User Panel, and Utilities Package
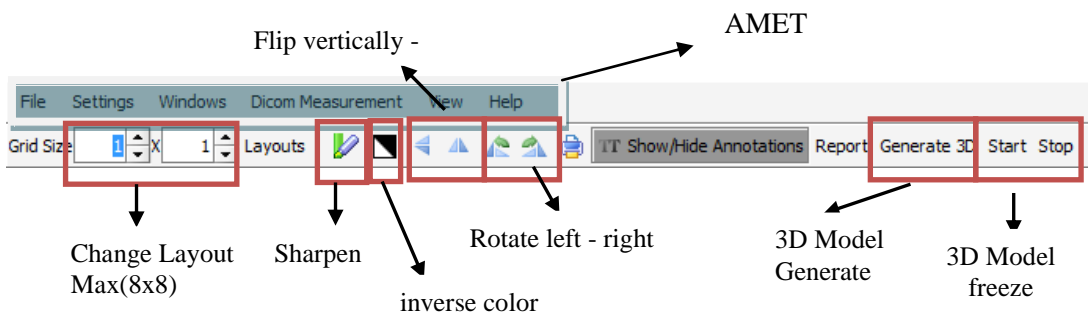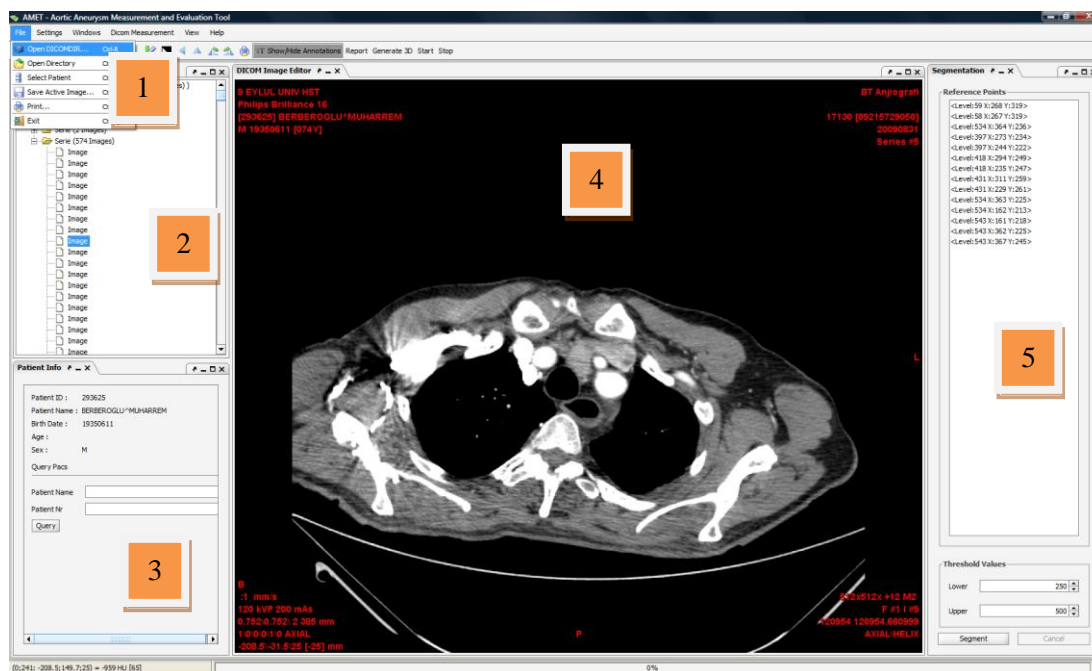
B. AMET

Figure B.1 AMET Toolbar

Figure B.2 DICOM Image Editor and Segmantation Panel of AMET (1) File Menu, (2) Patient DICOM ImageTree, (3) Patient Information, (4) DICOM Image Editor, (5) Segmantation Panel.

Figure B.3 AMET 3D View Mode (1) Windows Menu, (2) Slice View, (3) DICOM Image Editor, (4) 3D View Panel, (5) Measurement Panel, (6) Measurement History, (7) Measurement Report
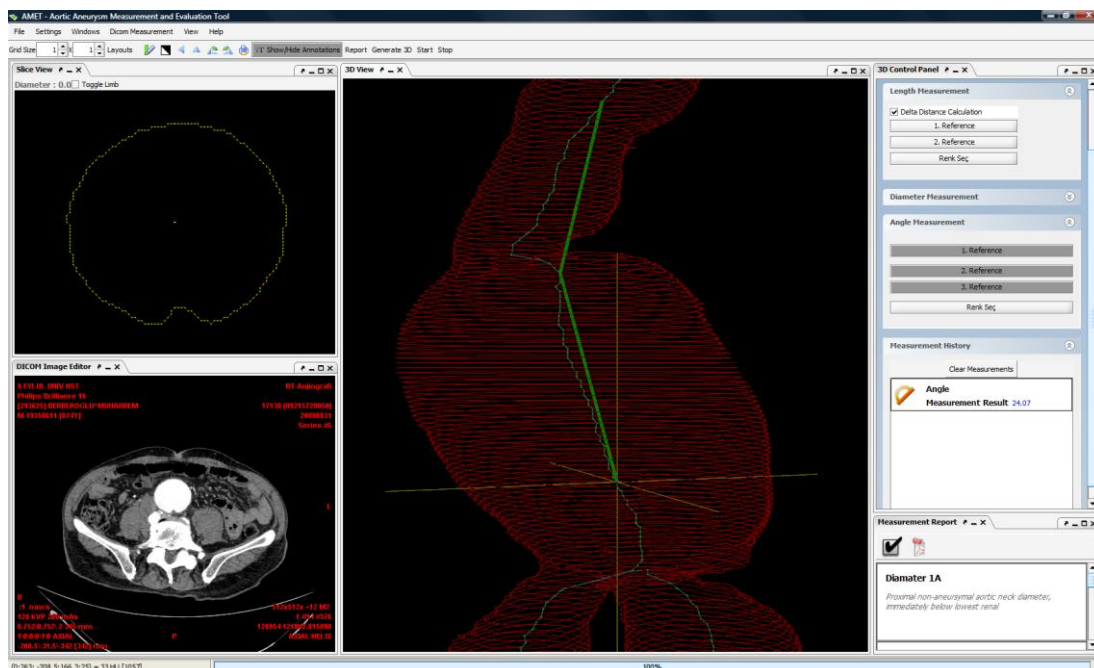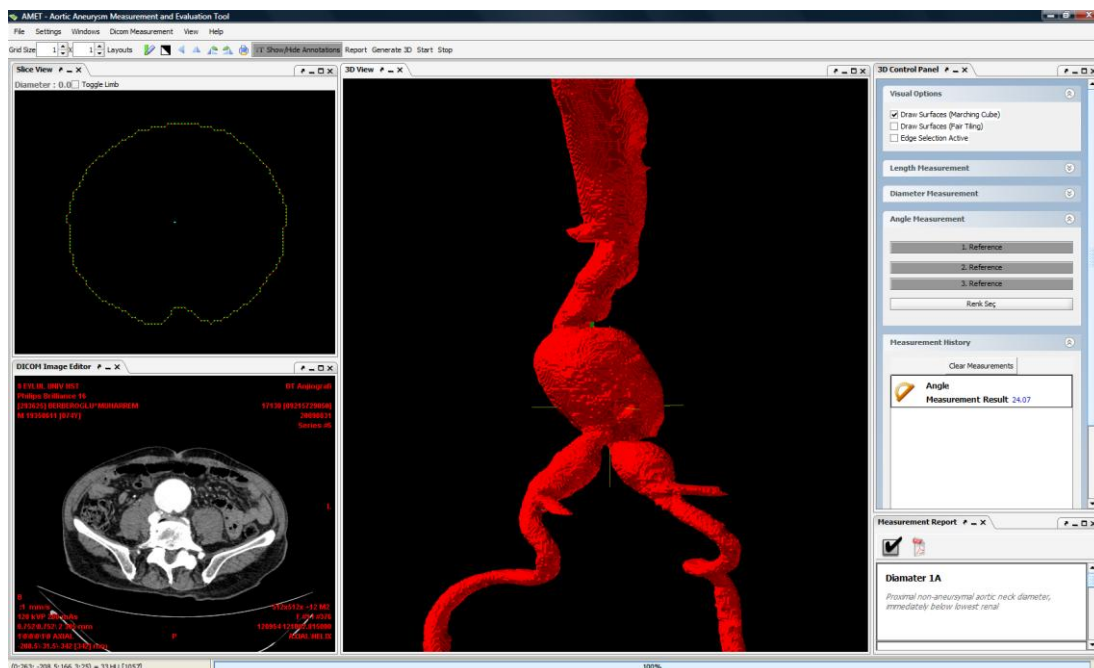
Figure B.4 AMET Angle Measurement

Figure B.5 A 3D View of Aorta (Draw Surface Marching Cube is enable)

C. Manual Measurement Methods

Figure C.1 Neck Diameter Measurement in Manual Method

The diameter of the neck is measured on the orthogonal cross − sections of the neck, from the outer wall to the outer wall. Each cross sections of the aorta is obtained in 1.5 mm intervals. Physicians can measure different aortic neck diameter at different positions. Physicians have to be find ideal circle to measure the neck diameter. Physicians have to find maximum diameter of the orthogonal cross − section just below the renal artery. The diameter is used to decide suitable patients for endovascular repair. The stent graft is applied to the patient if the neck is suitable size. In figure C.1 the neck diameter measurement is shown in manual method.

Figure C.2 Aneursym Length Measurement in Manual Method

Aortic length is the length between the lowermost renal artery and the aortic bifurcation. Figure C.2 shows the length measurement of the aneurysm in manual method.

Figure C.3 Proximal Neck Length

The measurement of the length for proximal fixation zone is calculated between the lowermost renal artery and the start point of the aneurysm. Figure C.3 shows to measurement of the proximal neck length in manual method.

Aorta can be segmented in three parts. The first part is the aorta above the renal arteries, the second part is aortic neck and the last part is the aneurysm. These three parts create two angles. These are supra-renal angle (α) and infra-renal angle (β). Supra – renal angle is the angle between proximal AAA neck and supra-renal aortic axis. Infra – renal angle is the angle between proximal AAA neck and main axis of AAA. Figure C.4 and C.5 shows the angle measurement of the abdominal aortic aneurysm in manual method.

Figure C.4 Supra – Renal Angle (α) of the aneursym

Figure C.5 infra-renal angle (β)

D. Abbreviations

AAA	Abdominal Aortic Aneurysm
AMET	Abdominal Aortic Aneurysm Measurement and Evaluation Tool
BSD	Berkeley Software Distribution
CT	Computed Tomography
DICOM	Digital Imaging and Communication Standard
DICOMDIR	Digital Imaging and Communication Standard Directory
EVAR	Endovascular Aneurysm Repair
HU	Hounsfield Unit
MDCT	Multi Detector Computed Tomography
MLCP	Median Luminal Center Path
MPR	Multi Planer Reformatted
MRI	Magnetic Resonance Imaging
OpenGL	Open Graphic Library